National Academy of Sciences of Ukraine
Institute of Mathematics

Qualifying scientific work
on the rights of the manuscript

MILIAIEV Anton Oleksandrovych

UDC 517.958:512.816

Machine learning of hydrodynamic reduced order models on nonlinear resonant liquid sloshing

113 Applied Mathematics

Thesis
for the degree of Doctor of Philosophy

The thesis contains the results of own research. The use of ideas, results and texts of other authors have an appropriate citation.

_____ A.O. Miliaiev

Supervisors
D.Sc., Academician of NAS of Ukraine
TYMOKHA Oleksandr Mykolayovych

Kyiv — 2026

Національна академія наук України
Інститут математики

Кваліфікаційна наукова
праця на правах рукопису

МІЛЯЄВ Антон Олександрович

УДК 517.958:512.816

Машинне навчання гідродинамічних моделей редукованого порядку нелінійного резонансного коливання рідини в баках

113 Прикладна математика

Дисертація
на здобуття ступеня доктора філософії

Дисертація містить результати власних досліджень. Використання ідей, результатів і текстів інших авторів мають посилання на відповідне джерело.

_____ О.О. Міляєв

Наукові керівники
доктор фіз.-мат. наук, академік НАН України
ТИМОХА Олександр Миколайович

Київ — 2026

Анотація

Міляєв А.О. Машинне навчання гідродинамічних моделей редукованого порядку нелінійного резонансного коливання рідини в баках. — Кваліфікаційна наукова праця на правах рукопису.

Дисертація на здобуття ступеня доктора філософії за спеціальністю 113 Прикладна Математика. – Інститут математики НАН України, Київ, 2026.

Динаміка резонансного хлюпання рідини є однією з найскладніших та найпривабливіших гідродинамічних систем через різноманітні застосування в аерокосмічній, морській, цивільній та хімічній інженерії. Ці системи характеризуються неоднозначним усталеним хвильовим розв'язком, мультистійкістю, хаосом та іншими сильно нелінійними явищами, які можуть залежати від в'язкого затухання. Моделі зменшеного порядку (нелінійні модальні системи), які, найімовірніше, залишаються єдиним аналітичним підходом до вивчення складної гідродинаміки хлюпання, однак походять від нев'язкої постановки задачі. Як показують сучасні експерименти, введення спекулятивних лінійних членів затухання в моделі зменшеного порядку не може забезпечити точний опис резонансних відгуків системи, особливо коли йдеться про фазові зсуви між гармонічним збуренням та вимушеними усталеними хвилями.

Застосовуючи так звану концепцію прихованої фізики, ця дисертація вперше в літературі розвиває підхід машинного навчання до відновлення нелінійних членів демпфування в асимптотичних нелінійних модальних системах типу Наріманова-Моїсеєва, використовуючи обмежений набір експериментальних даних про фазові зсуви. Основна увага приділяється вертикальним резервуарам прямокутної (двовимірні потоки) та круглої основи (тривимірні хвилі), а також поздовжнім збудженням найнижчої власної частоти коливання рідини, випадкам, для яких існують вищезгадані експериментальні дані.

У розділі 1 представлено розширений огляд мультимодальних (моделювання зменшеного порядку) методів з акцентом на аналітичні дослідження аналітичними методами стаціонарного резонансного хлюпання

в прямокутних (двовимірні та тривимірні рухт рідини) та вертикальних круглих контейнерах. Викладено відповідні модальні рівняння типу Наріманова-Моїсеєва, які ефективно описують амплітудні відгуки хвиль, включаючи їх останні версії Фальтінсена та Тімохи (2000 та 2016). У розділі також обговорюються проблеми нелінійного моделювання зменшеного порядку в нелінійному аналізі, що представляє концепцію прихованої фізики, та структуру цієї дисертаційної роботи.

У розділі 2 представлені необхідні елементи математичної теорії хлюпання рідини, яка складається з диференціальних, варіаційних та модальних формулювань, заснованих на ідеальній нестисливій гідродинамічній моделі. Для заміни диференціального та варіаційного формулювання системою звичайних диференціальних рівнянь прийнято схему моделювання зменшеного порядку з використанням проективної схеми типу Гальоркіна. У найзагальнішому вигляді таку систему вивели Майлз і Луковський. Система не містить членів, які відповідають за демпфування, проте можна включити такі лінійні члени, які в основному пов'язані з ефектом ламінарного в'язкого пограничного шару. Але цей підхід не працює для резонансних хвиль.

У наступних двох розділах демонструється, як відновити нелінійні члени демпфування. Процедура базується на методі машинного навчання, застосованому до так званої асимптотичної схеми Наріманова-Моїсеєва.

Розділ 3 зосереджений на випадку двовимірного резонансного хлюпання в прямокутному резервуарі та базується на підході машинного навчання, розробленому автором. Однодомінантна модальна система Фалтінсена і Тімохи оснащена нелінійними членами демпфування, структура яких повинна узгоджуватися з так званим асимптотичним упорядкуванням Моїсеєва. Дотримання цього правила доводить першу основну теорему розділу про загальну структуру членів «демпфування». Побудовано аналітичний асимптотичний періодичний розв'язок модальних рівнянь з демпфуванням. Цей аналітичний результат виражає другу основну теорему цього розділу.

Використання експериментальних даних німецьких дослідників (2021) для вивчення членів демпфування однодомінантних модальних рівнянь демонструє майже ідеальну відповідність з вимірюваннями, тоді як німецькі дослідники не змогли цього стверджувати, оскільки вони нехтували нелінійністю. Це (i) підтверджує, що ефектом демпфування вищих природних мод плескання не можна нехтувати; (ii) в'язке демпфування первинно збудженої (першої) власної форми коливання рідини, загалом кажучи, має бути функцією амплітуди резонансної хвилі; (iii) запропонований підхід машинного навчання є ефективним інструментом для оцінки в'язкого демпфування (логарифмічного декременту) найнижчої (домінантної) природної моди плескання.

Розділ 4 стосується резонансного хлюпання у вертикальному круговому резервуарі. Переглянуто модальні рівняння зменшеного порядку типу Наріманова-Моїсеєва Фальтінсена та Тімохи (2016). У лінійному випадку ці рівняння можна забезпечити лінійними членами демпфування, що відображають в'язкі ламінарні потоки на змоченій поверхні резервуара. Однак, використовуючи відповідні коефіцієнти демпфування, не вдалося досягти узгодженості з експериментальними даними щодо фазового зсуву, виміряними французькими дослідниками у 2007 році (премія EURMECH) для резонансних усталених кругових хвиль. Цей факт був детально обговорюється Райновським та Тимохою, які намагалися спекулятивно підібрати коефіцієнти демпфування. Дотримуючись підходу машинного навчання з розділу 3, асимптотичні модальні рівняння типу Наріманова-Моїссєва для хлюпань у вертикальному круглому резервуарі, були оснащені відповідними нелінійними членами демпфування та побудовано аналітичний асимптотичний періодичний розв'язок. Результат сформульовано як Теорема 4.1. Повідомляється про задовільну відповідність з експериментами. Основні висновки: (i) в'язке демпфування вищих власних форм не можна нехтувати; (ii) в'язке затухання первинно збуджених (перших) власних форм є сильно нелінійним і, отже, є функцією амплітуди резонансної хвилі.

У розділі 5 перераховано основні висновки дисертації та обговорено

майбутню роботу. Загалом, дисертація розв'язує кілька відкритих проблем щодо ролі ефектів в'язкого затухання та розробляє нові процедури машинного навчання для відновлення членів в'язкого затухання в нелінійних асимптотичних модельних рівняннях. Практичне значення поширюється на застосування в аерокосмічній інженерії, де точне прогнозування навантажень від хлюпання має вирішальне значення для проектування паливних баків, безпеки морських перевезень та налаштованих рідинних демпферів для контролю вібрації конструкцій. Розроблена методологія забезпечує систематичну основу для включення експериментальних даних у теоретичні моделі за допомогою машинного навчання, пропонуючи покращені можливості прогнозування для інженерного проектування у випадках, коли традиційні підходи до CFD стикаються з обчислювальними або моделюючими проблемами.

Ключові слова: гідродинамічна система, вільна поверхня, хлюпання, моделлювання обмеженого порядку, машинне навчання, в'язке демпфування.

Abstract

Miliaiev A.O. Machine learning of reduced order hydrodynamic models on nonlinear resonant liquid sloshing. — Qualifying scientific work on the rights of the manuscript.

Thesis for the degree of Doctor of Philosophy, speciality 113 Applied Mathematics. – Institute of Mathematics of NAS of Ukraine, Kyiv, 2026.

Resonant liquid sloshing dynamics is one from most challenging and attracting hydrodynamic systems due to various applications across aerospace, marine, civil, and chemical engineering. The systems are characterized by non-unique steady-state wave solution, multi-stability, chaos and other strongly nonlinear phenomena which may depend on viscous damping. Reduced order models (nonlinear modal systems) which remain, most probably, the only analytical approach to study of the complex sloshing hydrodynamics are, however derived from inviscid formulation. As present experiments show, introducing speculative linear damping terms in the reduced-order models is not able to provide accurate description of the resonant sloshing responses, especially, when it comes to phase lags between harmonic forcing and forced steady-state waves. By adopting the so-called hidden physics concept, this dissertation develops, firstly in the literature, a machine learning approach to restoring the nonlinear damping terms in asymptotic nonlinear modal systems of the Narimanov-Moiseev type by utilizing a limited set of experimental data on the phase lags. The main focus is on upright tanks of rectangular (two-dimensional flows) and circular base (three-dimensional waves) as well as longitudinal excitations of the lowest natural sloshing frequency, the cases, for which the aforementioned experimental data exist.

In Chapter 1, an extensive review on the multi-modal (reduced-order modeling) methods is presented with a focus on analytical studies by the analytical methods of steady-state resonant sloshing in rectangular (two-dimensional and three-dimensional flows) and upright circular containers. The corresponding Narimanov-Moiseev–type modal equations that effectively describe the steady-state wave amplitude responses are outlined including

their latest versions by Faltinsen & Timokha (2000 and 2016). The chapter also discusses challenges of the nonlinear reduced order modeling in nonlinear analysis, represents the hidden physics concept and structure of the present dissertation work.

Chapter 2 introduces necessary elements of mathematical sloshing theory, which consists of differential, variational and modal formulations based on ideal incompressible hydrodynamic model. In order to replace the differential and variational formulation by a system of ordinary differential equations, the Reduced Order Modeling scheme is adopted by employing a projective Galerkin–type scheme. In the most general form, the system was derived by Miles & Lukovsky. The system does not include damping terms, however, the linear damping terms can be incorporated which are mainly associated with laminar viscous boundary layer effect. This way fails for resonant waves. The next two chapters demonstrate how to restore the nonlinear damping terms. The procedure is based on the machine learning technique applied to the so-called Narimanov-Moiseev asymptotic scheme.

Chapter 3 focuses on the case of two-dimensional resonant sloshing in a rectangular tank and is based on machine learning approach developed by the author. The single-dominant modal system by Faltinsen & Timokha is equipped with the nonlinear damping terms whose structure should be consistent with the so-called Moiseev asymptotic ordering. Following this way proves the first main theorem of the chapter on general structure of the 'damping' terms. Analytical asymptotic periodic solution of the damping-equipped modal equations is constructed. The analytical result expresses the second main theorem of this chapter. Employing the experimental data of German researchers (2021) for learning the damping terms of the single-dominant modal equations demonstrates an almost perfect agreement with the measurements while the German researchers were not able to say that because they neglected the damping terms nonlinearity. This (i) confirms that damping effect of higher natural sloshing modes cannot be neglected; (ii) viscous damping of the primary-excited (first) natural sloshing mode should, generally speaking, be a function of the resonant wave amplitude; (iii) the

proposed machine learning approach is efficient tool for estimating the viscous damping (logarithmic decrements) of the lowest (dominant) natural sloshing mode.

Chapter 4 deals with resonant sloshing in an upright circular base tank. The Reduced Order Narimanov-Moiseev–type modal equations by Faltinsen & Timokha (2016) are revisited. In the linear case, these equations can be equipped with linear damping terms reflecting the viscous laminar flows at the wetted tank surface. However, using the corresponding damping rates was not able to get a consistency with experimental data on the phase-lag measured by French researchers in 2007 (EURMECH Award) for the swirling–type resonant steady-state sloshing. This fact was extensively discussed by Raynovskyy & Timokha who tried to speculatively to fit the measurements with varying the damping rates. Following the machine learning approach from the Chapter 3, the Narimanov-Moissev–type asymptotic modal equations for sloshing in an upright circular base tank are equipped with appropriate nonlinear damping terms and analytical asymptotic periodic solution is constructed. The result is formulated as Theorem 4.1. Satisfactory agreement with experiments is reported. The main conclusions are (i) viscous damping of higher natural sloshing modes cannot be neglected; (ii) viscous damping of the primary-excited (first) natural sloshing modes is strongly nonlinear and, therefore, is a function of the resonant wave amplitude.

The Chapter 5 lists the main conclusions to the dissertation and discusses the future work. Overall, the dissertation addresses several open problems on the role of viscous damping effects and develops a novel machine learning procedures to restore viscous damping terms in nonlinear asymptotic model equations. The practical significance extends to aerospace engineering applications, where accurate prediction of sloshing loads is critical for fuel tank design, marine transportation safety, and tuned liquid dampers for structural vibration control. The developed methodology provides a systematic framework for incorporating experimental data into theoretical models through machine learning, offering improved predictive capabilities for engi-

neering design in cases where traditional CFD approaches face computational or modeling challenges.

Keywords: hydrodynamic system, free surface, sloshing, reduced order modeling, machine learning, viscous damping

List of publications of the PhD candidate

1. Milyaev A.O., Timokha A.N., Learning the single-dominant model system on resonant sloshing in a rectangular tank, *Доповіді Національної Академії Наук України*, № 6 (2022), 46-53, 10.15407/dopovidi2022.06.046. (Фаховий журнал категорії Б).

2. Miliaiev A.O., Timokha A.N., Viscous damping of steady-state resonant sloshing in a clean rectangular tank, *Journal of Fluid Mechanics* **965**, R1 (2023), 11 pp., 10.1017/jfm.2023.372. (Scopus – Q1, WoS – Q1, SJR – Q1).

3. Miliaiev A.O., Timokha A.N., Damping of the swirling wave mode, *Нелінійні коливання* **27**, № 4 (2024), 517-528, 10.3842/nosc.v27i4.1494. (Фаховий журнал категорії А). Перевидано за кордоном: Miliaiev A.O., Timokha A.N., Damping of the swirling wave mode, *Journal of Mathematical Sciences (USA)* **295**, № 6 (2025), 726-738, 10.1007/s10958-026-08219-3. (Scopus – Q3, SJR – Q3).

4. Miliaiev A., Timokha A. Machine learning approach for studying damped resonant sloshing. VIII міжнародна наукова конференція СУЧАСНІ ПРОБЛЕМИ МЕХАНІКИ. Kyiv, 28-29 серпня 2025 року, Abstracts, http://tamd.univ.kiev.ua/wp-content/uploads/2025/08/ABSTRACTS_MPM_2025.pdf.

5. Miliaiev A.O., Timokha A.N. Differential equations of damped resonant sloshing. XX Міжнародна наукова конференція імені академіка Михайла Кравчука. 17–20 листопада 2025 р., Тези доповідей, сторінка 83, https://matan.kpi.ua/media/2025/kravchuk-conf-2025/kravchuk-conf-2025-abstracts.pdf.

Contents

Introduction

Relevance of research topic. The liquid sloshing dynamics remains one from most challenging topics for extensive studies in hydrodynamics and applied mathematics due to crucial applications across aerospace, marine, civil, and chemical engineering since analytical and numerical tools in solving the sloshing problems, especially, nonlinear, determine progress in designing and operating spacecraft fuel tanks, liquefied natural gas carriers, nuclear reactors, bioreactors, and seismic-resistant structures including liquid dampers [1]. The coupled rigid body and liquid sloshing motions imply a complex hybrid infinite-dimensional mechanical system where the body (container) has six degrees of freedom governed by ordinary differential equations but liquid sloshing is, in fact, a mechanical system with an infinite number of degrees of freedom that are often associated with natural sloshing wave modes.

To the author nest knowledge, the unique way to analytically study the liquid sloshing dynamics and/or coupled tank-sloshing motions consists of employing the reduced order modeling which is called in the literature on sloshing the multi-modal method (see, reviews on the method in [2–4]). Its idea consists of introducing the hydrodynamic generalized coordinates as an infinite set of time-depending functions characterizing perturbations of natural sloshing modes and, based on original differential or variational statement of the free-surface problem, as well as projective and asymptotic method, derive the so-called modal equations – systems of ordinary differential equations coupling these generalized hydrodynamic coordinates. In the nonlinear (resonant) case, the adopted specific asymptotic relations between the coordinates make it possible to sufficiently simplify the nonlinear modal system to a form, which admits analytical studies. This includes studying resonant steady-state sloshing regimes, their stability and multi-stability phenomena (two fully different wave regime exist with the same input data), secondary

resonances, as well as chaotic wave behaviors, the studies that remain challenging with the Computational Fluid Dynamics (see, [5] and [2]).

Recent catastrophic failures in aerospace missions and marine transport, along with the increasing use of liquid storage systems in seismic zones, have intensified the need for accurate prediction and control of *resonant* sloshing dynamics. A particularly challenging aspect that has gained attention is the role of viscous damping in nonlinear modal systems, which facilitate studies of the sloshing resonances especially for clean tanks without internal structures. By default, the the multimodal analysis is based on inviscid hydrodynamics and, as numerous studies have shown [2], because nonlinearity, in general, and nonlinear energy transfer from primary excited to higher natural sloshing modes, in particular, play most important role to damp the wave response, analytical results on wave / hydrodynamic force / hydrodynamic moment amplitudes by the nonlinear modal equations are in rather accurate agreement with experimental measurements [1]. However, recent experimental and theoretical investigations of resonant sloshing which are associated with modern applications, e.g., protein grows in containers, highlighted a series of wave phenomena that cannot be explained and modeled, even qualitatively, when neglecting the viscous damping in the complex dynamical system. An example is the co-called Ikeda's paradox [6] on swirling (rotary waves) in a square base basin due to diagonal excitations: elementary symmetry analysis states that wave elevations at perpendicular tank should be equal and do not depend on the swirling wave direction (co- or counter-clock) but measurements break this conclusion. Another example is co- and counter-directed rotary waves due to circular orbital resonant excitation of an upright circular container. In [7], inviscid analysis showed that both types of these waves may exist and be stable but the counter-directed swirling wave is not realized in model tests. In these two cases, one can show that introducing small but non-zero damping makes the multi-modal analysis consistent with experiments, at least, qualitatively.

In [8] and [4], where the two aforementioned paradoxes were explained by small viscous damping, the authors followed the standard strategy and in-

corporated linear damping terms in the nonlinear equations which described the asymptotically dominant generalized hydrodynamic coordinate. However, this strategy failed to describe the phase lag between harmonic forcing and resonant steady-state waves. This fact was found out and extensively discussed in [4, 9] documenting the failure with regard to experimental measurements in [10] (EUROMECH prize of 2008!) who reported the phase lags for swirling wave in an upright circular tank due to longitudinal excitation of the lowest natural sloshing frequency. Further, German researchers [11] conducted the dedicated experimental studies on the phase lag for resonant sloshing in a longitudinally excited rectangular tank and showed, in particular, that the classical single-dominant Faltinsen-Timokha modal system [3] with linear damping terms in the dominant equation is not able to describe, even qualitatively, the phase lag.

Based on the mentioned open problem that linear damping models fail to capture the complex dissipative mechanisms for resonant sloshing, the present dissertation studies make first step toward developing a machine learning technique, which would enable to restore the viscous damping in nonlinear modal equations.

Relation with academic programs, plans, themes, grants. This thesis was conducted at the Department of Mathematical Problems of Mechanics and Control Theory of the Institute of Mathematics of the National Academy of Sciences of Ukraine as part of the research projects "Development and investigation of mathematical models of complex objects of mechanics and control systems" (2021–2025, state registration number 0121U100317), "Complex dynamical system in sciences: theory, mathematical modelling, numerical methods and implementation to advanced technology" (National Research Foundation of Ukraine, 2020-2024, state registration number 0120U104004), "Mathematical modeling of complex dynamical systems and processes actual to the state security" (2024-2025, state registration number 0123U100853). The research aligns with the priority areas of fundamental research established by the National Academy of Sciences of Ukraine in fluid mechanics and applied mathematics.

Purpose and objectives of research. The primary purpose of this dissertation is to develop a comprehensive machine learning-enhanced multimodal framework for analyzing damped nonlinear resonant sloshing in clean containers of various geometries, with emphasis on rectangular tanks and circular cylindrical tanks. The specific objectives of the research include:

- To derive and validate damped nonlinear modal equations for two-dimensional resonant sloshing in rectangular tanks, incorporating viscous dissipation effects through solving a inverse coefficient problem.
- To extend the multimodal analysis to three-dimensional swirling-type resonant waves in circular cylindrical tanks.
- To develop machine learning algorithms for determining damping-related coefficients from experimental data, bridging the gap between theoretical predictions and observed behavior.
- To establish stability criteria and classify steady-state resonant wave regimes in the presence of nonlinear damping terms.
- To validate the theoretical framework through comprehensive comparison with experimental measurements of the phase shifts between harmonic excitation and steady-state resonant wave regime.

Scientific novelty of the obtained results. The main results that determine the scientific novelty of this thesis and are submitted for defense are:

- First systematic study on how account for nonlinear viscous damping effect in the nonlinear multimodal sloshing theory: Unlike previous approaches that relied on linear damping assumptions, this work develops a framework where damping coefficients depend nonlinearly on modal amplitudes and their derivatives, accurately captures the complex dissipative mechanisms in resonant sloshing.
- Novel learning methodology for the damping coefficients identification: A physics-informed approach is developed to learn damping-related co-

efficients from experimental data, to establish a data-driven bridge between inviscid potential flow theory and viscous reality.

- Adaptive asymptotic modal equations for cylindrical tanks: New third-order asymptotic relations are derived that accurately describe the modal interactions in swirling flows, extending the Narimanov–Moiseev theory to include the viscous–type effects.

- Quantitative validation of phase-shift phenomena: The developed theory successfully predicts the phase lag between tank excitation and liquid response, a critical parameter for resonance detection and control that was inadequately described by previous models.

Practical significance of the obtained results. The theoretical framework and computational tools developed in this thesis have direct applications in:

- Aerospace Engineering: Improved prediction of propellant behavior in spacecraft tanks, enabling more efficient fuel management strategies and safer mission design.

- Marine Transportation: Enhanced assessment of sloshing loads in LNG carriers and oil tankers, contributing to structural design optimization and operational safety guidelines.

- Seismic Engineering: Better understanding of liquid dampers' performance in earthquake-resistant structures, facilitating the design of more effective vibration control systems.

- Bioprocess Engineering: Accurate modeling of mixing dynamics in orbital shaken bioreactors, optimizing cell culture conditions and scaling-up procedures.

- Industrial Safety: Development of predictive tools for preventing sloshing-induced accidents in chemical storage facilities and nuclear cooling systems.

The machine learning algorithms developed can be adapted to other fluid-structure interaction problems where empirical damping models are required.

Personal contribution of the PhD candidate. The results presented in this thesis were obtained by the PhD candidate independently. The candidate personally:

- Derived all asymptotic modal equations and steady-state analytical solutions for steady-state waves when nonlinear damping may matter.
- Developed and implemented the machine learning algorithms for the coefficients identification
- Performed numerical simulations and validated results against experimental data
- Prepared publications and conference presentations

In collaborative works, the supervisors provided guidance on research direction, problem formulation, and manuscript revision, while the experimental data used for validation were obtained from published sources and collaborative partners.

Approbation of the thesis results. The main results of the thesis were reported and discussed at:

- Seminar of Department of Mathematical Problems of Mechanics and Control Theory (Kyiv, 2020–2026);
- Bogolyubov Kyiv Conference "Problems of Theoreticall and Mathematical Physics" dedicated to the 115th anniversary of MM Bogiolyubov (1909-1992), September 24-26, 2024, Kyiv, Ukraine;
- VIII міжнародна наукова конференція СУЧАСНІ ПРОБЛЕМИ МЕХАНІКИ. Київ, 28-29 серпня 2025 року;
- XX Міжнародна наукова конференція імені академіка Михайла Кравчука. 17–20 листопада 2025 р.

Publications. The results of the thesis have been published in following scientific publications:

1. Milyaev A.O., Timokha A.N., Learning the single-dominant model system on resonant sloshing in a rectangular tank, *Доповіді Національної Академії Наук України*, № 6 (2022), 46-53, 10.15407/dopovidi2022.06.046. (Фаховий журнал категорії Б).

2. Miliaiev A.O., Timokha A.N., Viscous damping of steady-state resonant sloshing in a clean rectangular tank, *Journal of Fluid Mechanics* **965**, R1 (2023), 11 pp., 10.1017/jfm.2023.372. (Scopus – Q1, WoS – Q1, SJR – Q1).

3. Miliaiev A.O., Timokha A.N., Damping of the swirling wave mode, *Нелінійні коливання* **27**, № 4 (2024), 517-528, 10.3842/nosc.v27i4.1494. (Фаховий журнал категорії А).
   Перевидано за кордоном:
   Miliaiev A.O., Timokha A.N., Damping of the swirling wave mode, *Journal of Mathematical Sciences (USA)* **295**, № 6 (2025), 726-738, 10.1007/s10958-026-08219-3. (Scopus – Q3, SJR – Q3).

4. Miliaiev A., Timokha A. Machine learning approach for studying damped resonant sloshing. VIII міжнародна наукова конференція СУЧАСНІ ПРОБЛЕМИ МЕХАНІКИ. Kyiv, 28-29 серпня 2025 року, Abstracts, http://tamd.univ.kiev.ua/wp-content/uploads/2025/08/ABSTRACTS_MPM_2025.pdf.

5. Miliaiev A.O., Timokha A.N. Differential equations of damped resonant sloshing. XX Міжнародна наукова конференція імені академіка Михайла Кравчука. 17–20 листопада 2025 р., Тези доповідей, сторінка 83, https://matan.kpi.ua/media/2025/kravchuk-conf-2025/kravchuk-conf-2025-abstracts.pdf.

Structure and volume of thesis. The thesis consists of an introduction, five chapters, conclusions, a list of references containing 232 items, and one appendix. The total volume is 12 pages, with the main text occupying 128 pages. The thesis includes 5 figures and 0 tables illustrating theoretical predictions, numerical results, and experimental validation.

Chapter 1

Overview of the literature and the dissertation studies concept

1.1. Reduced order modeling in liquid sloshing

The present dissertation centres around hybrid mechanical systems consisting of a rigid tank moving with, generally speaking, six degrees of freedom according to a prescribed time-dependent law (periodic and resonant in these studies) where the contained liquid has a free surface. In the literature, these free-surface liquid motions are called *sloshing*. Mathematically, the liquid sloshing dynamics in the rigid containers is described by an evolution initial-and-boundary value problem with an free boundary. Straightforward approaches to analyzing the hydrodynamic problem normally adopt diverse numerical methods of the so-called Computational Fluid Dynamics (CFD). The CFD methods are applied to solve the aforementioned initial-boundary value problems with diverse Cauchy conditions which determine an initial position of the free surface and initial liquid velocity field. For prescribed tank motions, the CFD solutions describe the so-called transient waves caused by initial perturbations and excitations (tank motions). When these excitations do not lead to resonances in the hydrodynamic system, employing the CFD methods looks a rather rational way in engineering the hybrid mechanical systems.

A fundamentally different physical problem arises when the moving rigid container undergoes periodic resonant excitations. In that case, transient sloshing tends to possess a steady-state wave regime that develops over long time scales after transient effects decay. The steady-state regimes may be of diverse type, coexist with each others or be unstable that yields the chaos.

Therefore, the specific periodic steady-state sloshing pattern that emerges is strongly dependent on the initial conditions (Cauchy conditions) so that small change of these condition can lead to different steady-state resonant wave regimes on a long time scale. Description of all possible steady-state wave regimes is called classification.

Because the problem on steady-state resonant sloshing may not have a unique solution but rather multiple solutions (different stable steady-state waves occurring for the same input physical parameters), to classify all possible steady-state waves by solving the original free-surface Cauchy problem. One should conduct an infinite set of numerical trial runs with different initial conditions. An even more challenging problem is how to discriminate real (mathematical and physical) hydrodynamic instability and numerical instability. Especially, when chaotic sloshing is detected in computations. Is that a physically real chaos in the hydrodynamic system or a product of inaccurate numerical simulations, a failure of the adopted CFD method? Hence, the nonlinear resonant sloshing problem on steady-state wave regimes and their classification (description of all possible stable/unstable steady-state resonance waves) requires development dedicated analytical approaches.

Such an appropriate approach could be the so-called nonlinear multimodal method which treats original evolution boundary value problem as a problem of analytical mechanics. The method is based on the Reduced Order Modeling concept. It makes it possible to reduce the original free-boundary value problem to a system of ordinary differential equations with respect to the generalized hydrodynamic coordinates which determine instant wave patterns. This system is a hydrodynamic analogy of the Euler-Lagrange–type equations and it has, generally, an infinite number of degrees of freedom. Once this (modal) system of differential equations has been derived and transformed to a finite-dimensional form, it becomes suitable for analytical studies, including for construction of analytical periodic solutions as well as implementation of other well-established methods known from the complex dynamical systems theory.

The key elements of the aforementioned Reduced Order Modeling ap-

proach and the present dissertation as well are: the projective multi-modal method based on the Bateman-Luke variational principle; the general infinite-dimensional nonlinear modal system of differential equations of the Miles-Lukovsky type; its finite-dimensional asymptotic Narimanov-Moiseev–type approximate form (for upright containers); nonlinear damping terms incorporated into the latter equations which, in the linear case, imply logarithmic decrements of the natural sloshing modes, if these modes are adopted in the modal representation of the instant wave patters where the generalised hydrodynamic coordinates appear as time-dependent coefficients in the modal representation; analytical studies of the finite-dimensional Narimanov-Moiseev–type asymptotic modal equations through construction of their stable/unstable periodic (steady-state) solutions; development of a *machine learning procedure* to restore the nonlinear damping terms by using a limited set of experimental measurements.

1.2. Natural sloshing modes and frequencies

Each degree of freedom in the Reduced Order Models, nonlinear modal systems is associated with perturbation of natural sloshing mode which is a standing wave occuring on the free surface in the motionless container. The natural sloshing modes were first mathematically and rigorously introduced and analyzed (for an upright container with a circular cross-section) by Mykhailo Ostrogradsky [12] in the early 19th century. As we noted, these modes constitute standing waves on the liquid free surface of the contained liquid with the corresponding natural sloshing frequencies and the container does not move but sloshing is described within the framework of linear approximation.

A generic mathematical theory for the corresponding spectral boundary value problems with a parameter on part of the boundary, which, properly, describes the natural modes and frequencies, was developed only in the 1960s [13]. According to the spectral theorems, any linear wave in stationary containers is a superposition of standing waves by the natural sloshing modes and frequencies. Moreover, any instantaneous surface pattern, even

for nonlinear sloshing in moving containers, can be expanded by a functional series in the natural modes. The nonlinear case assumes, additionally, that the tank walls are vertical at the free surface.

As we announced, the nonlinear multi-modal method introduces a set of hydrodynamic generalized coordinates associated with the perturbed (relative to the static position) liquid flows (perturbed velocity potential and free-surface patterns) via the natural sloshing modes. The method derives (modal) systems of nonlinear ordinary differential equations coupling the generalized coordinates and generalized velocities which are time-depending coefficients in functional representations of the free surface and velocity potential. These modal equations serve as analogs of the Euler-Lagrange equations for this type of hydro-mechanical system. The derivation of the nonlinear modal equations utilizes methods of analytical mechanics, which are, normally, based on variational formulations of the Hamilton-Ostrogradsky type. The derived modal systems can, theoretically, be used for direct simulation of nonlinear surface waves as well as associated hydrodynamic forces and moments (the first problem of mechanics), or for modeling the coupled body-liquid dynamics. In the latter case, the modal equations should be analytically coupled with equations of motions of the rigid container [1, 14, 15].

The multi-modal modeling currently represents virtually the most effective tool for studying resonance steady-state liquid sloshing, investigating their stability, internal resonances, chaos as well as the coupling between the rigid body and liquid motions. The derivation and machine learning of such modal systems, adapted for studying *damped* sloshing, is in focus of the present dissertation.

1.3. Appearance of linear and nonlinear multi-modal methods

The word 'multimodal' (modal) originates from the famous paper [3], which was published in 2000. However, historically speaking, the multi-modal method was proposed fifty years earlier, in the 1950s-60s, when researchers

first encountered the lack of knowledge on liquid sloshing and associated hydrodynamic loads in aircraft, spacecraft, and maritime containers. Scientific legacy of the initial steps toward the development of these methods is systematized in [14, 16–21] and [13, 22–30]. At that time, researchers basically focused on the theoretical analysis of linear (small-amplitude) liquid sloshing as well as experimental studies of nonlinear resonant phenomena. Experiments by the USA researchers were best documented in the NASA report [16]. Experiments by Soviet scientists were reported in [15, 24, 31–33].

The linear multi-modal method (see the original works [13, 25, 34–38], and modern studies [1, 39], which describe details of this method) was proposed in the 1950s. The method, when being applied to linear sloshing problem, derives an infinite set of uncoupled linear oscillators (uncoupled linear ordinary differential equations), collectively referred to as the linear modal system, in which inhomogeneous terms are functions of the six generalized coordinates (degrees of freedom) of the rigid body motions, and the unknowns are the hydrodynamic generalized coordinates which, as we already stated, imply perturbation of the free boundary by the natural sloshing modes.

The multi-modal method treats linear liquid sloshing as a linear mechanical system with an infinite number of uncoupled degrees of freedom. It is necessary to know the natural sloshing modes, φ_n, frequencies, σ_n, and the linear Stokes-Joukovskii potentials, $\mathbf{\Omega}_0 = (\Omega_{01}, \Omega_{02}, \Omega_{03})$ defined in the unperturbed liquid domain Q_0. Considering together the linear modal system and dynamic equations of the rigid container, and using the linearized Lukovsky formulas, which express hydrodynamic forces and moments in terms of hydrodynamic generalized coordinates, makes it possible to analyze coupled motions of the mechanical 'body-liquid' system.

In the linear modal system and the Lukovsky formulas, the hydrodynamic coefficients are integrals of $\mathbf{\Omega}_0, \varphi_n$ and their derivatives. This implies that having known $\mathbf{\Omega}_0$ and φ_n and using analytical and/or numerical methods for ordinary differential (modal) equations makes it possible to find a semi-analytical solution to the linear liquid sloshing problem (see, Chapter 5 in [1] and [40–43]), thereby describe the linear coupled dynamics.

The Stokes-Joukovski potentials, Ω_{0i}, $i = 1, 2, 3$, yield the coefficients at inhomogeneous terms of the linear modal equations associated with the three angular degrees of freedom of the rigid tank. They are solutions to the Neumann boundary value problems in the hydrostatic liquid domain Q_0 which were first derived by Nikolay Joukovski (1885) [44] who studied spatial motions of a rigid body with cavities completely filled by an ideal incompressible liquid. Exact analytical expressions for Ω_{0i} are rare exceptions (see, Chapter 5 in [1]).

The natural sloshing modes are eigenfunctions of a special spectral boundary value problem in the unperturbed (hydrostatic) liquid domain Q_0. The spectral parameter κ appears in the boundary condition on the mean free surface Σ_0, and the natural sloshing frequency $\sigma = \sqrt{\kappa g}$ (g is the Earth's gravitational acceleration). The traces $\varphi_n|_{\Sigma_0}$ define the standing wave shapes by the natural sloshing modes. These were first described by Mikhail Ostrogradsky for a vertical circular tank. His work [12] was submitted to the Paris Academy of Sciences in 1826 and subsequently generalized by Poisson [45] for other reservoir shapes.

Rigorous mathematical theory for the spectral problems on natural sloshing modes and frequencies was developed in the 1960s (see, Chapter VI in [13] and [39, 46]). Specifically, the theory states that (i) the spectrum consists solely of positive eigenvalues, κ, with a single accumulation point at infinity (compared to the external wave problem in ocean surfaces, where the spectrum is continuous), and (ii) $\varphi_n|_{\Sigma_0}$ constitute, within to a nonzero constant, a functional basis in $L_2(\Sigma_0)$. The point (i) is crucial for understanding why the Korteweg-de Vries and Boussinesq equations (infinite liquid volume) and modal systems (liquid in a container) arise from the same free-surface boundary value problem yet have different mathematical natures. The point (ii) is the fundamental fact for introducing the hydrodynamic generalized coordinates.

In the 1960s–1970s, Selim Krein [47, 48] (see also [49, 50]) generalized these spectral theorems to the case of viscous incompressible liquids, while Kopachevsky incorporated the surface tension effects (part II in [51] and

[47, 52]). The problem on natural liquid sloshing in elastic reservoirs is of particular interest, with various aspects studied in [22, 25, 26, 30, 53, 54].

In the 1950s–1980s, primary focus has been on deriving the analytical approximate natural sloshing modes and linear Stokes-Joukovski potentials. Owing to a need in satisfying the mass conservation, solutions in [37, 55] were based on the Trefftz method, often utilizing the so-called harmonic polynomials [37]. Completeness of the harmonic polynomials in two-dimensional and three-dimensional domains was proven in [56, 57] for star-shaped liquid volume geometry. The constructed Trefftz solutions are particularly effective and ensuring a uniform convergence when singularities [13, 58–61] near corner points are taken into account [40, 62]. Nowadays, harmonic polynomials are widely employed in computational schemes such as the Harmonic Polynomial Cell (HPC) method [63, 64]. With the advancement of computer capabilities in the 1990s, finding φ_n and $\mathbf{\Omega}_0$ has become much simpler. Exceptions may include non-smooth tanks containing partitions, grids, etc., leading to singular behavior of $\nabla\varphi_n$ [40, 62, 65–68].

1.4. Pioneering analytical mathematical studies on nonlinear liquid sloshing

Historically first studies of nonlinear sloshing were originated in the 1950s by Penny & Price [69], Moiseev [70], Narimanov [71], and Perko [72, 73]. Using the perturbation theory [69], Moiseev [70] constructed an asymptotic steady-state (periodic) solution for the nonlinear liquid sloshing problem in a rigid tank undergoing small-amplitude horizontal and/or angular harmonic motions with the forcing frequency σ close to the lowest natural sloshing frequency σ_1. He considered the case of finite liquid depth in a tank undergoing longitudinal motions and proved that if the non-dimensional forcing amplitude is of order $\epsilon \ll 1$, the lowest natural sloshing mode is excited with amplitude of the order $O(\epsilon^{1/3})$. Necessary condition of the Moiseev's asymptotic scheme is the relation

$$\frac{\sigma^2 - \sigma_1^2}{\sigma_1^2} = O(\epsilon^{2/3}),$$

which formalizes the closeness of the forcing frequency to the lowest natural sloshing frequency, $\sigma \to \sigma_1$. Moiseev's theory implicitly assumes the absence of internal (secondary) resonance [1, 74–77] in this hydrodynamic system.

Moiseev's asymptotic steady-state solution was analytically derived (in an explicit form) for a two-dimensional rectangular tank in [78, 79]. Other tank shapes were considered in [14, 80–82]. Deriving Moiseev's asymptotic solution analytically involves cumbersome calculations due to the need to solve a sequence of boundary-value problems analytically.

In the 1980s, while analyzing quasi-periodic liquid sloshing regimes, Miles [83,84] generalized Moiseev's results and derived the so-called Miles equations which couple slowly varying dominant amplitudes from Moiseev's theory. Miles considered horizontal harmonic tank excitations of a vertical circular cylindrical tank with the forcing frequency close to the lowest natural sloshing frequency. He used Moiseev's asymptotics for σ and σ_1 combining it with separating fast and slow timescales in the Bateman-Luke variational formulation [85–87]. Miles' equations were later derived for upright tanks with rectangular base. Usage of those equations for studying the quasi-periodic resonant sloshing, its stability and classification including for chaos is widely recognized as mainstream [83,84,88] in this applied mathematical field. Both horizontal and vertical (Faraday waves) harmonic excitations were considered [83,88–94]. The papers [95,96] utilized the Miles equations to study the coupled tank-liquid motions with an amplitude-constrained external force.

Using perturbation technique, Narimanov [71] first derived weakly nonlinear modal equations describing the resonant liquid sloshing. Narimanov was unaware of Moiseev's results but postulated an asymptotic relationship between hydrodynamic generalized coordinates and hydrodynamic generalized velocities in the same way as if that follows from the Moiseev periodic solution. The first Narimanov–type modal systems in [71] (similar to those in [97–100]) contained algebraic errors which were later corrected by Lukovsky [15, 101–103]. Narimanov's technique also results in extensive and cumbersome calculations, which significantly increase as the number of introduced hydrodynamic generalized coordinates grows. Consequently, all ex-

isting Narimanov modal systems are of small dimensionality, involving only two to five (out of an infinite number of) hydrodynamic generalized coordinates. Narimanov's modal systems were derived for circular, rectangular, conical, and spherical tanks, as well as for upright circular cylindrical tank with rigid-ring baffles [15, 102–104]. Nowadays, this method is almost unused and has arguably been supplanted by variational versions of the modal method [105–107], which are typically based on the Bateman-Luke–type variational formulation [1, 15, 85–87]. This variational formulation makes it possible to naturally derive both the dynamic and kinetic parts of the boundary-value problem on liquid sloshing [1, 15, 108–110].

1.5. Combining variational and multi-modal methods

The multi-modal method based on the Bateman-Luke–type variational formulation was firstly proposed in 1976 by John Miles and Ivan Lukovsky [102, 111]. They independently derived a nonlinear modal system in terms of generalized coordinates and generalized velocities for liquid sloshing in an upright tank and prescribed oscillatory translational tank motions. Later on, Lukovsky derived a nonlinear modal system, which is now known as the Miles-Lukovsky system. This system allows for arbitrary tank motions [3, 112]. Lukovsky also proposed a nonconformal mapping technique for tanks with non-vertical walls [101, 113–116] and derived the so-called Lukovsky formulas for hydrodynamic force and moment [15, 102] (see, Chapter 7 of [1] where an alternative derivation of these formulas is proposed). He also demonstrated how to use the Bateman-Luke variational formalism to derive the equations of motion for the coupled 'rigid tank-liquid' system [102, 117].

By considering specific asymptotic relations between the hydrodynamic generalized coordinates and generalized velocities, the Miles-Lukovsky modal system can be reduced to a weakly nonlinear form, now known as adaptive nonlinear (asymptotic) modal systems [1, 15, 118–120]. Both the Miles-Lukovsky and adaptive nonlinear modal systems require finding the natural sloshing modes, φ_n, and the nonlinear Stokes-Joukowski potentials, $\mathbf{\Omega}$, in an explicit analytical form. The analytical natural sloshing modes must also

be continuously defined above the hydrostatic free surface Σ_0. This and other limitations of nonlinear modal methods are discussed in more detail in Chapter 7 of the book [1] and in [113, 118, 120].

By expressing the velocity potential via functional series with time-dependent coefficients (generalized velocities) when the functional basis coincides with the set of natural sloshing modes, Perko [72, 73] developed a numerical modal method which used to model short-term transient waves. In the 1970s-1980s, the Perko method (with several modifications) was utilized by Chakhov [121, 122] and Limarchenko with his PhD students [123–125, 125–127] to simulate diverse transient sloshing phenomena associated with spacecraft applications. Specifically, to derive approximate nonlinear modal equations, Limarchenko employed the classical Hamilton-Ostrogradsky variational statement combining this statement with a perturbation technique and a Trefftz projective scheme. The latter was required because the variational formulation of the Hamilton-Ostrogradsky derives from the necessary extrema condition only dynamical boundary condition of the hydrodynamic problem while the kinematic one should be solved by the Trefftz method. As matter of the fact, Limarchenko's approach and simulations are a kind of realising the Perko method but in a weakly-nonlinear, third-order approximation. The Perko and, of course, Limarchenko views on the nonlinear sloshing are unsuitable for analytical studies of steady-state waves. The authors do not pretend conducting these studies but restrict themselves to calculating transient waves on a relatively short time scale.

1.6. Using nonlinear multi-modal systems in analytical studies

In the 2000s, studies on nonlinear liquid sloshing dynamics bifurcated into numerical and analytical branches which possessed their own life and developed almost independently. Achievements in numerical modeling of that time are well outlined in [5] (see also [128–134]). The computational schemes adopt hydrodynamic models of a viscous incompressible liquid. The published nu-

merical results demonstrate rather efficient computations of nonlinear liquid sloshing. Ability to model wave breakings and/or fragmentation of the free surface, overturning, wave impacts on walls, and flip-through phenomena is illustrated in several examples as well. The aforementioned phenomena cannot be accurately described within physical (mathematical) models employed in analytical studies of the liquid sloshing dynamics. These models are, normally, weakly nonlinear, assume an ideal incompressible liquid with potential flows and are restricted to assumptions on smooth and continuous free surfaces.

One should note that similar separation of numerical and analytical approaches have in the 20th century occurred in the ocean waves theory. At the present time, the ocean waves dynamics is studied, almost independently, by either CFD methods applied to the original free-surface boundary problems or employing approximate analytical surface wave models such as the Korteweg-de Vries and Boussinesq equations that are a very special classes of weakly-nonlinear partial differential equations [135]. The latter approximate analytical models are normally not used in engineering computations. Instead, the models appear as the main mathematical apparatus for qualitative analysis and classification of the ocean wave types, their stability, as well as establishing the chaos in hydrodynamic systems. They are also non invertible when the task consists of parametric studies of the solution versus initial scenarios and input parameters.

Because the Perko–type methods belong to direct numerical approaches to the liquid sloshing dynamics, albeit using simplified modal-type mathematical models, it is of limited interest for computing hydrodynamic loads and describing the aforementioned wave phenomena on the free surface, as well as for analytical studies. This explains why the Perko scheme is rarely used in modern studies. Examples are limited to *ad hoc* computations by either the fully nonlinear Miles-Lukovsky systems as it has been done in [136, 137] or weakly-nonlinear modal systems derived and utilized in [126, 138–144]. Another drawback of the Perko method is that the corresponding systems of ordinary differential equations are stiff in computing. To provide stable and

robust computations, at least, on a relatively short time scale, the adopted systems of ordinary differential equations require incorporating an artificial damping which suppresses spurious higher harmonics [138, 139]. Otherwise, because of amplification of, generally, infinite set of higher harmonics, the time-step integration becomes unstable over relatively long time intervals.

In view of the required damping in the modal systems, using the Perko–type methods for computations makes sense when containers are equipped with slosh-suppressed devices which cause/yield a huge damping in the hydrodynamic system. This makes, physically, the adopted modal systems non-stiff. Examples are tanks with perforated screens [142–144].

An intense usage of the nonlinear modal method as an effective tool for analytical studies has been, to some extent, associated with a growing practical interest to clean (without internal structures that have sharp edges) containers, including those carrying Liquefied Natural Gas (LNG). This happened in the 90's that motivated many researchers returning to ideas of the nonlinear modal method. In 2000 [3], this has been done by Faltinsen, Rognebakke, Lukovsky, and Timokha who revisited the Bateman-Luke–type variational formalism to derivation of nonlinear modal equations and demonstrated all the needed details on how the multi-modal modeling can explain stable asn unstable steady-state resonant wave regimes and simulate transients for the simplest possible case – the case of a rigid rectangular tank. Their studies initiated a new series of publications on nonlinear modal systems, mainly for rectangular and circular tanks, where exact analytical φ_n and $\mathbf{\Omega_0}$ can be constructed, and the liquid depth is finite.

Two-dimensional nonlinear resonant liquid sloshing in a *smooth rectangular tank* with a *finite liquid depth* were studied in [3, 75, 118, 145–149] by using various nonlinear modal systems. The resonance excitations of the tank were assumed being of small amplitude, of the asymptotic order $O(\epsilon) \ll 1$, and the excitation frequency σ close to the lowest natural sloshing frequency σ_1. The legendary weakly-nonlinear modal system that describes the resonantly-excited sloshing [3] utilises the Miles-Lukovsky equations and, by applying the Narimanov-Moiseev asymptotics to them, transforms the problem

to three coupled ordinary differential equations with respect to the generalized hydrodynamic coordinates responsible for amplification of the three lowest natural sloshing modes. Transient and steady-state wave regimes were successfully described for both prescribed harmonic oscillations [3] and for coupled motions (floating tank on the sea surface [150–152]).

The steady-state resonant liquid sloshing in two-dimensional rectangular container is then characterized by the soft-spring type response curves if the depth-to-the -tank-width ratio $> 0.3368\ldots$, and the character changes to the hard-spring type behavior as $< 0.3368\ldots$ [1, 153]. Mathematical analysis of the single-dominant nonlinear multimodal system is reported in [118, 145, 146].

The single-dominant nonlinear modal system [3] becomes physically inapplicable with increasing excitation amplitude, at the critical liquid depth $h = 0.3368...$, and when the mean liquid depth tends to zero (shallow liquid depth limit). This failure is a consequence of secondary (internal) resonances in the hydrodynamic system. These resonances occur when $n\sigma \approx \sigma_n$ for some integer n where σ is the forcing frequency and σ_n is the nth natural sloshing frequency. The secondary resonances lead to an increase in amplitude of the nth natural sloshing mode through a nonlinear energy transfer from the primary (σ_1) to secondary (σ_n) excited natural sloshing modes. To account for secondary resonance of the nearly steady-state resonant sloshing in a rectangular tank with a finite liquid depth when the lowest natural sloshing mode is excited, the so-called adaptive modal systems should be derived [75, 146]. The concept of the adaptive multi-modal modeling suggests introducing several (non-single) dominant hydrodynamic generalized coordinates (natural sloshing modes) which are secondarily resonance excited and possess the lowest asymptotic order $O(\epsilon^{1/3})$. These extra dominant natural sloshing modes are normally associated with the higher harmonics $n\sigma \approx \sigma_n$ in the nearly steady-state wave response. The adaptive multimodal method was validated by comparison with experimental measurements [75, 76, 139]. When the secondary resonances matter, the corresponding steady-state wave amplitude response curves are characterized by extra peaks in the primary

resonance region. More details for adaptive multi-modal systems and their structure can be found in Chapter 8 of the book [1].

Employing the adaptive multi-modal modeling, Hermann & Timokha [146] demonstrated that the critical liquid depth is a function of the excitation amplitude (with the limiting case as $\epsilon \to 0$ being $0.3368\ldots$) and explained discrepancy between its theoretical prediction and the measured value 0.28 observed in the classical experimental work [154]. Adaptive multi-modal systems [147–149] also exploit lower-order asymptotics of the secondary-excited generalized hydrodynamic coordinates.

Deriving the nonlinear multi-modal system [76] for resonant liquid sloshing in a rectangular tank with small (shallow or intermediate) liquid depth requires the fourth-order asymptotic ordering of the Boussinesq type. Formally, the Boussinesq–type asymptotics is a consequence of combining those by Moiseev and Korteweg-de Vries [79,155,156]. All the hydrodynamic generalized coordinates and the dimensionless liquid depth in the Boussinesq–type modal equations are of the same asymptotic order $O(\epsilon^{1/4})$. The corresponding nonlinear modal equations contain only the fourth-order polynomial nonlinearities. The system is formally infinite-dimensional. After truncating the infinite-dimensional system of ordinary differential equations and incorporating linear damping terms with damping coefficients associated with laminar viscous boundary layer on the mean wetted tank surface (as in Chapter 6 of [1] and [157–161]), one can numerically find steady-state (periodic) stable resonant waves as well as simulate transient sloshing. Following this way provides a good agreement with experimental measurements from [76,162,163]. As for the steady-state wave experimental response curves by Chester [76,162–164], theoretical amplitude-frequency curves confirmed a 'finger-like' shape with multiple peaks in the primary resonance zone (where $\sigma \approx \sigma_1$). Increasing the excitation amplitude and/or decreasing the liquid depth (passage to shallow water) renders the Boussinesq–type nonlinear modal system physically inapplicable [76] due to invertible wave breaking, overturning, and fragmentation of the free surface, and other phenomena which make the constructed fourth-order asymptotic theory disputable. Reasons are that the free-surface

representation suggests be smooth and the aforementioned phenomena cause significant viscous damping. A detailed classification of nonlinear resonant sloshing for shallow water with an emphasis on local surface phenomena is provided in Chapter 8 of [1]. It prescribes four different wave types.

Damping of nonlinear resonant liquid sloshing in a clean rectangular tank is difficult to model with linear damping terms associated with logarithmic decrement of the corresponding natural sloshing mode, especially, when damping mechanism is not continuous. Examples are free-surface fragmentation due to breaking waves or, e.g., ceiling impact, whose effect can be incorporated into nonlinear modal systems [3, 75] by employing Wagner's theory [165]. In the latter case, the damping rate is a non-continuous function of the time.

Further, the viscous damping can be caused by a viscous turbulent layer during liquid flow through porous screens, i.e., when the tank is not clean and contains internal sharp structures. How to account for damping in screen-equipped containers is shown in [138, 142, 166, 167]. The screen is setup in the middle and may be characterised by different screen porosity ratio. For smaller screen porosity ratios, $0 < S_n < 0.5$, and relatively small excitation amplitudes, using the pressure drop condition across the screen [168], integral terms were derived to be incorporated in nonlinear modal systems [142, 166] to account for the viscous damping effect. The modified nonlinear modal systems demonstrated results that were both quantitatively and qualitatively consistent with experimental data. For higher porosity ratios, $0.5 < S_n < 1$, the screen sufficiently changes the natural sloshing modes and frequencies [65] that modifies analytical structure of linear [167] and nonlinear [138] modal systems. Secondary resonances become then more pronounced, and the amplitude-frequency response curve peaks in the primary resonance region differ from those observed in a clean rectangular tank. Nonlinear modal systems for tanks with porous screens have been derived, studied, and validated in [142–144, 169, 170].

Generalizations of the two-dimensional flow results on single-dominant modeling [3] to the case of a three-dimensional resonant sloshing in upright

tanks with a rectangular base are reported in [171]. The primary focus is on a nearly square cross-section which results in a situation where the two lowest oscillation modes have equal natural sloshing frequencies. The corresponding nonlinear modal system of the Narimanov-Moiseev–type was derived in [171,172]. It has nine degrees of freedom and couples two dominant, $O(\epsilon^{1/3})$, hydrodynamic generalized coordinates which correspond to the lowest natural sloshing frequency. This asymptotic nonlinear modal system effectively provides an analytical classification of steady-state wave regimes (planar, diagonal, nearly diagonal, and circular waves) for longitudinal and diagonal harmonic excitations of the tank [171,173] and, later on, for arbitrary periodic resonant tank motions [174]. The classification was made by constructing analytical periodic solutions of the nonlinear Narimanov-Moiseev–type modal system. The solutions depend on four lowest-order amplitude parameters whose analysis makes it possible to compute and draw steady-state wave amplitude response curves, particularly when the aspect ratio of the tank dimensions is perturbed near unity [172,175,176]. A good qualitative agreement with experiments was shown, including estimates of frequency ranges where chaotic waves occur. On the other hand, theoretical transient and steady-state waves were not quantitatively supported by experiments due to the secondary resonance effect, which becomes especially pronounced for swirling, even at sufficiently small excitation amplitudes. Including the secondary resonance effect led to adaptive modal systems [139,177].

1.7. Nonlinear multi-modal reduced order models of resonant sloshing in upright axisymmetric tanks

In the 1980s, Lukovsky [102,117,178] derived a finite-dimensional nonlinear asymptotic modal system of the Narimanov-Moiseev–type, which couples five hydrodynamic generalized coordinates. This system describes resonant liquid sloshing in an upright circular cylindrical tank exposed to longitudinal harmonic excitations with the forcing frequency close to the lowest natural sloshing frequency. He also constructed analytical asymptotic periodic

solutions of this system to demonstrate occurrence of planar and swirling steady-state waves, analysed their stability by using the linear (first) Lyapunov method, as well as validated these semi-analytical results by comparing them with experimental data [179]. In [180], this nonlinear asymptotic modal system has been re-derived to classify steady-state wave regimes (as in [15, 117]) but the steady-state analysis was mainly based on numerical approaches.

The Lukovsky five-dimensional weakly-nonlinear modal system [15, 102] and its periodic solutions were in focus of [181] whose authors analyzed the behavior of nodal curves on the liquid surface for transient and steady-state resonant waves. These visualizations showed that the nodal curves are far from straight lines as wrongly claimed in other (simpler) theories. This is due to significant contribution of higher-order natural sloshing modes. Existing experimental observation qualitatively confirmed that behavior of the nodal curves as they are predicted by Lukovsky's theory. Faltinsen & Timokha [1] (Chapter 9) in their fundamental textbook revisited analytical studies of steady-state resonant sloshing in an upright circular base tank by exploiting the Lukovsky modal system and compared these theoretical results with experimental findings presented in [10].

Even though Lukovsky restricted his analysis to five degrees of freedom, the Narimanov-Moiseev asymptotics for axisymmetric tanks requires, generally, accounting for an infinite number of second- and third-order hydrodynamic generalized coordinates when deriving the corresponding nonlinear asymptotic modal systems [113, 120]. For a vertical circular cylindrical tank, an infinite-dimensional modal system of the Narimanov-Moiseev–type was first derived and analyzed in [119]. The infinite number of second- and third-order hydrodynamic generalized coordinates had little effect on Lukovsky's qualitative results regarding periodic steady solutions (waves), except for certain liquid depths and frequencies where secondary (internal) resonances occurred in the infinite-dimensional system as predicted in [7, 74, 104].

As we stated above, Lukovsky also analytically derived and analyzed periodic solutions of the five-dimensional nonlinear modal system [102, 182, 183]

which correspond to resonant steady-state sloshing in a vertical annular cylindrical tank when the excitation frequency is close to the lowest natural sloshing frequency. In [184], his modal system was re-derived and modified by including additional third-order hydrodynamic generalized coordinates (degrees of freedom). The latter paper also reports experimental studies on resonant sloshing due to longitudinal tank excitations. Comparing the experimental and theoretical steady-state wave amplitude response curves [184] demonstrated good agreement for the planar standing wave mode, but, even with the inclusion of speculative additional terms (for alignment with experimental baseline data), a visual discrepancy between theory and experiments for the circular wave was apparent. An attempt to derive a nonlinear modal system of the Narimanov-Moiseev–type for an off-center column position was made in [185]. Liquid sloshing a vertical annular tank with transverse partitions were studied in [186, 187].

For tanks with non-vertical walls, to the author best knowledge, exact analytically-presented natural sloshing modes do not exist in the literature, and, furthermore, a normal (single-valued) presentation of the free surface becomes impossible. These two problems on the analytical natural sloshing modes and free-surface presentation, can be solved by employing the so-called non-conformal mapping technique proposed in 1975 by Lukovsky [101, 103, 188, 189]. This analytical technique was combined in [101, 103] with Narimanov's third-order perturbation scheme. The results are low-dimensional weakly-nonlinear (modal) systems of ordinary differential equations with respect to the generalised hydrodynamamic coordinates to describe resonant sloshing. This combined approach has also been utilised in the manner of the Perko method by Limarchenko [126, 127, 141] to simulate transient waves. Finally, the non-conformal mapping technique has been adopted in the variational method by Miles-Lukovsky [15, 102, 113]. This made it possible to derive the Miles-Lukovsky infinite-dimensional nonlinear modal system for tanks with non-vertical walls as well as diverse weakly-nonlinear nodal equations.

The multidimensional nonlinear modal systems of the Narimanov-

Moiseev–type have been derived for conical and spherical containers. Using these systems facilitated studies of resonant sloshing in these containers caused by excitations of the lowest natural sloshing frequency [113,114]. The main difficulty in implementation of the non-conformal mapping technique to other tank shapes remains the absence of an effective and highly accurate analytical approximation of the natural sloshing modes such that the approximate natural sloshing modes accurately satisfy the Laplace equation and zero Neuman condition on the tank walls for any admissible instant shape of the liquid domain. The approximate natural sloshing modes should also allow for analytical continuation across the free surface. There are other limitations of the nonlinear modal method for tanks with non-vertical walls that are described in [15,120] and Chapter 9 of the book [1].

According to the results in [80,190,191], the unperturbed flat (horizontal) static free surface in a circular conical tank with a small opening angle can be replaced by a spherical 'cap', in order to construct an analytical solution to the spectral boundary problem on natural sloshing modes and frequencies in terms of spherical functions. Using such approximations of the natural sloshing modes, a nonlinear modal system of the Narimanov-Moiseev–type was constructed in [192, 193]. This result was improved and generalised in [102, 114, 194–198] (see also references therein).

In [194, 196, 197], approximate natural sloshing modes were constructed without the aforementioned replacement of the unperturbed free surface. Based on these natural sloshing modes, a five-dimensional nonlinear modal system of the Narimanov-Moiseev type was derived and investigated for truncated and non-truncated circular V-conical tanks [114, 196]. In contrast to Lukovsky' modal system for circular cylindrical tank [102, 117, 178], these Narimanov-Moiseev–type equations contain additional nonlinear terms that reflect the so-called geometric nonlinearity (non-verticality of the tank walls). In the work [199], attention is paid to the behavior of nodal lines on the oscillating free surface which looks rather similar to those observed in [181]. The theoretical analysis of secondary resonances [114, 196] and the comparison of the theoretical results with experiments [114, 195, 200] showed that the

secondary resonances indeed play significant role for conical reservoirs.

Analytical approximations of the natural sloshing modes for the spherical tank were constructed in [66, 67, 201, 202]. Based on the constructed analytical approximate solutions from [66, 202], an infinite-dimensional nonlinear modal system of the Narimanov-Moiseev–type (generalization of [119]) was explicitly derived in [113,203]. The results of studying periodic (steady-state) resonant waves by using this modal system were validated by experiments from [19] for the depth-to-radius ratios ≤ 0.5. Secondary resonances and experimentally observed fragmentation of the free surface (along with overturning waves) make this weakly-nonlinear modal system practically unsuitable for higher liquid depths and when the excitation amplitude increases.

An infinite-dimensional nonlinear modal system of the Narimanov-Moiseev–type was constructed but not analyzed for the two-dimensional circular tank in [204]. This case exhibits secondary resonance for almost all fill levels of the tank [31, 40] and makes [204] weakly applicable.

1.8. Challenges of the nonlinear reduced order modeling in nonlinear sloshing analysis

There are several challenges in the field of analytical studies of the nonlinear liquid sloshing dynamics, in general, and for the nonlinear multi-modal modeling, in particular, as a kind of the Reduced Order Modeling in the nonlinear hydrodynamics. Most of them are discussed in [2]. Whilst extensive ideas and works mainly concern generalization and extension of the multi-modal method to new, practically important liquid sloshing problems (see, for example, Chapter 1 [1] and [15,205]), intensive efforts focus on improving the multi-modal method and weakly-nonlinear modal systems (from both physical and mathematical perspectives), as well as a thorough mathematical work uniquely presented in [118, 145, 146], dealing with modal systems from [3, 75].

A class of generalizations of the nonlinear multi-modal modeling is associated with derivations of the corresponding modal systems and their analysis

for tanks of complex geometric shapes. This implies constructing an appropriate set of analytical approximate natural liquid sloshing modes of special types and improving the tensor algebra of curvilinear coordinates adopted in the non-conformal mapping technique by Lukovsky [15]. Finally, since deriving weakly nonlinear modal systems for complex tank shapes is particularly cumbersome, a task may consist of writing a computer algebra code that enables derivation based on computer calculations, as was done for the vertical circular cylindrical tank in [206].

The multi-modal modeling, both linear and nonlinear, is based on the hydrodynamic model of an ideal incompressible liquid with irrotational lows. This implies, in particular, that viscous damping is neglected. In this context, it is also worth noting the reviews in Chapter 6 of the book by Faltinsen & Timokha [1]. They give an overview of analytical methods and approaches that allow for estimating the energy dissipation in the sloshing problem with a focus on the linear sloshing as well as demonstrate how the associated viscous damping effect can be incorporated into the linear modal theories. Chapter 6 of [1] explains how to account for damping in nonlinear modal systems due to flow separation at sharp edges of the immersed structures. The corresponding procedure was realized for rectangular tanks containing porous screens [138, 142, 167].

Caused by modal modeling of resonant sloshing in bioreactors, a series of experimental and theoretical studies in the physical domain have been conducted for sloshing in a clean upright circular container which moves translatory in the horizontal plane along an elliptic trajectory. Experimental studies are mainly associated with PhD Thesis by Reclari [207] and research papers [9, 208–212]. Specifically, resonant sloshing in clean bioreactors is characterized by non-negligible viscous damping. Furthermore, the main type of the stable steady-state sloshing is swirling due to the circular orbital resonant forcing. The first step towards analyzing the associated waves has been made in [7]. Its authors did not account for damping. How to introduce linear damping into the corresponding modal systems from [7], construct and study the analytical steady-state wave motions (periodic solutions of

systems, study stability), and analyze the types of surface waves depending on the trajectory of tank motion (including circular orbital) has been the goal in [9, 212]. The results summarized in the book [4]. Two important conclusions are the following. Firstly, the viscous damping plays crucial role in explaining why the counter-directed swirling does not exists for the circular orbital excitations, even though it should occur and be stable within the framework of the inviscid theory [7]. Secondly, taking the linear damping prediction and incorporating it into the nonlinear modal models is not able to provide a consistency with experiments for swirling wave mode.

Analogously, the linear damping terms inserted into the single Narimanov-Moiseev–type modal system [3] failed to correctly describe resonant sloshing in rectangular tank. The latter was shown in [11] where one can find new experimental measurements including for the phase-shift between the harmonic longitudinal tank excitations.

The latter two cases, with resonant sloshing in a rectangular clean tank and resonant swirling in an upright circular base tank, showed that viscous damping in the nonlinear multimodal modelling is strongly nonlinear and can, physically, be affected by various factors. e.g., fragmentation of the free surface and dynamic contact angle [213, 214]. A way to account for these factors consists of developing the machine learning technique. It is originated in the present dissertation.

1.9. Concept and structure of the present dissertation work

The forthcoming main text of the PhD Thesis is separated into three chapter. The next chapter introduces elements of general mathematical theory of the liquid sloshing dynamics. This theory consists of differential, variational and modal formulations. An ideal incompressible liquid with irrotational flows is considered. The chapter presents the corresponding free-surface problem with respect to the velocity potential and a function which describes, implicitly, instant free-surface shape. The Luke-Bateman varia-

tional formulation whose action is a function of the velocity potential and the aforementioned function on the free surface is given. The necessary extrema condition of the action, as the theorem proves derives the governing equation and all the boundary conditions of the free-surface boundary problem.

In order to replace the differential and variational formulation by a system of ordinary differential equations, the Reduced Order Modeling scheme is adopted by employing a projective Galerkin–type scheme. For this purpose, both the free surface and velocity potential are presented in the form of functional series with time-dependent coefficients, $\beta_i(t)$ and $R_n(t)$. These are treated as the generalised hydrodynamic coordinates and velocities, respectively. The necessary extrema condition of the Luke-Bateman action leads then to the desired system of ordinary differential equations coupling $\beta_i(t)$ and $R_n(t)$. The system consists of kinematic and dynamic parts where the second part can be interpreted as a kind of Euler-Lagrange equations. In the most general form, the derived system appears as the so-called Miles-Lukovsky nonlinear modal system (equations). The system is infinite-dimensional and is fully equivalent to the original differential boundary value problem with free (unknown) boundary.

A physically important particular case of the Miles-Lukovsky modal equation is when liquid sloshing can effectively described in the linear approximation. In that case, adopting the natural sloshing modes (standing waves occurring on the free surface in the rest container) in the functional representations of the free surface and velocity potential yields a system of uncoupled linear oscillators whose right-hand side is a function of the six generalised coordinates for the rigid body (tank) motions. Specifically, the linear equations do not include damping terms since the original statement neglects the viscous phenomena. However, the linear damping terms can be incorporated into the linear modal sloshing theory and one can even estimate the damping rates assuming these are mainly associated with laminar boundary layer effect and bulk viscous damping. The chapter exemplifies that fact and even writes down Keulegan–type prediction for the damping rates when the tank

has rectangular shape. This prediction of the damping rates is however too rough and may even become wrong for resonant sloshing. A reason is that the resonant waves cause nonlinear energy transfer from primary excited to higher natural sloshing modes (generalized hydrodynamic coordinates) and, moreover, the damping terms in the modal equations should then be of nonlinear structure. The next two chapters, 3 and 4, demonstrate how to restore the nonlinear damping terms in nonlinear modal equations for the two cases: resonant sloshing in two-dimensional rectangular tank and upright circular cylindrical tank when the tanks are excited longitudinally with the forcing frequency close to the lowest natural sloshing frequency. The restoring procedure is based on the machine learning technique applied to the so-called Narimanov-Moisev asymptotic reduced order modal equations. Choosing these tank shapes is due to requirement in the measured data on the phase-lag between harmonic forcing and resonant wave response in the machine learning procedures. Unfortunately, those data exist in the literature only for these tanks [10, 11].

Chapter 3 focuses on the case of two-dimensional resonant sloshing in a rectangular tank and is based on a machine learning approach developed by the author in [215, 216]. It starts with deriving the asymptotic single-dominant multi-modal system of the Narimanov-Moiseev–type by following [3] but in a non-dimensional statement where the characteristic dimension is the tank width but the characteristic time is associated with the highest natural sloshing period. The forcing period of the horizontal tank motion suggests being close to the latter highest period. The single-dominant modal system is further equipped with the nonlinear damping terms whose structure should be consistent with the Moiseev asymptotic ordering in derivations [3]. This proves the first main theorem of the Chapter 3. Furthermore, an asymptotic periodic solution of the damping-equipped modal equations is constructed. The secular (necessary solvability) condition links the dominant resonance wave amplitude, phase-lag between the harmonic forcing and the wave response, as well as the non-dimensional forcing frequency. This analytical results expresses the second main theorem of this chapter. Employing

the experimental data from [11] to learn the damping terms of the single-dominant modal equations demonstrates almost perfect agreement with the nature while [11] was not able to say that because they neglected the damping nonlinearity.

Chapter 4 deals with resonant sloshing in an upright circular base tank when the forcing amplitude is small but the forcing frequency is close to the lowest natural sloshing frequency. The Reduced Order Narimanov-Moiseev–type modal equations from [4] are re-derived. In the linear case, the modal equations can be equipped with linear damping terms reflecting the viscous laminar flows at the wetted tank surface and the viscous bulk damping. This is similar to the rectangular tank geometry. However, the estimated damping rates were not able to get a consistency with experimental data on the phase-lag measured in [10] for the swirling–type resonant steady-state sloshing regime. This fact was extensively discussed in [4] who conducted speculative investigations by trying to fit the measurements with varying the damping coefficients. Situation appeared similar to the discussed in the Chapter 3 for rectangular tank shape.

Following the research approach from the Chapter 3, the Narimanov-Moissev–type asymptotic modal equations for sloshing in an upright circular base tank are equipped with appropriate nonlinear damping terms. Procedure of finding an asymptotic periodic solution of the modal equations with linear damping from [4] is generalized the considered case. The result is formulated as Theorem 4.1 which is the main result of the present chapter. The constructed asymptotic solution may effectively draw the response curves within analytical way and, thereby, provides a base for the machine learning procedure which makes it possible to restore the damping terms. The measurements from [10] are collected to learn. Rather satisfactory agreement is reported in the contrast to speculative manipulations with the dominant linear damping coefficient in [4].

The Chapter 5 lists the main conclusions to the dissertation work.

Chapter 2

Differential, variational, and modal formulations of the problem

2.1. Introduction

Throughout the present dissertation, we consider the liquid sloshing dynamics in a mobile rigid container which moves periodically with, generally speaking, six degrees of freedom as shown in Fig. 4.1. The oscillatory tank motions are prescribed and of small amplitude relative to the inner tank dimension (normally, it is the characteristic linear size of the hydrostatic free surface). Whereas the tank motions are assumed be known input parameters, the task consists of getting the hydrodynamic characteristics of the liquid sloshing. This includes the velocity field, pressure and associated hydrodynamic loads (hydrodynamic force and moment) on the wetted tank surface. This means that we solve the so-called *first problem of the dynamics*.

Specifically, the liquid sloshing dynamics is described in the non-inertial coordinate system $Oxyz$ which is rigidly fixed with the moving (oscillating) container. As usually in the literature, the Oxy plane is assumed coinciding with the unperturbed (mean, hydrostatic) free surface of the contained liquid. The hybrid rigid tank-liquid mechanical system or, alternatively, the coordinate system moves in the gravitational field whose potential written in the $Oxyz$ tank-fixed system takes the form

$$U_g = -\boldsymbol{g} \cdot \boldsymbol{r}' = -\boldsymbol{g} \cdot \boldsymbol{r} - \boldsymbol{g} \cdot \boldsymbol{r}'_{\mathbf{0}}, \tag{2.1}$$

where $\boldsymbol{g}$ is the gravity acceleration vector, $\boldsymbol{r} = (x, y, z)$ is the radius-vector relative to O, and $\boldsymbol{r}'_O$ is the radius-vector of the origin O relative to the origin O' of an inertial coordinate system $O'x'y'z'$.

The liquid domain does not contain gas cavities and surface tension can be neglected due to relatively large tank size causing the Bond number exceeding 100 (see, [1], chapter 2). The forthcoming mathematical analysis also assumes that the contained liquid is ideal, incompressible and the liquid flows are irrotational (there is a velocity potential). The viscous laminar boundary layer on the wetted tank surface, which is not zero in reality, is of rather small thickness, that is, its value is much smaller than the tank dimension. This justifies the above assumption on ideal liquid with irrotational flows, i.e., the thin viscous boundary layer and associated rotational (vortex) flows are then located only in the vicinity of the tank surface and do not affect the dominant liquid flow component.

Neglecting the viscous boundary layer does not imply that one can fully neglect the viscous damping in the hydrodynamic system including that caused by this viscous boundary layer. This only means that viscous flows are of local character, e.g., these are localized in a think layer at the wetted tank surface and do not affect, globally, the liquid sloshing. This fact is confirmed by experiments, at least, for qualitative analysis of the hydrodynamic response. However, non-zero damping in the hydrodynamic system plays significant role for prediction of the phase lag between the forcing and response signals, as well as for swirling waves when the damping prevents counter-directed wave propagation due to the orbital tank excitations [4, 174]. The latter implies that the adopted governing equations for the liquid sloshing dynamics within the framework of our assumptions (ideal incompressible liquid with irrotational flows) should on a certain stage be modified to include the damping effect, at least, caused by the laminar viscous layer.

When considering unmovable container, viscous damping in the hydrodynamic system can physically be associated with logarithmic decrement of standing waves occurring due to initial free-surface disturbances. In that case, liquid sloshing is linear so that the free-surface motions and associated viscous damping are simply a decomposition by the standing waves (natural sloshing modes). The energy dissipation of each natural sloshing mode is then mainly caused by the viscous boundary layer on the *mean* wetted tank

surface. Other physical factors may matter but play a secondary role for relatively large containers.

Contrary, resonant liquid sloshing is a strongly nonlinear wave phenomenon and, as consequence, there appears a nonlinear energy flow from primary excited to higher natural sloshing modes which can, under certain circumstances, be interpreted as a kind of the energy dissipation. This fact is extensively discussed in [139]. Examples of other physical factors which could affect energy dissipation for nonlinear resonant sloshing are viscous boundary layer at the *dynamically changing* wetted tank surface, bulk damping, free-surface contamination, and wave breaking.

A correct and accurate account for *all physical factors of the viscous damping for resonant liquid sloshing is the main goal* of the present dissertation studies. The problem will be solved by a machine learning technique applied not to the original free-surface boundary problem which, as we already stated, neglects viscosity, but to a reduced-order discrete mathematical model derived from the inviscid mathematical formulation. The mathematical model will appear as the co-called nonlinear modal system of ordinary differential equations with respect to the generalized hydrodynamic coordinates responsible for perturbations of the natural sloshing modes.

The first step towards getting the reduced-order nonlinear modal system consists of utilizing the Bateman-Luke–type variational principle for the considered free-surface boundary problem. This variational principle is formulated with respect to the two unknowns, which are associated with the instant free surface pattern and velocity potential defined in the time-changing liquid domain, respectively. When these two functions are expanded into functional series by the natural sloshing modes with time-dependent coefficients $\beta_i(t)$ and velocities $R_n(t)$, respectively, one can interpret these coefficients as generalized hydrodynamic coordinates and velocities of the hydrodynamic system.

The necessary extrema condition by $\beta_i(t)$ and $R_n(t)$ of the Bateman-Luke–type action leads to a (modal) system of ordinary differential equations with respect to the generalised hydrodynamic coordinates and velocities. Un-

der certain circumstances, the modal system is mathematically equivalent to the original free-surface problem. It is a sort of the Euler-Lagrange equations.

In their linear approximation, the nonlinear coupling in the modal equations disappears and we arrive at an infinite set of linear uncoupled oscillators by $\beta_i(t)$. Incorporating appropriate linear damping terms into each uncoupled linear equation with respect to $\beta_i(t)$ implies accounting for logarithmic decrement of the corresponding standing wave (natural sloshing modes). The corresponding damping rates can then be estimated by using Keulegan's approach [158] described in details in Chapter 6 of [1].

Transition from the original free-surface boundary value problem to the infinite-dimensional nonlinear modal equations with respect to the generalized hydrodynamic coordinates and velocities will be described in the present chapter. We will also discuss the aforementioned linear case and outline formulas for the Keulegan's damping rates.

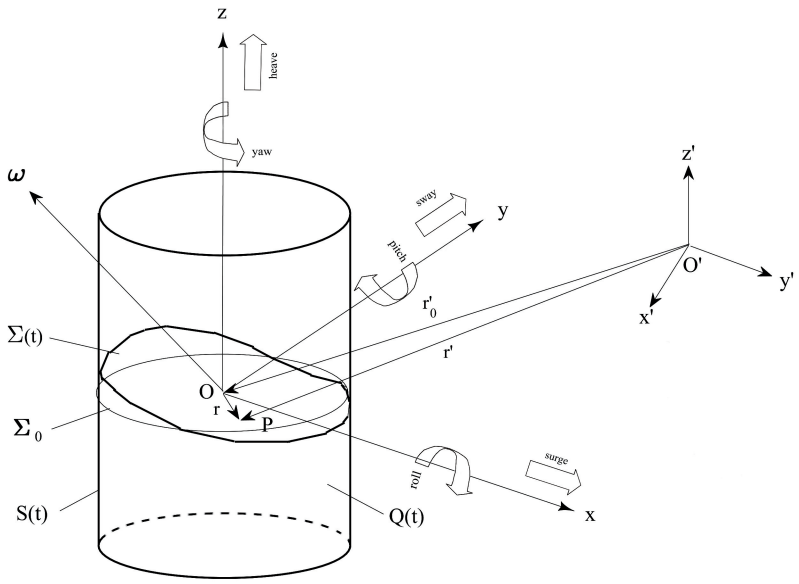

Figure 2.1. Sketch of a moving rigid tank partially filled with a liquid. The non-inertial $Oxyz$ coordinate system is rigidly fixed with the tank. The $O'x'y'z'$ coordinate system is an artificial inertial coordinate one which is normally associated with the earth. Prescribed motions of the rigid tank (coordinate system $Oxyz$) are governed by the translatory velocity vector $\boldsymbol{v}_O = d\boldsymbol{r}'_O/dt = \dot{\boldsymbol{r}}'_O$ of the origin O and the instantaneous angular velocity $\boldsymbol{\omega}(t)$.

2.2. Free-surface boundary value problem

Let $Q(t)$ denote the liquid domain, $\Sigma(t)$ is the free surface, and $S(t)$ is the wetted tank surface. The unperturbed (hydrostatic) liquid domain is denoted as Q_0, the static (unperturbed) free surface is Σ_0, and the mean wetted tank surface is denoted as S_0.

2.2.1. Governing hydrodynamic equations. Because liquid motions are considered in the body-fixed movable, non-inertial coordinate system $Oxyz$, the first task consists of writing down the governing hydrodynamic equations of an ideal incompressible liquid with irrotational flows in this non-inertial coordinate system.

The absolute velocity field in $Q(t)$ is described by the velocity potential

$$\boldsymbol{v} = \nabla\Phi(x, y, z, t),$$

which satisfies the Laplace equation as a consequence of the continuity (mass conservation), $\nabla \cdot \boldsymbol{v} = 0$ [1], whereas the pressure in the time-varied liquid domain $Q(t)$ can be computed using the Bernoulli equation [1]. Because the Laplace equation expresses the mass conservation, it remains invariant in any Cartesian coordinate system, inertial or non-inertial), therefore,

$$\nabla^2\Phi = \Delta\Phi \equiv \frac{\partial^2\Phi}{\partial x^2} + \frac{\partial^2\Phi}{\partial y^2} + \frac{\partial^2\Phi}{\partial z^2} = 0 \quad \text{in } Q(t) \tag{2.2}$$

but the Bernoulli equation is invariant only in inertial coordinate systems.

The Bernoulli equation takes the form

$$p + \rho\left(\left.\frac{\partial\Phi}{\partial t}\right|_{\text{inertial}} + \frac{1}{2}(\boldsymbol{v})^2 + U_g\right) = C(t), \tag{2.3}$$

where $C(t)$ is an arbitrary time-dependent function. The Bernoulli equation is a result of integrating Euler equation that became possible for irrotational flows. To express the Bernoulli equation in the non-inertial coordinate system $Oxyz$, we need to modify the quantity $\partial\Phi/\partial t$, which denotes in the inertial system the time derivative of Φ at fixed points with coordinates (x', y', z').

In the $Oxyz$ coordinate system, we also operate with the time derivative of Φ at fixed points (x, y, z), meaning

$$\left.\frac{\partial \Phi}{\partial t}\right|_{\text{in non-inertial } Oxyz} = \lim_{\Delta t \to 0} \frac{\Phi(x, y, z, t + \Delta t) - \Phi(x, y, z, t)}{\Delta t}.$$

Assume that the point (x, y, z) coincides with point (x', y', z') at the time t and consider the difference between (x, y, z) and (x', y', z') at $t + \Delta t$, up to nonlinear terms. It is equal to $\boldsymbol{v}_b\, \Delta t$, where, according to the Euler formula for rigid bodies,

$$\boldsymbol{v}_b = \boldsymbol{v}_O + \boldsymbol{\omega} \times \boldsymbol{r} \tag{2.4}$$

is the velocity of the rigid body point defined by the radius vector $\boldsymbol{r} = (x, y, t)$, $\boldsymbol{v}_O$ is the velocity of the origin O, and $\boldsymbol{\omega}$ is the instantaneous angular velocity of the rigid body around O. The Taylor series expansion of $\Phi(x, y, z, t + \Delta t)$ in the vicinity of (x', y', z') derives

$$\begin{aligned}\left.\frac{\partial \Phi}{\partial t}\right|_{\text{in non-inertial } Oxyz} &= \\ &= \lim_{\delta t \to 0} \frac{\Phi(x', y', z', t + \Delta t) + \boldsymbol{v_b} \cdot \nabla \Phi \Delta t - \Phi(x, y, z, t)}{\Delta t} \\ &= \left.\frac{\partial \Phi}{\partial t}\right|_{\text{in inertial } O'x'y'z'} + \boldsymbol{v}_b \cdot \nabla \Phi \end{aligned} \tag{2.5}$$

and, therefore, the Bernoulli equation (2.3) in the non-inertial system $Oxyz$ can be written down as

$$p + \rho\left(\left.\frac{\partial \Phi}{\partial t}\right|_{\text{non-inertial}} - (\boldsymbol{v}_O + \boldsymbol{\omega} \times \boldsymbol{r}) \cdot \nabla \Phi + \frac{1}{2}(\nabla \Phi)^2 + U_g\right) = C(t), \tag{2.6}$$

where, as usually, $C(t)$ is an arbitrary function of time, ρ is the liquid density, U_g is defined by (2.1), and p is the liquid pressure.

The gravity potential U_g was defined in (2.1) as $U_g = -\boldsymbol{g} \cdot \boldsymbol{r'}$. Because $\boldsymbol{r'} = \boldsymbol{r}'_O + \boldsymbol{r}$, and $\boldsymbol{g} \cdot \boldsymbol{r}'_O$ is only function of time (any potential is defined within to a function of time), we can assume that

$$U_g = -\boldsymbol{g} \cdot \boldsymbol{r}; \quad \boldsymbol{r} = (x, y, z). \tag{2.7}$$

in the non-inertial coordinate system $Oxyz$.

We choose the coordinate system $Oxyz$ in such a way that the plane $z = 0$ coincides with the unperturbed free surface (static position). Assuming that the atmospheric pressure is constant and equal to p_0, one can choose $C(t)$ such that the pressure equals p_0 on the unperturbed free surface. The Bernoulli equations (2.6) takes then the following form

$$p - p_0 = -\rho\left(\frac{\partial\Phi}{\partial t} + \frac{1}{2}(\nabla\Phi)^2 - \nabla\Phi\cdot(\boldsymbol{v}_O + \boldsymbol{\omega}\times\boldsymbol{r}) + U_g\right). \tag{2.8}$$

This makes it possible to compute the pressure $p(x, y, z, t)$ in $Q(t)$ by using the velocity potential $\Phi(x, y, z, t)$.

2.2.2. Boundary conditions. The boundary condition on the wetted tank surface $S(t)$ requires that there is no normal flow through $S(t)$, i.e., the normal velocity on the wetted surface is equal to the normal component of the rigid body velocity, i.e.,

$$\boldsymbol{v}\cdot\boldsymbol{n} = \boldsymbol{v}_O\cdot\boldsymbol{n} + [\boldsymbol{\omega}\times\boldsymbol{r}]\cdot\boldsymbol{n} \quad \text{on } S(t), \tag{2.9}$$

where $\boldsymbol{n}$ is the outer normal vector to $S(t)$ and $\boldsymbol{v}$ is the absolute liquid velocity. One can rewrite (2.9) as

$$\frac{\partial\Phi}{\partial n} = \boldsymbol{v}\cdot\boldsymbol{n} = \boldsymbol{v}_O\cdot\boldsymbol{n} + \boldsymbol{\omega}\cdot[\boldsymbol{r}\times\boldsymbol{n}] \quad \text{on } S(t). \tag{2.10}$$

Because the hydrodynamic pressure on the free surface equals to the gas pressure p_0, using (2.8), the so-called dynamic boundary condition on the free surface reads as

$$\frac{\partial\Phi}{\partial t} + \frac{1}{2}(\nabla\Phi)^2 - (\boldsymbol{v}_O + \boldsymbol{\omega}\times\boldsymbol{r})\cdot\nabla\Phi + U_g = 0 \quad \text{on } \Sigma(t). \tag{2.11}$$

As a consequence, we derived two boundary conditions: on the wetted tank surface (2.10) and the unknown free surface (2.11). The free-boundary problem also requires the kinematic boundary condition on the free surface.

The kinematic boundary condition ensures that any liquid particle remains on the free surface at any instant time t. When the non-inertial coordinate system $Oxyz$ is used, the most general implicit definition of the free surface is of implicit form and can be determined by the equation

$$Z(x, y, z, t) = 0, \tag{2.12}$$

where Z is, generally, unknown and should be found from the boundary value problem together with the velocity potential Φ. When liquid particles remain on the free surface implies that the material derivative of Z in the inertial coordinate system $O'x'y'z'$ equals to zero, i.e.

$$0 = \frac{D'Z}{Dt} = \left.\frac{\partial Z}{\partial t}\right|_{O'x'y'z'} + \boldsymbol{v}\cdot\nabla Z$$
$$= \left.\frac{\partial Z}{\partial t}\right|_{Oxyz} - \boldsymbol{v}_b\cdot\nabla Z + \nabla\Phi\cdot\nabla Z \quad \text{on } \Sigma(t), \quad (2.13)$$

where we used the formula for the time derivative in the non-inertial coordinate system derived in (2.5).

The outer normal vector (to the free surface $\Sigma(t)$) can be written as

$$\boldsymbol{n} = \frac{\nabla Z}{|\nabla Z|} \quad \text{on } \Sigma(t), \quad (2.14)$$

which transforms (2.13) to

$$\frac{\partial\Phi}{\partial n} = \boldsymbol{v_0}\cdot\boldsymbol{n} + \boldsymbol{\omega}\cdot[\boldsymbol{r}\times\boldsymbol{n}] - \frac{\partial Z/\partial t}{|\nabla Z|} \quad \text{on } \Sigma(t), \quad (2.15)$$

where the time derivative is computed in the $Oxyz$ coordinate system.

In the considered cases when the tank walls are parallel to the z-axis, the normal form of the free surface representation is possible, i.e.,

$$Z(x,y,z,t) = z - \zeta(x,y,t) = 0. \quad (2.16)$$

The kinematic boundary condition (2.15) takes then the form

$$\frac{\partial\Phi}{\partial z} - \frac{\partial\Phi}{\partial x}\frac{\partial\zeta}{\partial x} - \frac{\partial\Phi}{\partial y}\frac{\partial\zeta}{\partial y} = (\boldsymbol{v}_O + \boldsymbol{\omega}\times\boldsymbol{r}).(-\frac{\partial\zeta}{\partial x}, -\frac{\partial\zeta}{\partial y}, 1) + \frac{\partial\zeta}{\partial t} \quad \text{on } \Sigma(t), \quad (2.17)$$

or

$$\frac{\partial\Phi}{\partial n} = (\boldsymbol{v}_O + \boldsymbol{\omega}\times\boldsymbol{r})\cdot\boldsymbol{n} + \frac{\partial\xi/\partial t}{\sqrt{1+(\nabla\xi)^2}} \quad \text{on } \Sigma(t). \quad (2.18)$$

2.2.3. Mass (volume) conservation condition. The mass of an incompressible liquid must remain constant, i.e.,

$$M_l = \int\limits_{Q(t)} \rho dQ = \rho\, Vol = const, \quad (2.19)$$

where M_l and Vol are the mass and volume of the contained liquid, respectively.

Equation (2.19) is not automatically satisfied. It imposes a restriction on admissible class of functions Z (or ζ), which define the free surface. Integral condition (2.19) represents a geometric (holonomic) constraint.

2.2.4. Initial and periodicity conditions. Equations (2.2), (2.10), (2.11), (2.13), and (2.19) constitute a free-surface boundary value problem describing the liquid sloshing dynamics in a container moving by prescribed law. Solving this problem requires either initial conditions or, in the case of periodic vector-functions $\boldsymbol{v_0}(t)$ and $\boldsymbol{\omega}(t)$ – periodicity conditions.

Physically, adopting the initial conditions implies introducing an initial scenario so that the corresponding solution of the initial boundary value problem describes the so-called transient sloshing affected by the prescribed tank motion $(\boldsymbol{v}_O(t), \boldsymbol{\omega}(t))$ as well as initial perturbations of the free surface and liquid velocity field.

The initial (Cauchy) conditions read as

$$Z(x,y,z,t_0) = Z_0(x,y,z); \quad \left.\frac{\partial \Phi}{\partial n}\right|_{\Sigma(t_0)} = V_0(x,y,z)|_{\Sigma(t_0)}, \tag{2.20}$$

where the given function Z_0 defines the initial position of the free surface $\Sigma(t_0)$: $Z_0(x,y,z) = 0$ and $V_0(x,y,z)$ specifies the initial absolute normal velocities on the given initial surface $\Sigma(t_0)$. Using the kinematic condition (2.15), the initial conditions (2.20) can be rewritten in the form

$$Z(x,y,z,t_0) = Z_0(x,y,z); \quad \left.\frac{\partial Z}{\partial t}\right|_{t=t_0} = Z_1(x,y,z)|_{\Sigma(t_0)}, \tag{2.21}$$

where Z_0 and Z_1 are prescribed functions of spatial variables.

The boundary value problem (2.2), (2.10), (2.11), (2.13), and (2.19) with periodicity conditions determines periodic (steady-state) wave motions. Physically, stable steady-state waves are realized after initially occurring transients caused by initial perturbations (2.21). Mathematically, the periodicity conditions read as

$$Z(x,y,z,t+T) = Z(x,y,z,t), \tag{2.22}$$

provided, as stated before, by the periodicity of the prescribed tank motions, $\boldsymbol{v}_O(t+T) = \boldsymbol{v}_O(t)$ and $\boldsymbol{\omega}(t+T) = \boldsymbol{\omega}(t)$, where T is the prescribed period. Condition (2.22) ensures periodicity of the velocity field determined from the Neumann boundary value problem (2.2), (2.9), and (2.18).

2.3. The Luke-Bateman variational principle

Theorem 1.1 *Smooth solutions to the boundary value problem with a free surface (2.2), (2.10), (2.11), (2.13), (2.19) coincide with extrema of the Luke-Bateman action*

$$W(Z,\Phi) = \int_{t_1}^{t_2} L\,\mathrm{d}t,$$

$$L = \int\limits_{Q(t)} (p-p_0)dQ = -\rho \int\limits_{Q(t)} \left[\frac{\partial \Phi}{\partial t} + \frac{1}{2}(\nabla\Phi)^2 - \nabla\Phi\cdot(\boldsymbol{v}_O + \boldsymbol{\omega}\times\boldsymbol{r}) + U_g\right] dQ, \tag{2.23}$$

for the isochronous independent smooth variations

$$\begin{aligned} &\delta\Phi(x,y,z,t_1) = 0; \quad \delta\Phi(x,y,z,t_2) = 0, \\ &\delta Z(x,y,z,t_1) = 0; \quad \delta Z(x,y,z,t_2) = 0. \end{aligned} \tag{2.24}$$

Theorem 1.1 was proven in [217].

Let us describe some details of this proof.

Suppose that two unknown functions, Z and Φ can be represented as $\Phi = \Phi(x,y,z,t,\alpha_1)$ and $Z = Z(x,y,z,t,\alpha_2)$ where the two small parameters α_1 and α_2 are independent, and their zeros correspond to the extrema points of the functional W. Substituting Φ and Z into (2.23) gives a function of two real variables α_1 and α_2, i.e. $W = W(\alpha_1,\alpha_2)$. The variation calculation at the point $\alpha_1 = \alpha_2 = 0$ is then as follows

$$dW(0,0) = \left.\frac{\partial W}{\partial \alpha_1}\right|_{0,0} d\alpha_1 + \left.\frac{\partial W}{\partial \alpha_2}\right|_{0,0} d\alpha_2 = \delta W \frac{\partial W}{\partial Z}\underbrace{\frac{\partial Z}{\partial \alpha_2}d\alpha_2}_{\delta Z} + \frac{\partial W}{\partial \Phi}\underbrace{\frac{\partial \Phi}{\partial \alpha_1}d\alpha_1}_{\delta\Phi}$$

$$-\rho\int_{t_1}^{t_2}\left(-\int_{\Sigma(t)}\left[\frac{\partial\Phi}{\partial t} + \frac{1}{2}(\nabla\Phi)^2 - \nabla\Phi\cdot(\boldsymbol{v_0} + \boldsymbol{\omega}\times\boldsymbol{r}) + U_g\right]\frac{\delta Z}{|\nabla Z|}dS\right.$$

$$+\int\limits_{Q(t)}\left[\nabla\Phi\cdot\nabla(\delta\Phi)+\frac{\partial(\delta\Phi)}{\partial t}-\nabla(\delta\Phi)\cdot(\boldsymbol{v_0}+\boldsymbol{\omega}\times\boldsymbol{r})\right]dQ\Big)dt=0, \quad (2.25)$$

where we accounted for the gravity potential U_g and $(\boldsymbol{v_0}+\boldsymbol{\omega}\times\boldsymbol{r})$ do not depend on α_1 and α_2 and, furthermore, their variations are zero.

Because δZ and $\delta\Phi$ are independent, we can choose $\delta\Phi=0$. Considering arbitrary variations δZ, equality (2.25) leads to the dynamic boundary condition (2.11) on $\Sigma(t)$. When $\delta Z=0$, $\delta\Phi\neq 0$, the integral from (2.25) can be modified by using Green's formula, Gauss's theorem, and the Reynolds transport theorem

$$\int\limits_{Q(t)}\nabla\Phi\cdot\nabla(\delta\Phi)\,\mathrm{d}Q=\int\limits_{S(t)+\Sigma(t)}\delta\Phi\frac{\partial\Phi}{\partial n}\,\mathrm{d}S-\int\limits_{Q(t)}\nabla^2\Phi\delta\Phi\,\mathrm{d}Q,$$

$$\int\limits_{Q(t)}\boldsymbol{v}_O\cdot\nabla(\delta\Phi)\,\mathrm{d}Q=\int\limits_{Q(t)}\nabla(\boldsymbol{v}_O\cdot\boldsymbol{r})\cdot\nabla(\delta\Phi)\,\mathrm{d}Q=\int\limits_{S(t)+\Sigma(t)}\delta\Phi(\boldsymbol{v}_O\cdot\boldsymbol{n})\,\mathrm{d}S,$$

$$\int\limits_{Q(t)}(\boldsymbol{\omega}\times\boldsymbol{r})\cdot\nabla(\delta\Phi)\,\mathrm{d}Q=\int\limits_{S(t)+\Sigma(t)}\delta\Phi((\boldsymbol{\omega}\times\boldsymbol{r})\cdot\boldsymbol{n})\,\mathrm{d}S,$$

$$\int\limits_{Q(t)}\frac{\partial(\delta\Phi)}{\partial t}\,\mathrm{d}Q=\frac{d}{dt}\int\limits_{Q(t)}\delta\Phi\,\mathrm{d}Q+\int\limits_{\Sigma(t)}(\delta\Phi)|_{\Sigma(t)}\frac{\partial Z/\partial t}{|\nabla Z|}\,\mathrm{d}S. \quad (2.26)$$

These convert the final integral into the variational equality

$$\delta W|_{\delta Z=0}=\rho\int\limits_{t_1}^{t_2}\Bigg(\int\limits_{S(t)}\left[\frac{\partial\Phi}{\partial n}-(\boldsymbol{v}_O+\boldsymbol{\omega}\times\boldsymbol{r})\cdot\boldsymbol{n}\right]\delta\Phi\,\mathrm{d}S-\int\limits_{Q(t)}\nabla^2\Phi\delta\Phi\,\mathrm{d}Q$$
$$+\int\limits_{\Sigma(t)}\left[\frac{\partial\Phi}{\partial n}-(\boldsymbol{v}_O+\boldsymbol{\omega}\times\boldsymbol{r})\cdot\boldsymbol{n}+\frac{\partial Z}{\partial t}/|\nabla Z|\right]\delta\Phi\,\mathrm{d}S\Bigg)\,\mathrm{d}t$$
$$-\rho\int\limits_{Q(t)}\delta\Phi\,\mathrm{d}Q|_{t=t_1}^{t=t_2}=0, \quad (2.27)$$

where the last term, $\rho\int Q(t)\delta\Phi\,\mathrm{d}Q|_{t=t_1}^{t=t_2}=0$, gives zero contribution since $\delta\Phi=0$ for $t=t_1,t_2$ according to (2.24). From the variational equality (2.27), the kinetic relations of the boundary value problem follow.

2.4. The Miles-Lukovsky nonlinear modal equations

We employ the Luke-Bateman variational principle and the so-called nonlinear multimodal method to derive a system of nonlinear modal equations, a system of ordinary differential equations with respect to the generalized coordinates and velocities of the hydrodynamic system. Analytical methods that make this fundamentally possible were proposed in [1,3,102].

2.4.1. Modal representation of the free surface and velocity potential. The multimodal method utilizes representations of solutions by functional series with time-dependent coefficients. Because functions describing the free surface and velocity potential (Z and Φ) are considered independent in the variational formulation, two separate functional representations are required: one functional series for the free surface Z and another one for the velocity potential Φ.

When the free surface $\Sigma(t)$ is expressed by the equation

$$z = \zeta(x, y, t) \quad (Z(x, y, z, t) = z - \zeta(x, y, t) = 0)$$

in the non-inertial coordinate system $Oxyz$, the first functional series is

$$\zeta(x, y, t) = \sum_{i=1}^{\infty} \beta_i(t) f_i(x, y), \tag{2.28}$$

where the functional basis $\{f_i(x, y)\}$ does not necessarily represent the natural sloshing modes but must be a complete set of basis functions in appropriate functional space and the time-dependent functions $\{\beta_i\}$ could be interpreted as *generalized hydrodynamic coordinates*. The functional basis should satisfy the necessary volume conservation condition

$$\int_{\Sigma_0} f_i(x, y)\, dxdy = 0,$$

where Σ_0 is the unperturbed (hydrostatic) free surface. This condition is equivalent to (2.19).

A functional series is also required for the velocity potential:

$$\Phi(x,y,z,t) = \boldsymbol{v}_O(t)\cdot\boldsymbol{r} + \boldsymbol{\omega}(t)\cdot\boldsymbol{\Omega}(x,y,z,t) + \underbrace{\sum_{n=1}^{\infty} R_n(t)\varphi_n(x,y,z)}_{\varphi(x,y,z,t)}, \quad (2.29)$$

where the functional basis $\{\varphi_n\}$ is not necessarily associated with the natural sloshing modes and

$$\boldsymbol{\Omega} = (\Omega_1(x,y,z,t), \Omega_2(x,y,z,t), \Omega(x,y,z,t))^T$$

is the vector Stokes-Joukowski potential, which is a vector function of spatial and generalized hydrodynamic coordinates coming from the following Neumann boundary value problem

$$\bigtriangledown^2 \boldsymbol{\Omega} = 0 \text{ in } Q(t); \quad \frac{\delta\Omega_1}{\partial n} = yn_z - zn_y; \ \frac{\partial\Omega_2}{\delta n} = zn_x - xn_z; \\ \frac{\delta\Omega_3}{\partial n} = xn_y - yn_x \text{ on } S(t)\cup\Sigma(t), \quad (2.30)$$

where we denote components of the outward normal vector as

$$\boldsymbol{n} = (n_x, n_y, n_z).$$

The functional basis $\{\varphi_n(x,y,z)\}$ in (2.29) must be complete for any admissible liquid shapes of $Q(t)$. In practical applications, $\{\varphi_n(x,y,z)\}$ usually coincides with the natural sloshing modes. In this case, Φ (from equation (2.29)) automatically satisfies the Laplace equation and boundary conditions on the wetted tank surface. However, the two boundary conditions on the free surface are not fulfilled.

Because both the kinematic and dynamic boundary conditions naturally follow from the Luke-Bateman variational principle, the Luke-Bateman variational formalism can be considered a useful tool for derivation of ordinary differential equations which couple the time-dependent generalized hydrodynamic coordinates $\beta_i(t)$ and velocities $R_n(t)$. The differential equations, at least their dynamic component, can be treated as the Euler-Lagrange equation of the second kind with respect to β_i and R_n with an infinite number of degrees of freedom.

2.4.2. Modal equations. After substituting (2.29) into (2.23), the Lagrangian in the Luke-Bateman principle takes the following form

$$L = -\rho \int\limits_{Q(t)} \left[\frac{d\boldsymbol{v}_O}{dt} \cdot \boldsymbol{r} + \frac{\partial}{\partial t}(\boldsymbol{\omega}\cdot\boldsymbol{\Omega}) + \frac{1}{2}\nabla(\boldsymbol{\omega}\cdot\boldsymbol{\Omega})\cdot\nabla(\boldsymbol{\omega}\cdot\boldsymbol{\Omega}) - \boldsymbol{\omega}\cdot(\boldsymbol{r}\times\nabla(\boldsymbol{\omega}\cdot\boldsymbol{\Omega})) \right.$$
$$\left. - \frac{1}{2}\boldsymbol{v}_O^2 - \boldsymbol{\omega}\cdot(\boldsymbol{r}\times\boldsymbol{v}_O) - \boldsymbol{\omega}\cdot(\boldsymbol{r}\times\nabla\varphi) + \nabla(\boldsymbol{\omega}\cdot\boldsymbol{\Omega})\cdot\varphi \right] dQ + L_r, \quad (2.31)$$

where

$$L_r = -\rho \int\limits_{Q(t)} \left[\frac{\partial\varphi}{\partial t} + \frac{1}{2}(\nabla\varphi)^2 + U_g \right] dQ. \quad (2.32)$$

The integral expressions in (2.31) require simplifications. These follow from vector algebra, Gauss' theorem, and the Neumann boundary conditions (2.30). Two terms under the integral in (2.31) cancel each other, i.e.,

$$\int\limits_{Q(t)} \left[-(\boldsymbol{\omega}\times\boldsymbol{r})\cdot\nabla\varphi + \nabla(\boldsymbol{\omega}\cdot\boldsymbol{\Omega})\cdot\nabla\varphi \right] dQ$$
$$= \int\limits_{S(t)+\Sigma(t)} \left(\frac{\partial(\boldsymbol{\omega}\cdot\boldsymbol{\Omega})}{\partial n} - (\boldsymbol{\omega}\times\boldsymbol{r})\cdot\boldsymbol{n} \right) \varphi\, dS = 0. \quad (2.33)$$

Other quantities appearing in the integral (2.31) can be compactly written down in terms of the inertia tensor $J^1 = J^1(x,y,z,t)$ whose components are the following integrals with respect to the Stokes-Joukowski potential (2.30):

$$J^1_{11} = \rho \int\limits_{Q(t)} \left(y\frac{\partial\Omega_1}{\partial z} - z\frac{\partial\Omega_1}{\partial y} \right) dQ = \rho \int\limits_{S(t)+\Sigma(t)} \Omega_1 \frac{\partial\Omega_1}{\partial n} dS,$$
$$J^1_{22} = \rho \int\limits_{Q(t)} \left(z\frac{\partial\Omega_2}{\partial x} - x\frac{\partial\Omega_2}{\partial z} \right) dQ = \rho \int\limits_{S(t)+\Sigma(t)} \Omega_2 \frac{\partial\Omega_2}{\partial n} dS,$$
$$J^1_{33} = \rho \int\limits_{Q(t)} \left(x\frac{\partial\Omega_3}{\partial y} - y\frac{\partial\Omega_3}{\partial x} \right) dQ = \rho \int\limits_{S(t)+\Sigma(t)} \Omega_3 \frac{\partial\Omega_3}{\partial n} dS,$$

$$J^1_{12} = J^1_{21} = \rho \int\limits_{Q(t)} \left(z\frac{\partial\Omega_1}{\partial x} - x\frac{\partial\Omega_1}{\partial z} \right) dQ = \rho \int\limits_{Q(t)} \left(y\frac{\partial\Omega_2}{\partial z} - z\frac{\partial\Omega_2}{\partial y} \right) dQ$$

$$= \rho \int\limits_{S(t)+\Sigma(t)} \Omega_1 \frac{\partial \Omega_2}{\partial n} dS = \rho \int\limits_{S(t)+\Sigma(t)} \Omega_2 \frac{\partial \Omega_1}{\partial n} dS,$$

$$J_{13}^1 = J_{31}^1 = \rho \int\limits_{Q(t)} \left(x \frac{\partial \Omega_1}{\partial y} - y \frac{\partial \Omega_1}{\partial x} \right) dQ = \rho \int\limits_{Q(t)} \left(y \frac{\partial \Omega_3}{\partial z} - z \frac{\partial \Omega_3}{\partial y} \right) dQ$$

$$= \rho \int\limits_{S(t)+\Sigma(t)} \Omega_1 \frac{\partial \Omega_3}{\partial n} dS = \rho \int\limits_{S(t)+\Sigma(t)} \Omega_3 \frac{\partial \Omega_1}{\partial n} dS,$$

$$J_{23}^1 = J_{32}^1 = \rho \int\limits_{Q(t)} \left(x \frac{\partial \Omega_2}{\partial y} - y \frac{\partial \Omega_2}{\partial x} \right) dQ = \rho \int\limits_{Q(t)} \left(z \frac{\partial \Omega_3}{\partial x} - x \frac{\partial \Omega_3}{\partial z} \right) dQ$$

$$= \rho \int\limits_{S(t)+\Sigma(t)} \Omega_2 \frac{\partial \Omega_3}{\partial n} dS = \rho \int\limits_{S(t)+\Sigma(t)} \Omega_3 \frac{\partial \Omega_2}{\partial n} dS. \quad (2.34)$$

The inertia tensor is associated with the following quadratic form

$$-\frac{1}{2}\omega_1^2 J_{11}^1 - \frac{1}{2}\omega_2^2 J_{22}^1 - \frac{1}{2}\omega_3^2 J_{33}^1 - \omega_1\omega_2^2 J_{12}^1 - \omega_1\omega_3^2 J_{13}^1 - \omega_2\omega_3^2 J_{23}^1$$

$$+ \frac{1}{2}\rho \int\limits_{S(t)+\Sigma(t)} (\boldsymbol{\omega}\cdot\boldsymbol{\Omega}) \left(\frac{\partial \Omega}{\partial n} \cdot \boldsymbol{\omega} \right) dS$$

$$= \frac{1}{2}\rho \int\limits_{Q(t)} \left(\frac{1}{2} \nabla(\boldsymbol{\omega}\cdot\boldsymbol{\Omega}) \cdot \nabla(\boldsymbol{\omega}\cdot\boldsymbol{\Omega}) - \boldsymbol{\omega}\cdot(\boldsymbol{r}\times\nabla(\boldsymbol{\omega}\cdot\boldsymbol{\Omega})) \right) dQ. \quad (2.35)$$

The last volume integral is a part of equation (2.31). After simplifications, this equation takes the following form

$$L = -[\dot{v}_{O1} l_1 + \dot{v}_{O2} l_2 + \dot{v}_{O3} l_3 + \dot{\omega}_1 l_{1\omega} + \dot{\omega}_2 l_{2\omega} + \dot{\omega}_3 l_{3\omega} + \omega_1 l_{1\omega t} + \omega_2 l_{2\omega t} + \omega_3 l_{3\omega t}$$

$$- \frac{1}{2}(\omega_1^2 J_{11}^1 + \omega_2^2 J_{22}^1 + \omega_3^2 J_{33}^1) - \omega_1\omega_2 J_{12}^1 - \omega_1\omega_3 J_{13}^1 - \omega_2\omega_3 J_{23}^1$$

$$- \frac{1}{2} M_1 (v_{O1}^2 + v_{O2}^2 + v_{O3}^2) + (\omega_2 v_{O3} - \omega_3 v_{O2}) l_1$$

$$+ (\omega_3 v_{O1} - \omega_1 v_{O3}) l_2 + (\omega_1 v_{O2} - \omega_2 v_{O1}) l_3] + L_r, \quad (2.36)$$

where M_l is the liquid mass, and

$$l_{k\omega} = \rho \int\limits_{Qt} \Omega_k dQ; \; l_{k\omega t} = \rho \int\limits_{Qt} \frac{\partial \Omega_k}{\partial t} dQ;$$

$$l_1 = \rho \int\limits_{Q(t)} x dQ; \; l_2 = \rho \int\limits_{Q(t)} y dQ; \; l_3 = \rho \int\limits_{Q(t)} z dQ. \quad (2.37)$$

The vectors

$$\boldsymbol{l}(t) = (l_1, l_2, l_3);\ \boldsymbol{l_\omega}(t) = (l_{1\omega}, l_{2\omega}, l_{3\omega});\ \boldsymbol{l_{\omega t}}(t) = (l_{1\omega t}, l_{2\omega t}, l_{3\omega t})$$

are functions of $\{\beta_i\}$ and $\left\{\dot{\beta}_i\right\}$. Furthermore, component (2.32) must account for the modal representation (2.29), yielding the following expression

$$L_r = -\rho \int\limits_{Q(t)} \left[\sum_{n=1}^{\infty} \dot{R}_n \varphi_n + \frac{1}{2} \sum_{n,k=1}^{\infty} R_n R_k (\nabla\varphi_n \cdot \nabla\varphi_k) + U_s \right] dQ$$

$$= -\left[\sum_{n=1}^{\infty} A_n \dot{R}_n + \frac{1}{2} \sum_{n,k=1}^{\infty} A_{nk} R_n R_k - g_1 l_1 - g_2 l_2 - g_3 l_3 - m_1 g \cdot r_0' \right], \quad (2.38)$$

where

$$A_n = \rho \int\limits_{Q(t)} \varphi_n dQ; \quad A_{nk} = A_{kn} = \rho \int\limits_{Q(t)} \nabla\varphi_n \cdot \nabla\varphi_k \, dQ. \quad (2.39)$$

The Luke-Bateman variational principle, equations (2.23) and (2.24), consider L as a function of the two *independent* variables $\zeta(x, y, t)$ and $\Phi(x, y, z, t)$. When substituting representations (2.28) and (2.29), the Lagrangian L becomes expressed through equations (2.36) and (2.38), a function of the independent generalized coordinates $\{\beta_i\}$ and velocities $\{R_n\}$. Note, integrals in equations (2.34), (2.37), and (2.39) are functions of $\{\beta_i\}$. Independent variations of the action $W = \int_{t_1}^{t_2} L dt$ (via $\delta\zeta$ and $\delta\Phi$) must correspond to independent variations of $\delta\beta_i$ and δR_n, respectively. This yields the following variational equality

$$\delta W = \int\limits_{t_1}^{t_2} \Bigg[\sum_n A_n \delta\dot{R}_n + \sum_n A_{nk} R_k \delta R_n$$

$$+ \left(\sum_n \dot{R}_n \frac{\partial A_n}{\partial\beta_i} + \omega_1 \frac{\partial l_{1\omega t}}{\partial\beta_i} + \omega_2 \frac{\partial l_{2\omega t}}{\partial\beta_i} + \omega_3 \frac{\partial l_{3\omega t}}{\partial\beta_i} \right.$$

$$\left. + \frac{1}{2} \sum_{n,k} R_n R_k \frac{\partial A_{nk}}{\partial\beta_i} + \dot{\omega}_1 \frac{\partial l_{1\omega}}{\partial\beta_i} + \dot{\omega}_2 \frac{\partial l_{2\omega}}{\partial\beta_i} + \dot{\omega}_3 \frac{\partial l_{3\omega}}{\partial\beta_i} \right)$$

$$+ (\dot{v}_{O1} - g_1 + \omega_2 v_{O3} - \omega_3 v_{O2}) \frac{\partial l_1}{\partial\beta_i} + (\dot{v}_{O2} - g_2 + \omega_3 v_{O1} - \omega_1 v_{O3}) \frac{\partial l_2}{\partial\beta_i}$$

$$+ (\dot{v}_{O3} - g_3 + \omega_1 v_{O2} - \omega_2 v_{O1}) \frac{\partial l_3}{\partial\beta_i} - \frac{1}{2}\omega_1^2 \frac{\partial J_{11}^1}{\partial\beta_i} - \frac{1}{2}\omega_2^2 \frac{\partial J_{22}^1}{\partial\beta_i} - \frac{1}{2}\omega_3^2 \frac{\partial J_{33}^1}{\partial\beta_i}$$

$$- \omega_1\omega_2\frac{\partial J^1_{12}}{\partial\beta_i} - \omega_1\omega_3\frac{\partial J^1_{13}}{\partial\beta_i} - \omega_2\omega_3\frac{\partial J^1_{23}}{\partial\beta_i}\Bigg)\delta\beta_i$$
$$+ (\omega_1\frac{\partial l_{1\omega t}}{\partial\dot\beta_i} + \omega_2\frac{\partial l_{2\omega t}}{\partial\dot\beta_i} + \omega_3\frac{\partial l_{3\omega t}}{\partial\dot\beta_i})\delta\dot\beta_i\Bigg]dt = 0,\ i \geq 1. \quad (2.40)$$

The terms proportional to $\delta\dot Rn$ and $\delta\dot\beta i$ in the last expression (2.40) can be integrated by parts and, using the fact

$$\delta R_n(t_1) = \delta R_n(t_2) = \delta\beta_i(t_1) = \delta\beta_i(t_2) = 0,$$

can be reduced to expressions in terms of δR_n and $\delta\beta_i$ instead of $\delta\dot Rn$ and $\delta\dot\beta i$. We then obtain the following infinite system of nonlinear ordinary differential equations (the *Miles-Lukovsky* equations) with respect to $\{R_n(t)\}$ and $\{\beta_i(t)\}$

$$\sum_i \frac{\partial A_n}{\partial\beta_i}\dot\beta_i - \sum_k R_k A_{nk} = 0, \quad n = 1, 2, ..., \quad (2.41)$$

$$\sum_n \dot R_n\frac{\partial A_n}{\partial\beta_i} + \frac{1}{2}\sum_n\sum_k \frac{\partial A_{nk}}{\partial\beta_i}R_nR_k + \dot\omega_1\frac{\partial l_{1\omega}}{\partial\beta_i} + \dot\omega_2\frac{\partial l_{2\omega}}{\partial\beta_i} + \dot\omega_3\frac{\partial l_{3\omega}}{\partial\beta_i}$$
$$+ \omega_1\frac{\partial l_{1\omega t}}{\partial\beta_i} + \omega_2\frac{\partial l_{2\omega t}}{\partial\beta_i} + \omega_3\frac{\partial l_{3\omega t}}{\partial\beta_i} - \frac{d}{dt}\left(\omega_1\frac{\partial l_{1\omega t}}{\partial\dot\beta_i} + \omega_2\frac{\partial l_{2\omega t}}{\partial\dot\beta_i} + \omega_3\frac{\partial l_{3\omega t}}{\partial\dot\beta_i}\right)$$
$$+ (\dot v_{O1} - g_1 + \omega_2 v_{O3} - \omega_3 v_{O2})\frac{\partial l_1}{\partial\beta_i} + (\dot v_{O2} - g_2 + \omega_3 v_{O1} - \omega_1 v_{O3})\frac{\partial l_2}{\partial\beta_i}$$
$$+ (\dot v_{O3} - g_3 + \omega_1 v_{O2} - \omega_2 v_{O1})\frac{\partial l_3}{\partial\beta_i} - \frac{1}{2}\omega_1^2\frac{\partial J^1_{11}}{\partial\beta_i} - \frac{1}{2}\omega_2^2\frac{\partial J^1_{22}}{\partial\beta_i} - \frac{1}{2}\omega_3^2\frac{\partial J^1_{33}}{\partial\beta_i}$$
$$- \omega_1\omega_2\frac{\partial J^1_{12}}{\partial\beta_i} - \omega_1\omega_3\frac{\partial J^1_{13}}{\partial\beta_i} - \omega_2\omega_3\frac{\partial J^1_{23}}{\partial\beta_i} = 0,\ i = 1, 2, ... \quad (2.42)$$

If container is characterised by vertical (cylindrical) walls near the undisturbed free surface Σ_0, the values of $\partial l_k/\partial\beta_i$ can be written as

$$\frac{\partial l_3}{\partial\beta_i} = \rho\int\limits_{\Sigma_0} f_i^2 dS\beta_i = \lambda_{3i}\beta_i; \quad \frac{\partial l_2}{\partial\beta_i} = \rho\int\limits_{\Sigma_0} y f_i^2 dS = \lambda_{2i},$$
$$\frac{\partial l_1}{\partial\beta_i} = \rho\int\limits_{\Sigma_0} x f_i^2 dS = \lambda_{1i}. \quad (2.43)$$

The system (2.41)-(2.42) was independently derived by Miles and Lukovsky in 1976. Its final form (for an arbitrary motion of the tank) was obtained by Lukovsky.

2.5. Linear modal equations and viscous damping

Linear and weakly-nonlinear theories of sloshing are normally based on the natural sloshing modes in the modal representations (2.28), (2.29). This means that the natural sloshing modes φ_i are the eigenfunctions coming from the spectral boundary problem

$$\nabla^2\varphi_i = 0 \text{ in } Q_0; \quad \frac{\partial\varphi_i}{\partial n} = 0 \text{ on } S_0; \quad \frac{\partial\varphi_i}{\partial n} = \kappa_i\varphi_i \text{ on } \Sigma_0; \quad \int_{\Sigma_0}\varphi_i\, dS = 0 \quad (2.44)$$

where Q_0 is the mean liquid domain, S_0 is the mean wetted tank surface, and Σ_0 is the mean (unperturbed) free surface. Adopting the natural sloshing mode basis implicitly implies that φ_i are analytically expandable over Σ_0 to the "gas domain".

As derivations in Chapter 5 of [1] have shown, the orthogonality of $\{f_n(x,y) = \varphi_n(x,y,0)\}$ in $L_2(\Sigma_0)$ makes the matrices $\partial A_n/\partial\beta_i$ and A_{nk} containing only non-zero diagonal $O(1)$-order elements as $\beta_i \to 0$. Assuming both forcing and sloshing are small and of the same asymptotic order,

$$|\boldsymbol{v}_O| \sim |\boldsymbol{\omega}| \sim \beta_i \sim R_i = O(\epsilon) \ll 1$$

and excluding the $o(\epsilon)$ quantities in the modal equations (2.41), (2.42) reduces them, as one can see in [1], to the set of uncoupled linear ordinary differential equations

$$\ddot{\beta}_m + \boxed{2\xi_m\sigma_m\dot{\beta}_m} + \sigma_m^2\beta_m = K_m(t)$$
$$= \bar{\lambda}_{1m}(\ddot{\eta}_1 - g\eta_5) + \bar{\lambda}_{2m}(\ddot{\eta}_2 + g\eta_4) + \sum_{k=4}^{6}\bar{\lambda}_{(k-3)m}\ddot{\eta}_k, \quad (2.45)$$

where $\sigma_m^2 = g\kappa_m$ and the λ-type hydrodynamic coefficients are functions of integrals over the natural sloshing modes $\{\varphi_n\}$ and the linearised Stokes-Joukowski potentials $\boldsymbol{\Omega}_0(x,y,z) = \boldsymbol{\Omega}(x,y,z,\{0\})$ coming in the linear case from the Neumann boundary value problem

$$\nabla^2\boldsymbol{\Omega}_0 = 0 \text{ in } Q_0; \quad \frac{\partial\boldsymbol{\Omega}_0}{\partial n} = \boldsymbol{r}\times\boldsymbol{n} \text{ on } S_0\cup\Sigma_0. \quad (2.46)$$

Explicit expressions for the λ-coefficients are presented in Chapter 5 of [1].

Furthermore, the linear equations (2.45) contain the rigid body-motion generalized coordinates $\eta_i(t)$, $i = 1, \dots, 6$, which correspond to small-magnitude perturbations by six degrees of freedom of the rigid tank, namely, sway, surge, heave, roll, pitch, and yaw. These oscillatory perturbations are shown in Figure 2.1.

In the linear approximation, the generalized coordinates introduce the translatory and angular velocities by the rule

$$\boldsymbol{v}_O(t) = \dot{\eta}_1 \boldsymbol{e}_1 + \dot{\eta}_2 \boldsymbol{e}_2 + \dot{\eta}_3 \boldsymbol{e}_3; \quad \boldsymbol{\omega}(t) = \dot{\eta}_4 \boldsymbol{e}_1 + \dot{\eta}_5 \boldsymbol{e}_2 + \dot{\eta}_6 \boldsymbol{e}_3, \tag{2.47}$$

where $\boldsymbol{e}_i$ are the unit vectors of the $Oxyz$-coordinate frame.

Linear modal equations (2.45) are also equipped with the framed terms whose appearance *does not follow* from the inviscid infinite-dimensional multi-modal mathematical model. These terms imply viscous damping. According to original assumptions that liquid flows are mainly inviscid and irrotational, the non-dimensional damping rates ξ_m should be small and proportional to $\mathrm{Ga}^{-1/4}$ where

$$\mathrm{Ga} = \frac{gL^3}{\nu^2}$$

is the Galileo number (L is the characteristic dimension of Σ_0, ν is the kinematic viscosity).

A rigorous linear sloshing theory of viscous liquid was constructed by S. Krein in [48]. Krein's theorem states that only a finite number of oscillatory sloshing modes exists, i.e., interpreting his result in term of the linear oscillators (2.45), there exists N such that $\xi_i > 1$ for $i \geq N$. Numerical analysis in [218] also demonstrates that only lower viscous sloshing modes can be approximated by using the 'inviscid' eigensolution by (2.44). This means that the linear modal as well as weakly-nonlinear theories based on the original free-surface inviscid problem are only accurate if they involve a limited number of summands. The latter happens when only lower set of the generalised hydrodynamic coordinates possesses asymptotically-dominant character $\gg O(\epsilon)$ where the forcing amplitude holds the asymptotic order $O(\epsilon)$. This is expected for resonance excitations.

When associating $\xi_i \ll 1$ with logarithmic decrements of lower natural sloshing modes, the damping rates can be estimated from below [1] by using

asymptotic formulas which are derived by employing the laminar viscous boundary layer theory, and sometimes, in addition, by accounting for the bulk damping effect,

$$\xi_i^{(0)} = \underbrace{\xi_i^{layer}}_{O(\mathrm{Ga}^{-1/4})} + \underbrace{\xi_i^{bulk}}_{O(\mathrm{Ga}^{-1/2})} \lesssim \xi_i.$$

The authors in [1, 158, 160, 219] discussed why and when the bulk damping may matter as well as how other viscous damping mechanisms (dynamic contact angle, wave breaking, free-surface contamination, roof impact and so on) can increase the resulting dissipation in the hydrodynamic system.

Remark 2.1. Taking Keulegan's (1959) estimate for ξ_i^{layer} and ξ_i^{bulk} in [1] gives for *rectangular tanks* with width L and breadth B the following formula

$$\xi_i^{(0)} = \sqrt{\frac{\nu}{2\sigma_i}}\frac{1}{B}\left(1 + \frac{B}{L}\left[1 + \pi i \frac{1-2h}{\sinh(2\pi i h)}\right]\right) + 2\nu\frac{\pi^2 i^2}{L^2\sigma_i^2}, \tag{2.48}$$

where ν is the kinematic viscosity. Specifically, the formula provides $\xi_i^0 \to \infty$ as $i \to \infty$ but, as I stated above, the estimate (2.48) is valid only for lower indices i.

Remark 2.2. Estimate of the damping rates $\xi_i^{(0)}$ for an upright circular cylindrical tank is derived in the section 4.4 following the book [4]. The estimate also accounts for the laminar boundary layer effect and the bulk damping.

Remark 2.3. The generalised coordinate $\eta_3(t)$ does not appear in (2.45) that means that parametric waves (excited by vertical tank motions) cannot be described within the framework of the linear sloshing theory, i.e., the parametric waves are purely nonlinear phenomena. Further, the system (2.45) appears as an infinite set of linear uncoupled oscillators and admits exact analytical solution for any $\eta_i(t)$. This solution was derived in Chapter 5 by [1]. Practically, this means that if we know the natural sloshing modes from (2.44) and the Stokes-Joukowski potentials from (2.46), one can write down an analytical solution of the linear sloshing problem for any prescribed tank motions.

2.6. Conclusions to the chapter

Using variational principles of the hydrodynamics, herein, the Luke-Bateman variational formulation for the free-surface boundary value problem on liquid sloshing in moving containers and postulating a modal representation of the free boundary and velocity potential makes it possible to derive a (modal) system of nonlinear ordinary differential equations of the Miles-Lukovsky–type. The system nonlinearly couples the generalized hydrodynamic coordinates and velocities introduced in the above modal (functional) representation as time-dependent coefficients.

The functional base can coincide with the natural sloshing modes which imply the linear standing waves on the free surface of the motionless container. If making that, we implicitly assume that the natural sloshing modes are analytically expandable over the mean free surface Σ_0. The latter becomes possible when the tank wall is upright. Both the nonlinear and linearized modal equations possess then very special features that will further facilitate the analytical studies of the forthcoming chapters.

Because the original hydrodynamic model (statement) as well as the adopted variational principle neglect viscous damping, the derived Miles-Lukovsky–type modal system implies, in fact, a conservative infinite-dimensional mechanical system. In the linear case, the system transforms into an infinite set of uncoupled linear oscillators where each degree of freedom corresponds to perturbations of an associated natural sloshing mode. Each linear oscillator could be equipped with a linear damping term whose damping rate should be interpreted as that coming from the logarithmic decrement of the corresponding standing wave (natural sloshing mode). There are analytical approaches to estimating the damping rates if these are caused by the laminar boundary layer and viscous bulk. When dealing with small-amplitude sloshing, these predictions are rather satisfactory when the tank is clean (no baffles) and there are no other specific viscous damping sources alike the free surface contamination.

Situation becomes much more complicated for resonant sloshing when the resulting viscous damping may become strongly nonlinear, affected by

numerous weakly-elaborated physical factors (in addition to the boundary layer effect on the mean wetted tank surface) and also imply an energy transfer from primary-excited to other (higher) natural sloshing modes that can be treated as a nonlinear dissipative phenomenon as well. The forthcoming chapters are dedicated to construction of weakly-nonlinear modal equations with nonlinear damping terms which should model resonant sloshing in rectangular and upright circular cylindrical tank. The damping terms of these equations are restored from a machine (model) learning procedure.

Chapter 3

Damped two-dimensional nonlinear resonant sloshing in a clean rectangular tank

3.1. Introduction

When a clean rigid rectangular tank with a finite liquid depth is longitudinally excited with the forcing frequency close to the lowest natural sloshing frequency, liquid sloshing can keep two-dimensional flows in the excitation plane. The resonant sloshing becomes then strongly nonlinear and the linear sloshing theory (2.45) is not applicable to describe these flows anymore. The free-surface nonlinearity causes a transfer of energy from the lowest, primary-excited natural sloshing mode to higher ones [3, 220]. This nonlinear energy transfer becomes the prevailing mechanism preventing an infinite resonant wave-amplitude response of the primary excited sloshing mode while viscous damping plays only a secondary role [75].

The latter fact on the free-surface nonlinearity explains why diverse *undamped* weakly-nonlinear modal equations derived from the Miles-Lukovsky equations (2.41), (2.42) or similar provide satisfactory agreement with experimentally measured steady-state wave characteristics for both steady-state wave regimes and even transients on relatively short time period. This is even though they are based on the inviscid hydrodynamic statement and neglect viscous damping. Important thing is the nonlinear energy transfer is accounted for. Examples of the weakly-nonlinear equations for finite liquid depths are the single-dominant modal system which is valid for smaller excitation amplitudes [3] and their adaptive versions accounting for increasing forcing amplitude and critical liquid depth [75, 76]. On the other hand, all these undamped theories completely fail to accurately capture the phase-lag

response, which is theoretically a piecewise function (taking only two values, 0 and $\pm\pi$), whereas inclusion of a viscous damping, even very small, makes the response a smooth continuous function in the forcing frequency versus phase lag plane.

Section 2.5 shows how to incorporate viscous damping in the linear modal sloshing theory for clean tanks (without internal structures) and low-viscous liquid characterised by large Galileo number. The present chapter shows that having known a set of measured phase-lags and introducing physically and mathematically consistent *a priori* unknown damping terms into the single-dominant modal theory of resonant liquid sloshing in a rectangular tank, one can implement, following the hidden physics concept [221–223], a machine learning technique to deduce effective nonlinear viscous damping quantities in the modal system. The adopted procedure follows general concept of the so-called Reduced Order Modelling [223, 224] which suggests a simplification of the original physical model to a simple finite-dimensional equations but, on the next stage, restoring the lost model properties by using a learning technique and measured data, here, the measured phase-lags between the harmonic forcing the steady-state resonant sloshing regime.

An appropriate set of measured phase-lags for resonant steady-state sloshing in a clean rigid rectangular tank was recently reported in [11]. The authors exploited them to evaluate the liquid sloshing damping when adopting the Duffing equation as a phenomenological model for resonant steady-state oscillations of the liquid mass-center [225–228]. More precisely, the Duffing equation was adopted for description of horizontal coordinate of the liquid mass centre bearing in mind the horizontal centre motions move alike a spring-mass system with the linear eigen frequency equal to the lowest natural sloshing frequency.

In addition, the authors measured logarithmic decrement of the first (lowest) natural sloshing mode which has been at $\xi_1^{(0)} = 8.0 \cdot 10^{-3}$ that is generally not very far from $5.7 \cdot 10^{-3}$ by (2.48). However, adopting the linear damping term $2\sigma_1\xi_1\dot{\beta}_1$ in the Duffing mathematical model for modeling the resonant sloshing does not fit measurements on resonant steady-state waves. It had

to be significantly larger than $15 \cdot 10^{-3}$ to fit at least for a few of measured phase-lags.

In the present chapter, the single-dominant *inviscid* nonlinear modal system [3] is revisited and modified by incorporating theoretically consistent damping terms. By applying Moiseev's asymptotic method, a steady-state periodic solution of this system is derived, which depends on three *a priori* unknown parameters associated with damping in the approximate nonlinear modal theory. One parameter controls the damping ratio of the second generalized coordinate (mode), $\xi_2^{(0)}$, while the other two serve as coefficients in a linear regression, approximating the damping ratio of the first (lowest-order) mode as a function of the dominant dimensionless steady-state wave amplitude. To identify these three unknown parameters, a loss function is defined as the integral distance between the measured and theoretical phase-lag curves. Using the gradient descent optimization, the damping parameters are computed, demonstrating excellent agreement with the experimental phase-lag data in [11], where the single-dominant nonlinear modal model is applicable.

The numerical results highlight the importance of free-surface nonlinearity and associated energy transfer to higher sloshing modes, as well as the role of higher mode damping. Furthermore, the discrepancies between linear damping rates predicted theoretically [158], measured logarithmic decrements [11], and values obtained from the present machine learning approach are shown to be physically consistent and explainable.

3.2. The Miles-Lukovsky nonlinear modal equations for two-dimensional liquid flows

Consider two-dimensional liquid flows in the (x, z) plane exposed to oscillatory tank motions which are defined by

$$\boldsymbol{v}_O = (v_{O1}, 0, v_{O3}) \quad \text{and} \quad \boldsymbol{\omega} = (0, \omega(t), 0). \tag{3.1}$$

The two-dimensional liquid flows cause the two-dimensional surface mo-

tions which can be described by the free-surface decomposition

$$z = \zeta(x,t) = \sum_{i=1}^{\infty} \beta_i(t) f_i(x) \tag{3.2}$$

by the natural sloshing modes $\varphi_n(x,z)$ which constitute a harmonic function basis in Q_0 and $f_i(x) = \varphi_i(x,0)$ is the complete system of functions in $L_2(\Sigma_0)$.

The velocity potential $\Phi(x,z,t)$ should also possess the modal–type functional representation

$$\Phi(x,z,t) = v_{O1}x + v_{O3}z + \omega(t)\,\Omega(x,z,\{\beta_i(t)\}) + \sum_{n=1}^{\infty} R_n(t)\,\varphi_n(x,z), \tag{3.3}$$

where the Stokes-Joukowski vector potential

$$\boldsymbol{\Omega}(x,z,\{\beta_i(t)\}) = (0,\Omega(x,z,\{\beta_i(t)\}),0)$$

contains only the scalar Stokes-Joukovsky component Ω appearing as solution of the following boundary value problem

$$\Delta\Omega = 0 \quad \text{in} \quad Q(t); \qquad \frac{\partial\Omega}{\partial n}|_{S(t)+\Sigma(t)} = zn_x - xn_z \tag{3.4}$$

coming from the general three-dimensional statement (2.30) where n_x and n_z are projections of the outward normal vector on axes Ox and Oz.

The Miles-Lukovsky infinite-dimensional modal system of ordinary differential equations from previous section then simplifies and takes the following form

$$\sum_{i=1}^{\infty} \frac{\partial A_n}{\partial \beta_i}\dot{\beta}_i = \sum_{k=1}^{\infty} R_k A_{nk} = 0, \quad n = 1,2,\ldots; \tag{3.5}$$

$$\sum_{n=1}^{\infty} \dot{R}_n \frac{\partial A_n}{\partial \beta_i} + \frac{1}{2}\sum_{n=1}^{\infty}\sum_{k=1}^{\infty} \frac{\partial A_{nk}}{\partial \beta_i} R_n R_k + \dot{\omega}\frac{\partial l_{2\omega}}{\partial \beta_i} + \omega\frac{\partial l_{2\omega t}}{\partial \beta_i} - \frac{d}{dt}\left(\omega\frac{\partial l_{2\omega t}}{\partial \dot{\beta}_i}\right)$$
$$+ (\dot{v}_{O1} - g_1 + \omega v_{O3})\frac{\partial l_1}{\partial \beta_i} + (\dot{v}_{O3} - g_3 - \omega v_{O1})\frac{\partial l_3}{\partial \beta_i} - \frac{1}{2}\omega^2\frac{\partial J^1_{22}}{\partial \beta_i} = 0, \tag{3.6}$$

where, when dividing the equations by ρ, the nonlinear quantities with respect to the generalised hydrodynamic coordinates are as follows

$$A_n = \int\limits_{Q(t)} \varphi_n\,dxdz; \quad A_{nk} = A_{kn} = \int\limits_{Q(t)} \nabla\varphi_n \cdot \nabla\varphi_k\,dxdz, \tag{3.7}$$

$$\frac{\partial l_3}{\partial \beta_i} = \int\limits_{\Sigma_0} f_i^2 dx\, \beta_i = \lambda_{3i}\beta_i; \qquad \frac{\partial l_1}{\partial \beta_i} = \int\limits_{\Sigma_0} x f_i^2\, dx = \lambda_{1i}. \tag{3.8}$$

$$l_{2\omega} = \int\limits_{Q(t)} \Omega\, dxdz; \quad l_{2\omega t} = \int\limits_{Q(t)} \frac{\partial \Omega}{\partial t}\, dxdz, \tag{3.9}$$

$$J^1_{22} = \int\limits_{Q(t)} \left(z\frac{\partial \Omega}{\partial x} - x\frac{\partial \Omega}{\partial z} \right) dxdz. \tag{3.10}$$

3.3. Single-dominant asymptotic nonlinear modal equations for two-dimensional resonant sloshing in a rectangular tank

Following the classical paper [3], let us consider a mobile rectangular rigid tank of the width L filled partly by an inviscid incompressible liquid with a finite (non-small) mean liquid depth. In contrast to dimensional consideration in [3], we derive a single-dominant asymptotic nonlinear modal equations with respect to the L-scaled generalised hydrodynamic coordinates. The derivation will be done by simplifying the Miles-Lukovsky modal system (3.5), (3.6).

As above, the two–dimensional liquid flow are irrotational. The origin of the tank-fixed coordinate system is located at the center of the mean tank surface. The equation $z = \zeta(x,t)$ determines the perturbed free surface $\Sigma(t)$ so that non-dimensional liquid domain is as follows

$$Q(t) = \{(x,z) : -h < z < \zeta(x,t); -\tfrac{1}{2} < x < \tfrac{1}{2}\}, \tag{3.11}$$

where the nondimensional liquid depth is

$$h := \frac{h}{L} = O(1). \tag{3.12}$$

The natural sloshing modes $\varphi_i(x,z)$ and $f_i(x)$ comes from the spectral

boundary problem (2.44) which takes the form

$$\begin{gathered}\Delta\varphi_i = 0 \quad (-\tfrac{1}{2} < x < \tfrac{1}{2},\ -h < z < 0);\\ \left.\frac{\partial\varphi_i}{\partial x}\right|_{x=\pm\frac{1}{2}} = 0; \quad \left.\frac{\partial\varphi_i}{\partial z}\right|_{z=-h} = 0; \quad \left.\frac{\partial\varphi_i}{\partial z}\right|_{z=0} = \kappa_i\varphi_i;\\ \int\limits_{-1/2}^{1/2} \varphi_i|_{z=0}\, dx = 0\end{gathered} \tag{3.13}$$

and has the analytical solution

$$\begin{gathered}\kappa_i = \pi i \tanh(i\pi h); \quad \sigma_i^2 = \frac{g}{L}\kappa_i,\\ f_i(x) = \cos(\pi i(x+\tfrac{1}{2})); \quad \varphi_i(x,z) = f_i(x)\frac{\cosh(\pi i(z+h))}{\cosh(\pi i h)},\end{gathered} \tag{3.14}$$

which obviously satisfies the volume conservation condition

$$\int\limits_{-1/2}^{1/2} f_i(x)\, dx = 0. \tag{3.15}$$

The natural sloshing modes (3.14) should be substituted into the modal representations (3.2) and (3.3) to derive the modal equations (3.5), (3.6).

The latter equations can be simplified by assuming small-amplitude periodic excitations of the container by the body-motion generalized coordinates

$$\eta_1 \sim \eta_3 \sim \eta_5 = O(\epsilon) \ll 1 \tag{3.16}$$

so that, according to assumptions of the two-dimensional sloshing and neglecting the $o(\epsilon)$-terms, alike in the linear theory with (2.47), one can exclude the forcing terms in (3.5), (3.6) provided the generalised hydrodynamic coordinates and velocities are asymptotically small but, due to the resonance, can be of the lower asymptotic order than $O(\epsilon)$.

By keeping only terms up to highest asymptotic order $O(\epsilon)$ in the nonlinear modal system (3.5) and (3.6) we get (3.5) unchanged but (3.6) reads as

$$\sum_n \dot{R}_n \frac{\partial A_n}{\partial\beta_i} + \frac{1}{2}\sum_n\sum_k \frac{\partial A_{nk}}{\partial\beta_i} R_n R_k + \dot{\omega}\frac{\partial l_{2\omega}}{\partial\beta_i} + \omega\frac{\partial l_{2\omega t}}{\partial\beta_i} - \frac{d}{dt}\left(\omega\frac{\partial l_{2\omega t}}{\partial\dot{\beta}_i}\right)$$

$$+ (\dot{v}_{O1} - g_1)\lambda_{i1} - g_3\beta_i\lambda_{i3} = 0, \quad (3.17)$$

where

$$v_{O1} = \dot{\eta}_1; \quad g_3 = -\frac{g}{L}; \quad g_1 = \frac{g}{L}\eta_5(t). \quad (3.18)$$

and

$$\begin{aligned} \lambda_{i1} &= \int\limits_{-1/2}^{1/2} x\cos(i\pi(x+\tfrac{1}{2}))dx = \left(\frac{1}{i\pi}\right)^2((-1)^i - 1), \\ \lambda_{i3} &= \int\limits_{-1/2}^{1/2} \cos^2(i\pi(x+\tfrac{1}{2}))dx = \frac{1}{2} \end{aligned} \quad (3.19)$$

but

$$\frac{\partial l_{2\omega}}{\partial\beta_i}, \quad \frac{\partial l_{2\omega t}}{\partial\beta_i}, \quad \frac{\partial l_{2\omega t}}{\partial\dot{\beta}_i}$$

should be kept up to the $O(1)$ order by solving the problem on the Stokes-Joukowski potential Ω which comes from the boundary value problem (3.4) and parametrically depends on $\beta_i(t)$.

Because $\partial l_{2\omega}/\partial\beta_i$ and $\partial l_{2\omega t}/\partial\beta_i$ are multiplied by the forcing terms of the order $O(\epsilon)$ in (3.17), it is sufficient to include only linear terms in β_i in the integrals $l_{2\omega}$ and $l_{2\omega t}$. The problem (3.4) in a rectangular tank then takes the following form

$$\begin{aligned} &\Delta\Omega = 0 \ \text{ in } \ Q(t); \quad \left.\frac{\partial\Omega}{\partial z}\right|_{z=-h} = -x, \\ &\left.\frac{\partial\Omega}{\partial x}\right|_{x=\pm\frac{1}{2}} = z; \quad \left.\frac{\partial\Omega}{\partial n}\right|_{z=\zeta(x,t)} = -x\frac{1}{\sqrt{1+(\zeta_x)^2}} - z\frac{\zeta_x}{\sqrt{1+(\zeta_x)^2}}, \end{aligned} \quad (3.20)$$

whose zero-order approximation can be found by substitution of

$$\Omega = xz - 2\sum_{i=1}^{\infty} a_i f_i \frac{\sinh(\pi i(z+h/2))}{\cosh(\pi i h/2)} + \sum_{i=1}^{\infty}\chi_i(t) f_i \frac{\cosh(\pi i(z+h))}{\cosh(\pi i h)} \quad (3.21)$$

that computes a_i and $\chi_i(t) \equiv 0, \ i \geq 1$ in the lowest-order approximation ($\beta_i \equiv 0, \ i \geq 1$), i.e.,

$$\sum_{i=1}^{N} a_i f_i i\pi = x \quad \text{or} \quad a_i = \frac{2}{(i\pi)^3}[(-1)^i - 1]. \quad (3.22)$$

The functions $\chi_i(t)$ follow from (3.20) after substitution of (3.21) and (3.22) and performing Taylor series technique for free surface $\Sigma(t)$ (with respect to β_i). The linear terms of $l_{2\omega}$ and $l_{2\omega t}$ do not depend on $\chi_i(t)$. To show this we substitute (3.21) into the corresponding integrals

$$l_{2\omega} = -2\sum_{i=1}^{\infty} a_i \tanh\left(\tfrac{1}{2}i\pi h\right)\ \beta_i \int_{-1/2}^{1/2} f_i^2 dx + \sum_{i=1}^{\infty} \chi_i(t)\frac{1}{i\pi}\tanh(i\pi h)\int_{-1/2}^{1/2} f_i dx; \quad (3.23)$$

$$l_{2\omega t} = \sum_{j=1}^{\infty} \dot{\chi}(t)\frac{1}{i\pi}\tanh(i\pi h)\int_{-1/2}^{1/2} f_i dx. \quad (3.24)$$

It follows from the volume conservation condition (3.15) that

$$l_{2\omega t} = 0; \quad l_{2\omega} = -2\sum_{i=1}^{\infty} \beta_i \left(\frac{1}{i\pi}\right)^3 [(-1)^i - 1]\tanh\left(\frac{i\pi}{2}h\right) \quad (3.25)$$

and

$$\frac{\partial l_{2\omega t}}{\partial \beta_i} = 0; \quad \frac{\partial l_{2\omega}}{\partial \beta_i} = -2\left(\frac{1}{i\pi}\right)^3 [(-1)^i - 1]\tanh\left(\frac{i\pi}{2}h\right), \quad i \geq 1. \quad (3.26)$$

Finally, by remembering that angular position of the mobile coordinate system $Oxyz$ with respect to $O'x'y'z'$ is $\eta_5(t)$ we get correctly to $O(\epsilon)$ that the forcing terms in (3.17) are

$$\ddot{\eta}_5 \frac{\partial l_{2\omega}}{\partial \beta_i} + (-g_3)\beta_i\lambda_{3i} + (-g_1)\lambda_{1i}$$

caused by the pitch excitations can be rewritten as

$$-\left(\frac{1}{i\pi}\right)^2 [(-1)^i - 1]\left(\frac{2}{i\pi}\tanh\left(\frac{i\pi}{2}h\right)\ddot{\eta}_5(t) + \frac{g}{L}\eta_5(t)\right) + \frac{g}{L}\beta_i. \quad (3.27)$$

One can see that, as it happened in the linear sloshing theory, the forcing terms do not depend on the vertical excitations associated with the generalised coordinate $\eta_3(t)$.

Further, we consider two-dimensional weakly-nonlinear liquid sloshing in a rectangular tank of the width L and breadth B in fully non-dimensional statement so that, as earlier, L is the characteristic size and $T = 2\pi/\sigma_1$ is the characteristic time, where σ_1 is the lowest natural sloshing [circular] frequency by (3.14). In addition, as in [3], the container is filled with a finite liquid depth which means that the non-dimensional (L-scaled) depth $h \gtrsim 0.4$ [1, Chapter 8]. The tank oscillates with a small amplitude and the mean forcing frequency σ close to σ_1.

The classical paper [3] showed that, if the forcing amplitude is relatively small, the nonlinear resonant sloshing can be described by employing the so-called single-dominant nonlinear modal system. The paper derives this system by using the so-called Moiseev-Narimanov asymptotics where the hydrodynamic generalised coordinates $\beta_i(t)$ are small, appear in the functional [modal] representation of the free surface and possess the following asymptotics

$$z = \zeta(x,t) = \sum_{i=1}^{\infty} \beta_i(t) \cos(\pi i(x + \tfrac{1}{2})), \tag{3.28a}$$

$$\beta_1 = O(\epsilon^{1/3});\ \beta_2 = O(\epsilon^{2/3});\ \beta_3 = O(\epsilon);\ \beta_n \lesssim O(\epsilon),\quad n \geq 4, \tag{3.28b}$$

in which

$$\eta_1 \sim \eta_5 = O(\epsilon) \tag{3.29}$$

from (3.16).

The asymptotics (3.28b) is a consequence of the trigonometric algebra in (3.28a).

Asymptotic expansions of integrals A_i, A_{nk} have to be used to derive the single-dominant modal system from the modal equations (3.5), (3.17), (3.27). The functions A_i and A_{nk} are defined as integrals over the instantaneous liquid domain. Keeping terms up to ϵ gives

$$A_1 = \frac{1}{2}(\beta_1 + E_1(\beta_1\beta_2 + \beta_2\beta_3) + E_0(\beta_1^3 + 2\beta_1\beta_2^2 + \beta_1^2\beta_3)),$$

$$A_2 = \frac{1}{2}(\beta_2 + E_2(\beta_1^2 + 2\beta_1\beta_3) + 8E_0\beta_1^2\beta_2),$$

$$A_3 = \frac{1}{2}(\beta_3 + 3E_3\beta_1\beta_2 + 3E_0\beta_1^3); \tag{3.30}$$

$$A_{11} = (E_1 + 8E_1E_0\beta_1^2 - (2E_0 - E_1^2)\beta_2), \quad A_{22} = (2E_2),$$
$$A_{12} = A_{21} = ((4E_0 + 2E_1E_2)\beta_1 + (-4E_0 + 2E_1^2)\beta_3); \quad A_{33} = \rho 3E_3,$$
$$A_{13} = A_{31} = 3\rho(2E_0 + E_1E_3)(\beta_2 + 2E_4\beta_1^2),$$
$$A_{23} = A_{32} = 3\rho(4E_0 + 2E_2E_3)\beta_1, \quad (3.31)$$

in which

$$E_0 = \frac{1}{8}\pi^2; \qquad E_i = \frac{\pi}{2}\tanh(\pi i h), \quad i \geq 1. \quad (3.32)$$

Further, we express R_n as

$$R_n = \sum_i \gamma_i \dot{\beta}_i + \sum_{ij} \gamma_{ij} \dot{\beta}_j \beta_i + \sum_{ijk} \gamma_{ijk} \dot{\beta}_i \beta_j \beta_k + ...$$

and substitute it in (3.5). Explicit values of $\gamma_i, \gamma_{ij}, \gamma_{ijk}$ are found by gathering similar terms. The result is

$$R_1 = \frac{\dot{\beta}_1}{2E_1} + \frac{E_0}{E_1^2}\dot{\beta}_1\beta_2 - \frac{E_0}{E_1E_2}\dot{\beta}_2\beta_1 + \frac{E_0}{E_1}\left(-\frac{1}{2} + \frac{4E_0}{E_1E_2}\right)\beta_1^2\dot{\beta}_1,$$
$$R_2 = \frac{1}{4E_2}\left(\dot{\beta}_2 - \frac{4E_0}{E_1}\beta_1\dot{\beta}_1\right),$$
$$R_3 = \frac{\dot{\beta}_3}{6E_3} - \frac{E_0}{E_1E_3}\dot{\beta}_1\beta_2 - \frac{E_0}{E_2E_3}\dot{\beta}_2\beta_1$$
$$+ \dot{\beta}_1\beta_1^2\left(\frac{3E_2}{2E_3} - \frac{2E_0E_4}{E_1E_3} - E_4 + \frac{4E_0^2}{E_1E_2E_3} + \frac{2E_0E_2}{E_1E_3}\right);$$
$$R_i = \frac{\dot{\beta}_i}{2iE_i}, \quad i \geq 4 \quad (3.33)$$

and

$$\dot{R}_1 = \frac{\ddot{\beta}_1}{2E_1} + \frac{E_0}{E_1^2}\ddot{\beta}_1\beta_2 - \frac{E_0}{E_1E_2}\ddot{\beta}_2\beta_1 + \dot{\beta}_1\dot{\beta}_2\left(\frac{E_0}{E_1^2} - \frac{E_0}{E_1E_2}\right) + \frac{E_0}{E_1}\left(-\frac{1}{2} + \frac{4E_0}{E_1E_2}\right)\beta_1^2\ddot{\beta}_1$$
$$+ 2\frac{E_0}{E_1}\left(-\frac{1}{2} + \frac{4E_0}{E_1E_2}\right)\dot{\beta}_1^2\beta_1,$$
$$\dot{R}_2 = \frac{1}{4E_2}\left(\ddot{\beta}_2 - \frac{4E_0}{E_1}(\beta_1\ddot{\beta}_1 + \dot{\beta}_1^2)\right),$$
$$\dot{R}_3 = \frac{\dot{\beta}_3}{6E_3} - \frac{E_0}{E_1E_3}\ddot{\beta}_1\beta_2 - \frac{E_0}{E_2E_3}\ddot{\beta}_2\beta_1 - \left(\frac{E_0}{E_1E_3} + \frac{E_0}{E_2E_3}\right)\dot{\beta}_1\dot{\beta}_2$$
$$+ (\ddot{\beta}_1\beta_1^2 + 2\dot{\beta}_1^2\beta_1)\left(\frac{3E_2}{2E_3} - \frac{2E_0E_4}{E_1E_3} - E_4 + \frac{4E_0^2}{E_1E_2E_3} + \frac{2E_0E_2}{E_1E_3}\right);$$

$$\dot{R}_i = \frac{\ddot{\beta}_1}{2iE_i}, \quad i \geq 4. \quad (3.34)$$

When substituting above formulas in (3.17), we get the following system of ordinary differential equations asymptotically, up to the $O(\epsilon)$-terms describing the resonant liquid sloshing in rectangular tank performing small magnitude motions with the mean frequency close to the lowest natural sloshing frequency

$$\ddot{\beta}_1 + \beta_1 + d_1(\ddot{\beta}_1\beta_2 + \dot{\beta}_1\dot{\beta}_2) + d_2(\ddot{\beta}_1\beta_1^2 + \dot{\beta}_1^2\beta_1) + d_3\ddot{\beta}_2\beta_1 + P_1\left(\ddot{\eta}_1 - S_1\ddot{\eta}_5 - \frac{1}{2E_1}\eta_5\right) = 0, \quad (3.35a)$$

$$\ddot{\beta}_2 + \bar{\sigma}_2^2\beta_2 + d_4\ddot{\beta}_1\beta_1 + d_5\dot{\beta}_1^2 = 0, \quad (3.35b)$$

$$\ddot{\beta}_3 + \bar{\sigma}_3^2\beta_3 + d_6\ddot{\beta}_1\beta_2 + d_7\ddot{\beta}_1\beta_1^2 + d_8\ddot{\beta}_2\beta_1 + d_9\dot{\beta}_1\dot{\beta}_2 + d_{10}\dot{\beta}_1^2\beta_1 + P_3\left(\ddot{\eta}_1 - S_3\ddot{\eta}_5 - \frac{1}{6E_3}\eta_5\right) = 0 \quad (3.35c)$$

when the linear equations

$$\ddot{\beta}_i + \bar{\sigma}_i^2\beta_i + P_i(\dot{v}_{0x} - S_i\dot{\omega} - g\psi) = 0, \quad i \geq 4 \quad (3.36)$$

describe the higher hydrodynamic generalised coordinates. Here, the introduced hydrodynamic coefficients are calculated by the formulas

$$\bar{\sigma}_i^2 = \frac{\sigma_i^2}{\sigma_1^2} = \frac{iE_i}{E_1}; \quad P_{2i-1} = -\frac{8E_{2i-1}}{\pi^2(2i-1)}, \quad P_{2i} = 0,$$
$$S_i = \frac{2}{\pi i}\tanh\left(\frac{i\pi}{2}h\right), \quad i \geq 1, \quad (3.37)$$

where

$$d_1 = 2\frac{E_0}{E_1} + E_1; \quad d_2 = 2E_0\left(-1 + \frac{4E_0}{E_1E_2}\right); \quad d_3 = -2\frac{E_0}{E_2} + E_1,$$

$$d_4 = -4\frac{E_0}{E_1} + 2E_2; \quad d_5 = E_2 - 2\frac{E_0E_2}{E_1^2} - \frac{4E_0}{E_1}; \quad d_6 = 3E_3 - \frac{6E_0}{E_1},$$

$$d_7 = 9E_0 - 12\frac{E_0E_4}{E_1} - 6E_3E_4 + 24\frac{E_0^2}{E_1E_2} + 3\frac{E_0E_3}{E_1}; \quad d_8 = -6\frac{E_0}{E_2} + 3E_3,$$

$$d_9 = -6\frac{E_0}{E_1} - 6\frac{E_0}{E_2} - 6\frac{E_0E_3}{E_1E_2} + 3\frac{E_3E_1}{E_2},$$

$$d_{10} = 18E_0 - 2E_4\frac{12E_0 + 6E_1E_3}{E_1} + \frac{72E_0^2}{E_1E_2} + 12E_0\left(\frac{E_3}{E_1} - \frac{E_1}{E_2}\right). \quad (3.38)$$

The first two nonlinear equations of (3.35) couple β_1 with β_2 and do not depend on β_3. The third generalised hydrodynamic coordinate is excited by rigid body motions and depends on the first and second ones.

3.4. The damped single-dominant modal equations for longitudinal harmonic excitations

Consider longitudinal harmonic forcing with the nondimensional forcing frequency

$$\bar{\sigma} = \frac{\sigma}{\sigma_1}$$

and assume that there exists the viscous damping in the hydrodynamic system.

When the resonant sloshing is described by the single-dominant modal system (3.35), the latter reduces to the form

$$\ddot{\beta}_1 + \beta_1 + \boxed{2\xi_1\left[\dot{\beta}_1 + \Xi_1(\beta_m, \dot{\beta}_m|_{m=1,2})\right]} + d_1(\ddot{\beta}_1\beta_2 + \dot{\beta}_1\beta_2) + d_2(\ddot{\beta}_1\beta_1^2 + \dot{\beta}_1^2\beta_1) + d_3\ddot{\beta}_1\beta_1 = P_1\eta_{1a}\bar{\sigma}^2\cos(\bar{\sigma}t - \theta), \quad (3.39a)$$

$$\ddot{\beta}_2 + \bar{\sigma}_2^2\beta_2 + \boxed{2\bar{\sigma}_2\xi_2\left[\dot{\beta}_2 + \Xi_2(\beta_m, \dot{\beta}_m|_{m=1,2})\right]} + d_4\ddot{\beta}_1\beta_1 + d_5\dot{\beta}_1^2 = 0, \quad (3.39b)$$

$$\ddot{\beta}_3 + \bar{\sigma}_2^2\beta_3 + \boxed{2\bar{\sigma}_3\xi_3\left[\dot{\beta}_3 + \Xi_3(\beta_m, \dot{\beta}_m|_{m=1,2})\right]} + d_6\ddot{\beta}_1\beta_2 + d_7\ddot{\beta}_1\beta_1^2 + d_8\ddot{\beta}_2\beta_1 + d_9\dot{\beta}_1^2\beta_1 + d_{10}\dot{\beta}_1\dot{\beta}_2 = P_3\eta_{1a}\bar{\sigma}^2\cos(\bar{\sigma}t - \theta), \quad (3.39c)$$

$$\ddot{\beta}_n + \bar{\sigma}_n^2\beta_n + \boxed{2\bar{\sigma}_n\xi_n\dot{\beta}_2} = P_n\eta_{1a}\bar{\sigma}^2\cos(\bar{\sigma}t - \theta), \quad n \geq 4, \quad (3.39d)$$

where

$$\bar{\sigma}_i^2 = \frac{\sigma_i^2}{\sigma_1^2} = i\frac{\tanh(\pi i h)}{\tanh(\pi h)}; \quad P_i = \frac{2}{\pi i}\tanh(\pi i h)((-1)^i - 1) \quad (3.40)$$

but the hydrodynamic coefficients d_n depend on the non-dimensional liquid depth h. Further,

$$\eta_{1a} = O(\epsilon) \ll 1$$

is the non-dimensional forcing amplitude, and θ is the phase lag in the external horizontal harmonic forcing. The computed values of the hydrodynamic coefficients are tabled by [1, Chapter 8]. A novelty is the framed damping terms incorporated into the modal system.

Because (3.39) is based on the Narimanov-Moiseev asymptotic relations (3.28b) with neglecting the $o(\epsilon)$-order quantities, only β_1 and β_2 are nonlinearly coupled (there is an energy flow between these two lowest natural sloshing modes), β_3 is the 'driven' generalised hydrodynamic coordinate of the highest asymptotic order $O(\epsilon)$ but the higher natural sloshing modes, $n \geq 4$, are considered within the framework of the linear theory.

The same asymptotic relationships should be true for the incorporated *a priori* unknown damping terms, where Ξ_i are nonlinear function of the generalised hydrodynamic coordinates. Whereas $\eta_{1a} = 0$ (free oscillations), ξ_i, $i \geq 1$ can be associated with logarithmic decrements of the natural [Stokes] sloshing modes $\cos(\pi i(x + \frac{1}{2}))$ in (3.28a). The damping ratios ξ_i should be small for low-viscous liquids and, because our nonlinear analysis mainly centres around the two nonlinearly-coupled generalised coordinates, β_1 and β_1, one can assume, as the 'worse' case, that $\xi_1 \sim \xi_2$ possess the the lowest possible asymptotic order, i.e.,

$$\xi_1 \sim \xi_2 = O(\epsilon^{1/3}). \tag{3.41}$$

Furthermore, because the asymptotic modal theory neglects the $o(\epsilon)$-order contribution in (3.39), one concludes

$$\Xi_3 = \Xi_2 = 0 \quad \text{but} \quad \Xi_1 = \Xi_1(\beta_1, \dot{\beta}_1) \tag{3.42}$$

is a *quadratic* function, which we do not know *a priori* as well as the linear damping rates ξ_i.

This proves the first main theorem of the chapter:

Theorem 3.1. *Under assumption (3.41) on the viscous damping terms implying the boundary layer possesses the lowest-order amplitude of the single-dominant modal theory, the nonlinear differential equations of this theory with the damping terms (3.39) lead to (3.42) where* Ξ_1 *is a quadratic function.*

3.5. Steady-state resonant waves

The steady-state resonant sloshing is associated with periodic solutions of (3.39). Following Moiseev' asymptotic scheme [1, Chapter 8], one can find an asymptotic approximation of these solutions even if (3.39) is equipped with the damping terms. In the Moiseev's approximation, the lowest-order generalised hydrodynamic coordinates β_1 and β_2 take the form

$$\begin{aligned}\beta_1(t) &= a\cos(\bar{\sigma}t) + O(a^3),\\ \beta_2(t) &= a^2[l_0 + l_1\cos(2\bar{\sigma}t) + l_2\sin(2\bar{\sigma}t)] + O(a^3),\end{aligned} \tag{3.43}$$

where $a = O(\epsilon^{1/3}) > 0$ is the dominant wave amplitude,

$$\begin{aligned}l_0 &= \frac{d_4 - d_5}{2\bar{\sigma}_2^2},\\ l_1(\xi_2) &= \frac{(d_4 + d_5)(\bar{\sigma}_2^2 - 4)}{2((\bar{\sigma}_2^2 - 4)^2 + 16\bar{\sigma}_2^2\xi_2^2)},\\ l_2(\xi_2) &= \frac{2(d_4 + d_5)\bar{\sigma}_2\xi_2}{(\bar{\sigma}_2^2 - 4)^2 + 16\bar{\sigma}_2^2\xi_2^2};\end{aligned}$$

$a > 0$ and θ come from the so-called secular system

$$\begin{cases} a\left(m_1(\xi_2)a^2 + \hat{\sigma}^2 - 1\right) = \epsilon\cos\theta,\\ a\left(m_2(\xi_2)a^2 - 2\xi_1[1 + \xi a]\right) = \epsilon\sin\theta,\end{cases} \tag{3.44}$$

which is derived after substituting (3.43) into (3.39a) and collecting all quantities at $\cos(\bar{\sigma}t)$ and $\sin(\bar{\sigma}t)$; here,

$$\begin{aligned}m_1(\xi_2) &= -\tfrac{1}{2}d_2 - 2d_3l_1 + d_1(-l_0 + \tfrac{1}{2}l_1),\\ m_2(\xi_2) &= \tfrac{1}{2}l_2(d_1 - 4d_3), \quad \hat{\sigma} = \bar{\sigma}^{-1}\end{aligned}$$

and

$$\xi = -\frac{\bar{\sigma}}{\pi}\int_0^{2\pi/\bar{\sigma}} \Xi_1(\cos(\bar{\sigma}t), -\sin(\bar{\sigma}t))\sin(\bar{\sigma}t)dt \geq 0, \tag{3.45}$$

remembering that, from physical reasons,

$$\frac{\bar{\sigma}}{\pi}\int_0^{2\pi/\bar{\sigma}} \Xi_1(\cos(\bar{\sigma}t), -\sin(\bar{\sigma}t))\cos(\bar{\sigma}t)dt = 0. \tag{3.46}$$

Taking the sum of squares in (3.44) makes it possible to rewrite (3.44) to

$$a^2\left[\left(m_1(\xi_2)a^2 + (\hat{\sigma}^2 - 1)\right)^2 + \left(m_2(\xi_2)a^2 - 2\xi_1(1+\xi a)\right)^2\right] = \epsilon^2, \tag{3.47a}$$

$$\theta = \text{atan2}\left([m_2(\xi_2)a^2 - 2\xi_1(1+\xi a)],\ [m_1(\xi_2)a^2 + (\hat{\sigma}^2 - 1)]\right), \tag{3.47b}$$

which can be solved to get the phase-lag response curve in the $(\bar{\sigma}_1, \theta)$ plane. Indeed, (3.47a) gives

$$\begin{aligned}\bar{\sigma}^{-2}(a;\xi_1,\xi_2,\xi,\epsilon) &= \hat{\sigma}^2(a;\xi_1,\xi_2,\xi,\epsilon)\\ &= 1 - m_1(\xi_2)a^2 \pm \sqrt{\frac{\epsilon^2}{a^2} - [m_1(\xi_2)a^2 - 2\xi_1(1+\xi a)]^2},\end{aligned} \tag{3.48}$$

which has the physical meaning when both the right-hand side and expression under the square root are non-negative that yields the left and right bounds in

$$a_{\min}(\xi_1,\xi_2,\xi,\epsilon) \leq a \leq a_{\max}(\xi_1,\xi_2,\xi,\epsilon). \tag{3.49}$$

Furthermore, inserting (3.48) into (3.47b) derives

$$\begin{aligned}&\theta(a;\xi_1,\xi_2,\xi,\epsilon)\\ &\quad = \text{atan2}\left[m_2(\xi_2)a^2 - 2\xi_1(1+\xi a), m_1(\xi_2)a^2 + (\hat{\sigma}^2(a;\xi_1,\xi_2,\xi,\epsilon) - 1\right].\end{aligned} \tag{3.50}$$

As a consequence, when considering a in the interval (3.49) for fixed ξ_1, ξ_2, ξ, and ϵ, (3.48) and (3.50) parametrically define both the phase-lag response curve in the $(\bar{\sigma}, \theta)$-plane and the wave-amplitude response curve in the $(\bar{\sigma}, a)$-plane.

As matter of the fact, the following theorem is proved:

Theorem 3.2. *Under assumptions of Theorem 3.1, the ordinary differential equations of the single-dominant modal theory (3.39) have the asymptotic periodic solution whose dominant amplitude a in the lowest-order approximation (3.43), the unknown phase lag θ and the non-dimensional forcing frequency $\bar{\sigma}$ are coupled by the secular (solvability) equations (3.44) in which m_1 and m_2 and functions of h and ξ is coefficients following from integration of the quadratic term (3.45). The secular equations have analytical solution which gives the non-dimensional forcing amplitude $\bar{\sigma}$ (3.48) and the phase lag θ (3.50) the functions of the amplitude parameter a, (3.49).*

3.6. Learning the damping-related coefficients

The unknowns ξ_1, ξ_2, and ξ can be deduced from a set of experimental measurements by implementing a machine learning technique.

Let us consider the measured pairs $(\bar{\sigma}_1^{(i,n)}, \theta_i^{(n)})$ for the given forcing amplitudes

$$\epsilon_n = P_1 \eta_{2a}^{(n)}, \ n = 1, \ldots, N_{\eta_{2a}}.$$

Using (3.48)–(3.50), one can introduce the distance function D between the asymptotic theory and the fixed point $(\bar{\sigma}_1^{(i,n)}, \theta_i^{(n)})$ as follows

$$\begin{aligned} &D^2(n, i; \xi_1, \xi_2, \xi) \\ &= \min_{a_{\min} \le a \le a_{\max}} \left[\left(\bar{\sigma}(a; \xi_1, \xi_2, \xi, \epsilon_n) - \bar{\sigma}_1^{(i,n)} \right)^2 + \left(\theta(a; \xi_1, \xi_2, \xi, \epsilon_n) - \theta_i^{(n)} \right)^2 \right]. \end{aligned} \tag{3.51}$$

The 'total' distance function between all the measurement points $(\bar{\sigma}_1^{(i,n)}, \theta_i^{(n)})$ and the asymptotic prediction by (3.48)–(3.50) should be taken as the loss function

$$C(\xi_1, \xi_2, \xi) = \sum_{n=1}^{N_{\eta_{2a}}} \sum_i D(n, i; \xi_1, \xi_2, \xi) > 0. \tag{3.52}$$

The wanted parameters ξ_1, ξ_2 and ξ realise the absolute minimum of C. Minimising the loss function (3.52) can be done by using the gradient descent.

3.6.1. Employing the measured data by [11]. The experimental data on the liquid mass centre (horizontal steady-state wave amplitude and phase lag) were reported by [11]. Horizontal position of the liquid mass centre is, according to [1, Eq. (8.73)], described by

$$y_C(t) = -\frac{2}{\pi^2 h}\beta_1(t) + O(\epsilon) = -\frac{2}{\pi^2 h} a \cos \bar{\sigma} t + O(\epsilon). \tag{3.53}$$

This means that the theoretical steady-state phase lag and wave amplitude in experiments by [11] could in the lowest-order approximation be associated with θ and $2a/(\pi^2 h)$, respectively, coming from the asymptotic solution (3.48)–(3.50).

Experiments by [11] were done with the non-dimensional liquid depth $h = 0.8$ that implies (see, [1], Table 8.1):

$$d_2 = 3.142;\ d_2 = 2.533;\ d_3 = -0.021;\ d_4 = -0.042;\ d_5 = -3.225.$$

The forcing amplitudes $\eta_{2a} = 0.0009, 0.0017, 0.0032$, and 0.0064 were tested. At the same time, visual observations with $\eta_{2a} = 0.0064$ discovered wave breaking, overturning, and serious contribution of higher modes/harmonics that means that the single-dominant modal theory is not applicable for the experimental series with the largest forcing amplitude.

Utilizing three experimental series with $\eta_{2a} = 0.009, 0.0017$, and 0.0032 in the above-proposed 'machine learning technique' computes

$$\xi_1 = \xi_1^l = 0.007167965;\ \xi_2 = \xi_2^l = 0.01002107 \text{ and } \xi = \xi^l = 1.39803654.$$

Inserting these values into the asymptotic solution (3.48)–(3.50) draws the theoretical phase-lag response curves which are compared with measurements by [11] in Fig. 3.1 (a). The figure confirms applicability of the damped single-dominant modal theory (3.39) to fit the experimental data by [11]. Agreement is excellent, especially, in contrast to [11, Figure 14] who adopted in their computations by the single-dominant modal system $\xi_1 = \xi_1^{exp} = 8.4 \cdot 10^{-3}$ (coming from the measured logarithmic decrements) and $\xi_2 = \xi = 0$. The results in Fig. 3.1 (a) are also much better than with using the damped Duffing–type model by [11, Figure 13].

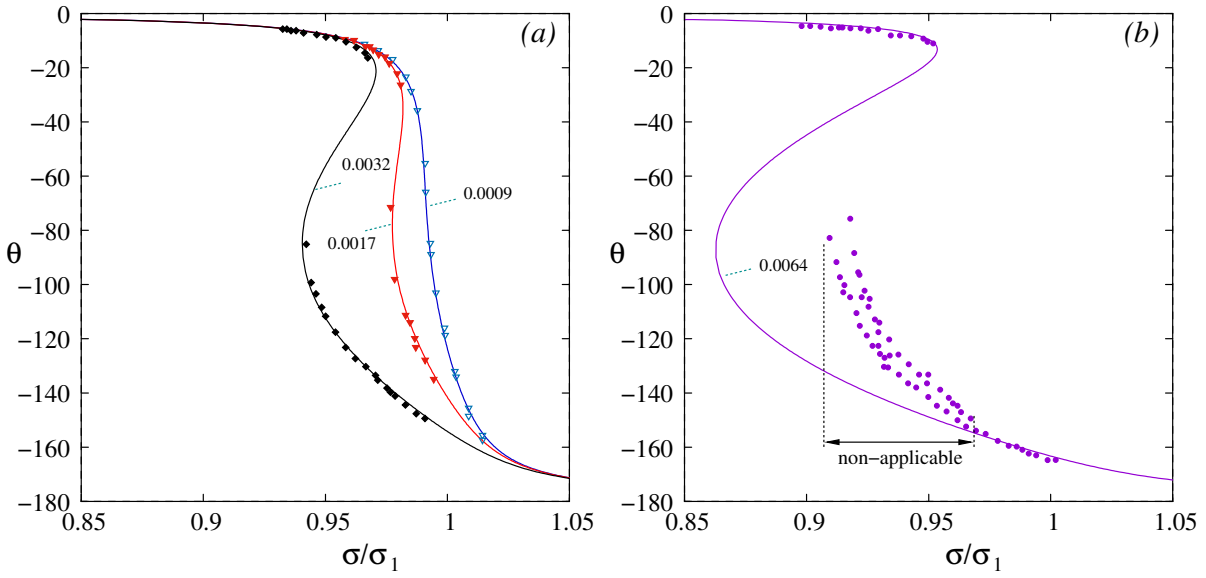

Figure 3.1. The theoretical (lines) and experimental (symbols) phase lag (in grads) response curves for the input parameters by [11]. The measured phase lag with the forcing amplitudes $\eta_{2a} = 0.0009$, 0.0017, and 0.0032 from the panel (a) were used to learn ξ_1, ξ_2 and ξ in the asymptotic solution (3.48)–(3.50) and compared with measurements by [11]. The computed damping coefficients are $\xi_1 = \xi_1^l = 0.007167965, \xi_2 = \xi_2^l = 0.01002107$ and $\xi = \xi^l = 1.39803654$. The panel (b) is drawn for the largest tested forcing amplitude $\eta_{2a} = 0.0064$ when the single-dominant modal system is, generally, not applicable; it detects a zone where this happens.

Even though, as we remarked above, the single-dominant modal system is, most probably, not applicable for the largest experimental forcing amplitude $\eta_{2a} = 0.0064$, the computed $\xi_1 = \xi_1^l, \xi_2 = \xi_2^l$ and $\xi = \xi^l$ were used in (3.48)–(3.50) with $\eta_{2a} = 0.0064$ to draw the theoretical phase-lag response curve and compare it with the measured phase lag θ. The results are shown in Fig 3.1 (b). The figure establishes a zone where the single-dominant modal theory is clearly non-applicable (wave breaking and other free-surface phenomena indeed matter!), discrepancy is here dramatically large. However, far from this zone, when experimental observations by [11] do not report on specific free-surface phenomena, the agreement is also excellent.

We used the asymptotic solution (3.48)–(3.50) to compare the theoretical mass-centre amplitude by (3.53) with measurements by [11]. The results are presented in Fig. 3.2, where the panel (a) is drawn for the cases from Fig. 3.1 (a) but (b) corresponds to the largest forcing amplitude $\eta_{2a} = 0.0064$. When analysing the results, one should remember that, according to [75], viscous damping weakly affects the resonant steady-state wave amplitude,

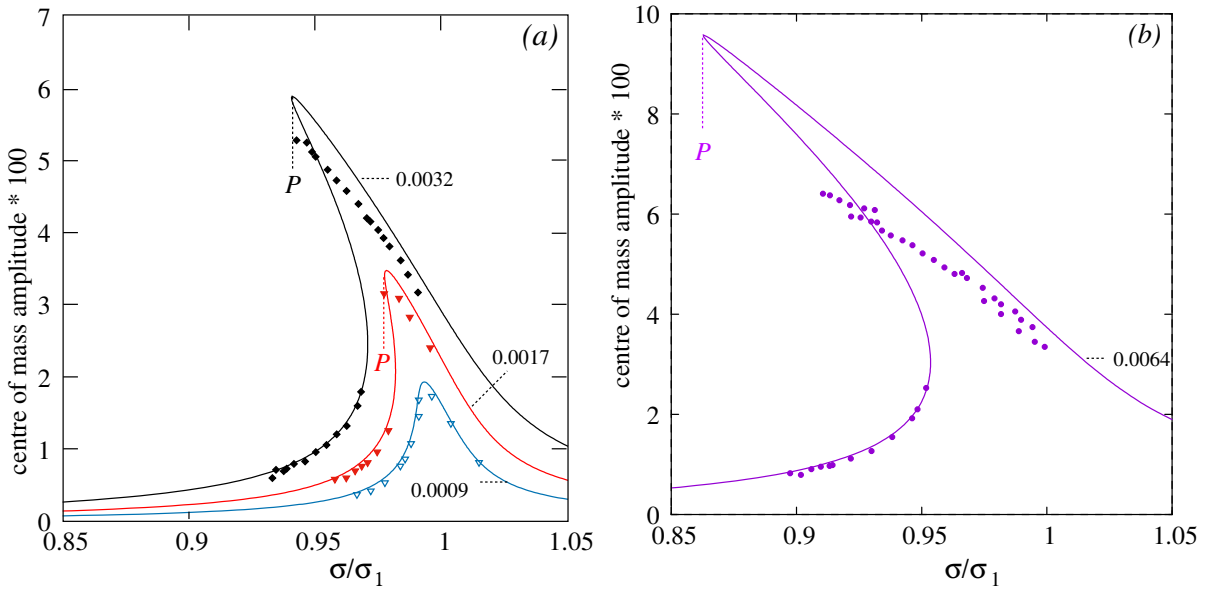

Figure 3.2. The same as in Fig. 3.1 but for the liquid mass-centre amplitude. Viscous damping is responsible for position of the jump-down bifurcation point P.

which is basically determined the free-surface nonlinearity and energy flow between the generalised hydrodynamic coordinates. However, viscous damping in both Duffing's and multimodal theories is responsible for horizontal position of the jump-down bifurcation point P.

In view of this fact, agreement between the 'learnt' asymptotic solution and measurements is very good in the panel (a). However, as it was expected, the analytical solution fails in the case (b). The paper [75] showed that if the single-dominant modal system overpredicts the steady-state wave amplitude response with increasing η_{2a} or at the critical depth, one should use an adaptive multimodal theory. For getting a better agreement in Figure 3.2 (a), one should generalise the proposed machine learning to the corresponding adaptive modal system.

3.6.2. Linear damping ratios. Neglecting nonlinear term in (3.39) leads to an infinite set of linear damped oscillators, the so-called linear modal theory by [1, Chapter 5], which is normally applicable for non-resonant sloshing of a low-viscous liquid. Furthermore, when posing $\eta_{2a} = 0$, its solution determines a superposition of decaying standing Stokes waves whose logarithmic decrements are associated with the linear damping ratios ξ_i.

Rigorous linear mathematical theory of viscous unforced sloshing was cre-

ated in [48]. Krein's theorem states that only a finite number of oscillatory sloshing modes exists, i.e., interpreting his result in term of the linear modal theory with $\eta_{2a} = 0$, there exists N such that $\xi_i > \bar{\sigma}_i$ for $i \geq N$. The latter fact contradicts to assumptions of the linear damped modal theory, which requires small ξ_i to weakly affect the natural sloshing frequencies and modes. Indeed, numerical analysis in [218] shows that only lower natural sloshing modes and frequencies of viscous liquids can be approximated within the framework of the inviscid hydrodynamic theory. In terms of the present damped multimodal theory, one must require $\xi_i \ll \bar{\sigma}_i$ on the corresponding asymptotic scale. Now, readers may understand why we postulated the asymptotic condition

$$O(\epsilon^{1/3}) = \xi_i \ll \bar{\sigma}_i = O(1), \ i = 1, 2,$$

that caused the main Theorem 3.1.

When associating ξ_i with logarithmic decrements of the (lower) natural sloshing modes of a low-viscous liquid, the corresponding linear damping ratios ξ_i can be estimated from below [1, Chapter 6] by using asymptotic formulas based on the laminar boundary layer theory and accounting for the bulk damping effects, $\xi_i^{(0)} = \xi_i^{layer} + \xi_i^{bulk} \lesssim \xi_i$. The papers [219], [160], and [1, Chapter 6] discuss why the bulk damping may matter as well as how other potentially-valuable damping mechanisms incl. dynamic contact angle, wave breaking, free-surface contamination, and roof impact can significantly increase the damping. Taking Keulegan's estimate for ξ_i^{layer} and Eq. (6.139) by [1] for ξ_i^{bulk} gives (2.48). Specifically, the formula provides $\xi_i^0/\bar{\sigma}_i \to \infty$ but, as we stated below, it may be only valid for lower indices i for which $\xi_i^{(0)} \lesssim O(1)$.

For the experimental input in [11, $L = 0.5$ m, $B = 0.05$ m, and $h = 0.8$], (2.48) gives $\xi_1^{(0)} = 0.0057$ and $\xi_2^{(0)} = 0.0047$; the computed values are practically not affected by the bulk damping and, therefore, one can say that it is the Keulegan's approximation. The Keulegan's damping ratios are definitely lower than $\xi_1^l = 0.007167965$ and $\xi_2^l = 0.01002107$ coming from the machine learning procedure, which were deduced from the experimental phase lags with $\eta_{2a} = 0.0009, 0.0017$, and 0.0032. The inequality is correct

because (2.48) estimates ξ_i from below.

The authors [11] conducted special model tests attempting to estimate ξ_1. To do that, they interrupted the forcing of the steady-state wave with $\eta_{2a} = 0.0064$ by making $\eta_{2a} = 0$ at an instant $t = t_0$ and, thereafter, measured logarithmic decrements of the wave decay. The mean experimental value of ξ_1 coming from these tests was $\xi_1 = \xi_1^{exp} = 0.0084$, which is larger of $\xi_1^l = 0.007167965$ because of, most probably, very special free-surface phenomena discovered for steady-state sloshing with $\eta_{2a} = 0.0064$, which could affect the logarithmic decrement even after interrupting the harmonic forcing.

On the other hand, the theoretical linear damping rate of the second natural sloshing mode, $\xi_2^{(0)} = 0.0047$, seems too low with respect to $\xi_2^l = 0.01002107$. Remembering Fig. 3.2, the discrepancy may be explained by a rather inaccurate modelling of energy flow between the second and some higher modes. In other words, because viscous damping of the higher modes ($i \geq 3$) is not included into the single-dominant analysis, the computed value $\xi_2^l = 0.01002107$, in fact, tries to 'accumulate' the amount damping of all natural sloshing modes starting with $i = 2$. Using an adaptive modal system by [75] would lead to a more accurate distribution of $\xi_i,\ i \geq 2$ and improve agreement in Fig. 3.2 (a).

3.7. Conclusions to the chapter

An estimate of viscous damping in the liquid sloshing dynamics can be done by applying a machine learning technique to the Reduced Order Models which are a common in analytical studies of the resonant waves. Originally, the latter models appear as multi-dimensional modal systems without damping terms. Their learning consists of incorporating damping terms with unknown *a priori* coefficients and deducing the coefficients by using a set of experimental data on the steady-state liquid response, preferably, the response parameters must be chosen which are most sensible to the viscous damping. These can, for instance, be phase lags between the harmonic forcing and the steady-state waves.

The present chapter realizes this idea for the case of resonant sloshing in

a two-dimensional clean rectangular tank exposed to horizontal excitations with the forcing frequency close to the lowest natural sloshing frequency. This kind of resonant sloshing can satisfactory be described by the single-dominant asymptotic modal system [3] whose extensive analysis, for transient and steady-state sloshing can be found in the textbook [1]. The modal system becomes, however, invalid in modeling the phase lag response curves and, as it was shown in 2001 [75], when the secondary resonances in the hydrodynamic system matter.

In the present chapter, the single-dominant modal equations from [3] are re-derived and, furthermore, equipped with *a priori* unknown damping terms. Theorem 3.1 establishes analytical structure of these terms to fit the Narimanov-Moiseev–type asymptotics that is a basis of the single-dominant modal theory. Theorem 3.2 of the chapter deals with the steady-state wave (periodic) solution of the damped modal equations. The solution is analytically derived by using the Moiseev's asymptotic scheme.

The derived analytical solution becomes a function of three unknown parameters, ξ_1, ξ_2 and ξ which are responsible for damping in the hydrodynamic system. Having known experimental measurements of the phase lags makes it possible to compute the aforementioned three *a priori* unknown parameters. Measurements by [11] are employed by the author [215] to demonstrate abilities of the proposed machine learning procedure. In contrast to numerical exercises with damping coefficients in [11], an excellent agreement is demonstrated except when, according to visual observations in [11], the single-dominant system is not applicable.

One conclusion from our numerical results is a confirmation that damping effect of higher natural sloshing modes cannot be neglected. Reason is nonlinear energy transfer from the primary-excited to higher modes with forthcoming viscous damping of these modes. Furthermore, viscous damping of the primary-excited (first) natural sloshing mode should, generally speaking, be a function of the resonant wave amplitude and, moreover, for the considered case, this function is just the linear regression. Finally, the proposed learning technique can be an efficient tool for estimating the viscous

damping (logarithmic decrements) of the lowest (dominant) natural sloshing mode, but it fails for higher (order) natural sloshing modes. To get more accurate estimate of the linear damping rate ξ_2 (the second mode), one should use an adaptive multi-modal system from [75] where the asymptotics $\beta_1 \sim \beta_2$ is adopted. Such adaptive modal system is also required for better prediction of the resonance steady-state wave-amplitude response curves.

Derivations of the steady-state wave (periodic) solution does not require an exact expression for the nonlinear damping terms in the modal equations $\Xi_1(\beta_1, \dot{\beta}_1)$. According to Theorem 3.1, any analytical quadratic form of Ξ_1 is allowed if it deduces the two integrals (3.45) and (3.46). En example could be

$$\Xi_1(\beta_1, \dot{\beta}_1) = \frac{3\pi}{8}|\dot{\beta}_1|\,\dot{\beta}_1, \tag{3.54}$$

which physically implies the quadratic drag force. Based on experimental measurement in [3] and other authors, one should check whether (3.54) is applicable.

Chapter 4

Damped swirling-type resonant wave in a circular cylindrical tank

4.1. Introduction

The learning technique developed in the previous chapter for rectangular tanks can be extended to the case of an upright circular cylindrical container. When such a clean rigid container is resonantly excited at a frequency close to its lowest natural sloshing frequency, similar nonlinear interactions between the natural sloshing modes cause a kinetic energy flow from the primary excited mode to higher natural sloshing modes [1,220]. This nonlinear energy transfer, along with viscous damping, prevents an unbounded resonant wave response.

Specifically, the resonant sloshing in the upright circular base tank can demonstrate different types of steady-state regimes and even become chaotic in certain forcing frequency ranges. One from most attractive steady-state waves is the co-called swirling – rotary waves propagating along the tank wall counter- or co-clockwise. The swirling-type resonant wave is normally realized at the linear resonance zone, i.e., when the forcing frequency σ equals or is very close to the lowest natural sloshing frequency σ_1. This wave type is accompanied by visible activation of higher natural sloshing modes and wave breaking, therefore, damping of any type for that kind of sloshing cannot be neglected. Nevertheless, semi-analytical nonlinear modal theories, derived under the inviscid-liquid assumptions [1,4], provide satisfactory predictions for the steady-state wave amplitudes and accurately predicts frequency ranges for all wave regimes and the chaos zone.

However, the inviscid theories are inadequate for quantifying the phase-lag between the harmonic tank excitation and periodic liquid oscillations. In the inviscid case, the phase-lag dependence on the forcing frequency remains a piecewise function, while real liquid damping renders it continuous. The inviscid theory also wrongly predicts directions of stable swirling waves: for circular orbital excitations of the upright circular base tank, the theory foresees the stable swirling in both directions, co- and counter-clockwise, whereas only co-directed (with excitation direction) swirling is realized in model tests. The reason is non-zero damping in the mechanical system. Incorporating a non-zero linear damping term in the corresponding modal equation, this fact was theoretically confirmed in [4, 9]. On the other hand, even speculatively varying the damping rate in the incorporated damping term, these authors were not able to fit experimental data on the phase-lag, even qualitatively. This means that the damping is, most probably, nonlinear and one needs a learning of the damping terms by the measured phase-lag values in the swirling wave regime.

Following the machine learning procedure from previous chapter (there, implemented for rectangular tanks [215]), one can restore appropriate nonlinear damping terms in the modal systems for sloshing in a circular base container derived in [7]. In this section, we revisit the Narimanov–Moiseev-type nonlinear modal system [7] and utilize the experimental measurements on the phase-lags reported in [10] to learn it for accounting the viscous damping. This makes it possible to generalize the data-driven damping identification strategy to resonant swirl-type sloshing in upright circular cylindrical tanks.

4.2. The general modal system (2.41), (2.42) for an upright circular cylindrical tank

Similar to [4], the present chapter focuses on the (special) explicit form of the multi-modal system for an upright circular base container of radius R_0, oscillating with a small amplitude in space. These oscillatory motions are described by the generalized body-related coordinates $\eta_1(t)$ and $\eta_2(t)$

(responsible for the horizontal translational movements) and angular oscillations are described by $\eta_4(t)$ and $\eta_5(t)$. Rotational motions around the Oz axis (yaw) cannot generate sloshing within the framework of the ideal liquid model. Vertical tank motions are not considered. The smallness of the angular disturbances means that nonlinearities in $\eta_4(t)$ and $\eta_5(t)$ could be neglected. Thus, the instantaneous angular velocity is $\boldsymbol{\omega} = (\dot{\eta}_4, \dot{\eta}_5, 0)$.

The geometric notations in Fig. 4.1 include the time-dependent liquid domain $Q(t)$ with the free surface $\Sigma(t)$ and the wetted surface $S(t)$. The free surface $\Sigma(t)$ is given by $z = \zeta(r, \theta, t)$, and the motion of the liquid is described by the velocity potential $\Phi(r, \theta, z, t)$. The unknowns ζ and Φ are defined in a cylindrical coordinate system, which is attached to the tank. The functions ζ and Φ can be found either from the corresponding boundary-value problem or from the equivalent variational formulation. All geometric and physical parameters are further normalized by R_0, which is considered the characteristic size.

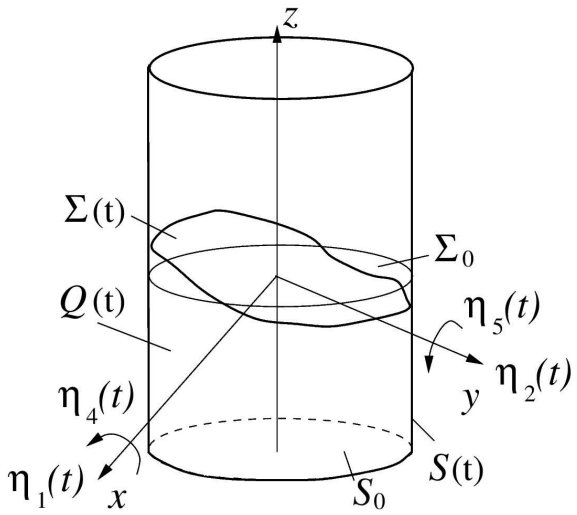

Figure 4.1. The liquid domain $Q(t)$ is bounded by the free surface $\Sigma(t)$ and the wetted tank surface $S(t)$. The liquid wave motions are considered in the non-inertial coordinate system $Oxyz$ rigidly fixed with the tank so that the coordinate plane Oxy coincides with the unperturbed (static) free surface Σ_0, and Oz is the axis of symmetry. The small-amplitude oscillatory tank motions are determined by the generalized coordinates $\eta_1(t)$ (surge), $\eta_4(t)$ (roll), $\eta_2(t)$ (sway), and $\eta_5(t)$ (pitch).

As shown in the previous section, the Luke-Bateman variational principle serves as the basis for the multi-modal method, which is based on the Fourier series decomposition of the solution, here, ζ and Φ. The time-dependent coefficients in these functional series are considered independent time variables

(generalized coordinates and velocities). The series for ζ and Φ are usually based on the natural sloshing modes which are the eigenfunctions of the spectral boundary-value problem (2.44) formulated in the hydrostatic domain Q_0 with $S_0 = S_{0e} + S_{0i} + S_{0b}$ and the mean (static, unperturbed) free surface Σ_0.

In the present chapter, the mathematical problem is rewritten in a dimensionless form after introducing the characteristic linear dimension R_0 (radius) and the characteristic time $T = 1/\sigma$, where T is the characteristic time period (σ is the circular frequency of the tank excitations). We also introduce a small parameter $\epsilon \ll 1$, which characterizes the dimensionless perturbation of the container, i.e.,

$$\eta_i(t) = O(\epsilon),\ i = 1, 2, 4, 5. \tag{4.1}$$

The normalized spectral boundary (2.44) on the natural sloshing modes and frequencies has the analytical solution (throughout the text we adopt notation from [229]) (see [1, 15])

$$\varphi_{Mi}(r, z, \theta) = \mathcal{R}_{Mi}(r)\, \mathcal{Z}_{Mi}(z) \begin{matrix}\cos\\ \sin\end{matrix}(M\theta), \quad M = 0, \ldots;\ i = 1, \ldots, \tag{4.2}$$

where

$$\mathcal{R}_{Mi}(r) = \alpha_{Mi} J_M(k_{Mi} r); \quad \mathcal{Z}_{Mi}(z) = \frac{\cosh(k_{Mi}(z + h))}{\cosh(k_{Mi} h)}. \tag{4.3}$$

Here, $J_M(\cdot)$ is the Bessel function of the first kind and rhe radial wave numbers k_{Mi} are determined from the equations

$$J'_{Mi}(k_{Mi}) = 0.$$

The normalization factors α_{Mi} follow from the orthogonality condition

$$\int_0^1 r\, \mathcal{R}_{Mi}(r)\, \mathcal{R}_{Mj}(r)\, dr = \delta_{ij}, \quad i, j = 1, \ldots, \tag{4.4}$$

where δ_{ij} is the Kronecker delta.

The spectral parameter κ_{Mi} and the natural sloshing frequencies σ_{Mi} are determined by the formulas

$$\kappa_{Mi} = k_{Mi} \tanh(k_{Mi} h); \quad \sigma^2_{Mi} = \kappa_{Mi} \frac{g}{R_0}, \tag{4.5}$$

where g is the gravity acceleration (dimensional).

Next, we consider only low-amplitude angular tank motions (4.1), so we will need only the linearized Stokes-Joukovsky potentials $\Omega_{0i}(r,z,\theta)$, $i=1,2,3$, which are harmonic functions satisfying the Neumann boundary conditions

$$\frac{\partial\Omega_{01}}{\partial n}=-(zn_r-rn_z)\sin\theta;\ \frac{\partial\Omega_{02}}{\partial n}=(zn_r-rn_z)\cos\theta;\ \frac{\partial\Omega_{03}}{\partial n}=0 \qquad (4.6)$$

on Σ_0 and S_0, where n_r and n_z are the corresponding projections of the outward normal in the r- and z-directions, such that $n_z=0$ on the vertical walls, but $n_r=0$ on Σ_0. The solution of (4.6) takes the form [4]

$$\Omega_{01}=-F(r,z)\sin\theta;\quad \Omega_{02}=F(r,z)\cos\theta;\quad \Omega_{03}=0,$$

where

$$F(r,z)=rz+\sum_{n=1}^{\infty}-\frac{2\,P_n}{k_{1n}}\,\mathcal{R}_{1n}(r)\frac{\sinh(k_{1n}(z+\frac{1}{2}h))}{\cosh(\frac{1}{2}k_{1n}h)};\quad P_n=\int_0^1 r^2\,\mathcal{R}_{1n}(r)\,dr. \qquad (4.7)$$

The nonlinear modal system of Miles-Lukovsky (2.41), (2.42) can be rewritten in terms of the generalized coordinates ($p_{Mi}(t)$ and $r_{mi}(t)$) and velocities ($P_{Mi}(t)$ and $R_{mi}(t)$),

$$\zeta(r,\theta,t)=\sum_{M,i}^{I_\theta,I_r}\mathcal{R}_{Mi}(r)\cos(M\theta)\,p_{Mi}(t)+\sum_{m,i}^{I_\theta,I_r}\mathcal{R}_{mi}(r)\sin(m\theta)\,r_{mi}(t), \qquad (4.8a)$$

$$\begin{aligned}\Phi(r,\theta,z,t)=\dot\eta_1(t)\,r\cos\theta+\dot\eta_2(t)\,r\sin\theta+F(r,z)[-\dot\eta_4(t)\sin\theta+\dot\eta_5(t)\cos\theta]\\ +\sum_{M,i}^{I_\theta,I_r}\mathcal{R}_{Mi}(r)\,\mathcal{Z}_{Mi}(z)\,\cos(M\theta)\,P_{Mi}(t)\\ +\sum_{m,i}^{I_\theta,I_r}\mathcal{R}_{mi}(r)\,\mathcal{Z}_{mi}(z)\,\sin(m\theta)\,R_{mi}(t),\end{aligned} \qquad (4.8b)$$

$I_\theta,,I_r\to\infty$. *Here and henceforth*, all the large summation indices denote summation from zero to I_θ, but the small indices indicate changes from one to I_θ or I_r.

The modal representation (4.8) is a special form of (2.28), (2.29). Using (4.8) leads, in turn, to a special structure in the Miles-Lukovsky modal equations (2.41), (2.42), provided that we additionally assume (4.1) and consider only the resonant excitations, where the hydrodynamic *generalized coordinates* are asymptotically larger than the tank excittion amplitude. Mathematically, this means that

$$O(\epsilon) \lesssim p_{Mi}(t),\ r_{mi}(t) \text{ and } O(\epsilon) \lesssim P_{Mi}(t),\ R_{mi}(t). \tag{4.9}$$

Next, we also neglect terms of the order $o(\epsilon)$, and thus, the series of terms in (2.42), which are related to the nonlinear Stokes-Joukovskii potential, now linearly depend on $\eta_i(t)$, $i = 4, 5$, as is the case of the linear sloshing theory. At the same time, due to (4.9), we retain the full nonlinearity with respect to the generalized hydrodynamic coordinates and velocities.

The *nonlinear modal system* (2.41), (2.42), rewrites in the form

$$\sum_{M,n}^{I_\theta,I_r} \frac{\partial A^p_{Ab}}{\partial p_{Mn}} \dot{p}_{Mn} + \sum_{m,n}^{I_\theta,I_r} \frac{\partial A^p_{Ab}}{\partial r_{mn}} \dot{r}_{mn} = \sum_{M,n}^{I_\theta,I_r} A^{pp}_{(Ab)(Mn)} P_{Mn} + \sum_{m,n}^{I_\theta,I_r} A^{pr}_{(Ab),(Mn)} R_{mn}, \tag{4.10a}$$

$$\sum_{M,n}^{I_\theta,I_r} \frac{\partial A^r_{ab}}{\partial p_{Mn}} \dot{p}_{Mn} + \sum_{m,n}^{I_\theta,I_r} \frac{\partial A^r_{ab}}{\partial r_{mn}} \dot{r}_{mn} = \sum_{M,n}^{I_\theta,I_r} A^{pr}_{(Mn),(ab)} P_{Mn} + \sum_{m,n}^{I_\theta,I_r} A^{rr}_{(ab)(mn)} R_{mn}, \tag{4.10b}$$

$A = 0, \dots, I_\theta$; $a = 1, ..., I_\theta$; $b = 1, \dots, I_r$; $I_\theta, I_r \to \infty$ (the kinematic subsystem), and

$$\sum_{M,n}^{I_\theta,I_r} \frac{\partial A^p_{Mn}}{\partial p_{Ab}} \dot{P}_{Mn} + \sum_{m,n}^{I_\theta,I_r} \frac{\partial A^r_{mn}}{\partial p_{Ab}} \dot{R}_{mn} + \frac{1}{2} \sum_{ML,nk}^{I_\theta,I_r} \frac{\partial A^{pp}_{(Mn)(Lk)}}{\partial p_{Ab}} P_{Mn} P_{Lk}$$
$$+ \sum_{Ml,nk}^{I_\theta,I_r} \frac{\partial A^{pr}_{(Mn),(lk)}}{\partial p_{Ab}} P_{Mn} R_{lk} + \frac{1}{2} \sum_{ml,nk}^{I_\theta,I_r} \frac{\partial A^{rr}_{(mn)(lk)}}{\partial P_{Ab}} R_{mn} R_{lk} + g \Lambda_{AA}\, p_{Ab}$$
$$+ (\ddot{\eta}_1 - g\eta_5 - S_b \ddot{\eta}_5) \Lambda_{1A} P_b = 0, \tag{4.11a}$$

$$\sum_{M,n}^{I_\theta,I_r} \frac{\partial A^p_{Mn}}{\partial r_{ab}} \dot{P}_{Mn} + \sum_{m,n}^{I_\theta,I_r} \frac{\partial A^r_{mn}}{\partial r_{ab}} \dot{R}_{mn} + \frac{1}{2} \sum_{ML,nk}^{I_\theta,I_r} \frac{\partial A^{pp}_{(Mn)(Kl)}}{\partial r_{ab}} P_{Mn} P_{Lk}$$

$$+\sum_{Nl,nk}^{I_\theta,I_r}\frac{\partial A^{pr}_{(Mn),(lk)}}{\partial r_{ab}}P_{Mn}R_{lk}+\frac{1}{2}\sum_{ml,nk}^{I_\theta,I_r}\frac{\partial A^{rr}_{(mn)(lk)}}{\partial r_{ab}}R_{mn}R_{lk}+g\Lambda_{aa}r_{ab}$$
$$+(\ddot{\eta}_2+g\eta_4+S_b\ddot{\eta}_4)\Lambda_{1a}P_b=0, \quad (4.11b)$$

$A=0,\ldots,I_\theta$; $a=1,...,,I_\theta$; $b=1,\ldots,I_r,,\ I_\theta,I_r\to\infty$ (the dynamic subsystem), where the comma between index pairs such as $(Ab),(Mn)$ indicates that the pairs do not commute; the coefficients P_b are defined in (4.7),

$$S_b=2\,k_{1b}^{-1}\,\tanh(k_{1b}\tfrac{h}{2}),\quad \Lambda_{IJ}=\begin{cases}2\pi, & I=J=0,\\ \pi\delta_{IJ}, & \text{otherwise},\end{cases} \quad (4.12)$$

where δ_{IJ} is the Kronecker delta. The modal system (4.10), (4.11) contains the following nonlinear expressions by generalized hydrodynamic coordinates

$$A^{pp}_{(Ab)(Mn)}=\int_0^1\int_{-\pi}^{\pi}r\Big[\cos A\theta\,\cos M\theta\,\mathcal{G}^{(1)}_{(Ab)(Mn)}+\sin A\theta\,\sin M\theta\,\mathcal{G}^{(2)}_{(Ab)(Mn)}\Big]d\theta dr,$$
$$A^{rr}_{(ab)(mn)}=\int_0^1\int_{-\pi}^{\pi}r\,\Big[\sin a\theta\,\sin m\theta\,\mathcal{G}^{(1)}_{(ab)(mn)}+\cos a\theta\,\cos m\theta\,\mathcal{G}^{(2)}_{(ab)(mn)}\Big]\,d\theta\,dr,$$
$$A^{pr}_{(Ab),(mn)}=\int_0^1\int_{-\pi}^{\pi}r\Big[\cos A\theta\,\sin m\theta\,\mathcal{G}^{(1)}_{(Ab)(mn)}-\sin A\theta\,\cos m\theta\,\mathcal{G}^{(2)}_{(Ab)(mn)}\Big]\,d\theta dr,$$
$$A^{p}_{Ab}=\int_0^1\int_{-\pi}^{\pi}r\cos(A\theta)\,\mathcal{G}^{(0)}_{Ab}\,d\theta\,dr,\ \ A^{r}_{ab}=\int_{r_1}^1\int_{-\pi}^{\pi}r\sin(a\theta)\,\mathcal{G}^{(0)}_{Ab}\,d\theta\,dr, \quad (4.13)$$

where

$$\mathcal{G}^{(0)}_{Ab}=\mathcal{R}_{Ab}(r)\int_{-h}^{\zeta}\frac{\cosh(k_{Ab}(z+h))}{\cosh(k_{Ab}h)}\,dz=\mathcal{R}_{Ab}(r)\,I^{(0)}_{(Ab)},$$
$$\mathcal{G}^{(1)}_{(Ab)(Mn)}=\mathcal{R}'_{Ab}(r)\,\mathcal{R}'_{Mn}(r)\,I^{(1)}_{(Ab)(Mn)}+\mathcal{R}_{Ab}(r)\,\mathcal{R}_{Mn}(r)\,k_{Ab}k_{Mn}I^{(2)}_{(Ab)(Mn)},$$
$$\mathcal{G}^{(2)}_{(Ab)(Mn)}=AM\,r^{-2}\,\mathcal{R}_{Ab}(r)\mathcal{R}_{Mn}(r)\,I^{(1)}_{(Ab)(Mn)}; \quad (4.14)$$

$$I^{(1)}_{(Ab)(Mn)} = \int\limits_{-h}^{\zeta} \frac{\cosh(k_{Ab}(z+h))\ \cosh(k_{Mn}(z+h))}{\cosh(k_{Ab}h)\ \cosh(k_{Mnh})}\, dz,$$
$$I^{(2)}_{(Ab)(Mn)} = \int\limits_{-h}^{\zeta} \frac{\sinh(k_{Ab}(z+h))\ \sinh(k_{Mn}(z+h))}{\cosh(k_{Ab}h)\ \cosh(k_{Mnh})}\, dz. \tag{4.15}$$

The system of ordinary differential equations (4.10)-(4.11) has, in general, infinite dimensional, as $I_\theta, I_r \to \infty$. If finite values of I_θ and I_r are taken, the Cauchy problem for (4.10), (4.11) can be solved numerically, describing the transient motions of the hydrodynamic system with the corresponding initial conditions. As we wrote in the literature review, such use of the modal system (4.10), (4.11) is associated with the Perko method.

Our further goal is an analytical study of the periodic (steady-state) motions of the system using (4.10)-(4.11). The studies become possible under additional simplifications in (4.10)-(4.11) via the use of special asymptotic relationships between the generalized hydrodynamic coordinates instead of (4.9). Moreover, we must consider viscous damping terms.

4.3. Adaptive asymptotic modal equations

The nonlinear modal system (4.10), (4.11) accounts for the smallness of amplitude of the container motions which are associated with the generalized coordinates $\eta_i(t)$, $i = 1, 2, 4, 5$. However, it does not introduce the asymptotic order for the generalized hydrodynamic coordinates $p_{Mi}(t)$ and $r_{mi}(t)$ on the introduced asymptotic scale $O(\epsilon)$. This makes the system (4.10), (4.11) raher complex and unsuitable for analytical studies, which are the primary goal of the dissertation. To simplify (4.10), (4.11), it is necessary to introduce additional asymptotic assumptions with respect to P_{Mi}, r_{mi}, and R_{Mi}, P_{mi}.

The most general assumptions for non-small liquid depth are associated with the so-called adaptive approach, where the resonantly excited eigenmodes with indices $(M_1 i_1)$ have the order $O(\epsilon^{1/3})$, some number of eigenmodes $(M_2 i_2)$ are of order $O(\epsilon^{2/3})$, and there is also a set of modes $(M_3 i_3)$

of third order $O(\epsilon)$ but all other eigenmodes can be neglected since these are of the order $o(\epsilon)$.

It is evident that the most general case of adaptive modal systems occurs when all generalized coordinates satisfy

$$p_{Mi} \sim r_{mi} = O(\epsilon^{1/3}).$$

This case is purely hypothetical and does not lead to nonlinear modal equations that can be studied analytically. The simplest case is the linear modal system which is associated with no resonances in the hydrodynamic system, so that all p_{Mi} and r_{mi} are of order $O(\epsilon)$. This last linear case will be necessary for the physically correct introduction of damping in this mechanical system through the estimation of logarithmic decrements of the attenuation of the natural sloshing modes.

In the most general case, the adaptive third-order modal system refers to the situation where the amplitude of the forcing amplitude is of the order $O(\epsilon) \ll 1$, but (4.1) and the generalized hydrodynamic coordinates and velocities are of order $O(\epsilon^{1/3})$, i.e.,

$$r_{mi} \sim R_{Mi} \sim P_{Mi} \sim p_{Mi} = O(\epsilon^{1/3}). \tag{4.16}$$

If the quantities of $o(\epsilon)$ are neglected, using assumptions (4.16) and (4.1) makes it possible to simplify (4.10), (4.11) and, thereby, derive a system of ordinary differential equations with respect to *only* the generalized hydrodynamic coordinates $r_{mi}(t)$ and $p_{Mi}(t)$. The derivation procedure is rather complicated. We will describe only some of its steps.

The first derivation stage of the adaptive system involves expanding $I^{(0)}_{(Ab)}, I^{(1)}_{(Ab)(Mn)}$, and $I^{(2)}_{(Ab)(Mn)}$ in Taylor series with respect to ζ, where $\zeta = O(\epsilon^{1/3})$. Analysis of (2.41), (2.42) shows that $I^{(0)}_{(Ab)}$ should be expanded to the third order of smallness, but $I^{(1)}_{(Ab)(Mn)}$ and $I^{(2)}_{(Ab)(Mn)}$ require expansion only to the second order, i.e.

$$I^{(0)}_{(Ab)} = k^{-1}_{Ab} \tanh(k_{Ab}h) + \zeta + \tfrac{1}{2}\kappa_{Ab}\zeta^2 + \tfrac{1}{6}k^2_{Ab}\zeta^3 + \ldots, \tag{4.17a}$$

$$I^{(1)}_{(Ab)(Mn)} = O(1) + \zeta + \tfrac{1}{2}(\kappa_{Ab} + \kappa_{Mn})\zeta^2 + \ldots, \tag{4.17b}$$

$$I^{(2)}_{(Ab)(Mn)} = O(1) + \kappa_{Ab}\kappa_{Mn}\zeta + \tfrac{1}{2}(k^2_{Ab}\kappa_{Mn} + k^2_{Mn}\kappa_{Ab})\zeta^2 + \dots . \tag{4.17c}$$

Substituting (4.17b) and (4.17c) into (2.13) gives

$$\begin{aligned}\mathcal{G}^{(1)}_{(Ab)(Mn)} &= O(1) + (\mathcal{R}'_{Ab}\mathcal{R}'_{Mn} + \mathcal{R}_{Ab}\mathcal{R}_{Mn}\kappa_{Ab}\kappa_{Mn})\,\zeta \\ &\quad + \tfrac{1}{2}[(\kappa_{Ab}+\kappa_{Mn})\mathcal{R}'_{Ab}\mathcal{R}'_{Mn} + \mathcal{R}_{Ab}\mathcal{R}_{Mn}(k^2_{Ab}\kappa_{Mn} + k^2_{Mn}\kappa_{Ab})]\zeta^2, \end{aligned}\tag{4.18a}$$

$$\begin{aligned}\mathcal{G}^{(2)}_{(Ab)(Mn)} &= O(1) + r^{-2}AM\mathcal{R}_{Ab}\mathcal{R}_{Mn}\,\zeta \\ &\quad + \tfrac{1}{2}r^{-2}AM(\kappa_{Ab}+\kappa_{Mn})\mathcal{R}_{Ab}\mathcal{R}_{Mn}\,\zeta^2. \end{aligned}\tag{4.18b}$$

At the second derivation stage, A^p_{Ab} and A^r_{ab} should be expanded to the order $O(\epsilon)$ in terms of the corresponding generalized hydrodynamic coordinates,

$$\begin{aligned}A^p_{Ab} = \Lambda_{AA,p_{Ab}} &+ \tfrac{1}{2}\sum_{MN,ij}^{I_\theta,I_r}\chi^{pp}_{(Mi)(Nj),(Ab)}p_{Mi}p_{Nj} + \tfrac{1}{2}\sum_{mn,ij}^{I_\theta,I_r}\chi^{rr}_{(mi)(nj),(Ab)}r_{mi}r_{nj} \\ &+ \tfrac{1}{3}\sum_{MNK,ijl}^{I_\theta,I_r}\chi^{ppp}_{(Mi)(Nj)(Kl),(Ab)}p_{Mi}p_{Nj}p_{Kl} \\ &+ \sum_{Mnk,ijl}^{I_\theta,I_r}\chi^{prr}_{(Mi),(nj)(kl),(Ab)}p_{Mi}r_{nj}r_{kl}, \end{aligned}\tag{4.19a}$$

$$\begin{aligned}A^r_{ab} = \Lambda_{,aa}r_{ab} &+ \sum_{Mn,ij}^{I_\theta,I_r}\chi^{pr}_{(Mi),(nj),(ab)}p_{Mi}r_{nj} + \tfrac{1}{3}\sum_{mnk,ijl}^{I_\theta,I_r}\chi^{rrr}_{(mi)(nj)(kl),(ab)}r_{mi}r_{nj}r_{kl} \\ &+ \sum_{MNk,ijl}^{I_\theta,I_r}\chi^{ppr}_{(Mi)(Nj),(kl),(ab)}p_{Mi}p_{Nj}r_{kl}, \quad I_\theta, I_r \to \infty, \end{aligned}\tag{4.19b}$$

where

$$\begin{aligned}\chi^{pp}_{(Mi)(Nj),(Ab)} &= \kappa_{Ab}\Lambda_{AMN,}\lambda_{(Ab)(Mi)(Nj)}, \\ \chi^{rr}_{(Mi)(nj),(Ab)} &= \kappa_{Ab}\Lambda_{A,mn}\lambda_{(Ab)(mi)(nj)}, \\ \chi^{ppp}_{(Mi)(Nj)(Kl),(Ab)} &= \tfrac{1}{2}k^2_{Ab}\Lambda_{AMNK,}\lambda_{(Ab)(Mi)(Nj)(Kl)}, \\ \chi^{prr}_{(Mi),(nj)(kl),(Ab)} &= \tfrac{1}{2}k^2_{Ab}\Lambda_{AM,nk}\lambda_{(Ab)(Mi)(nj)(kl)}, \\ \chi^{pr}_{(Mi),(nj),(ab)} &= \kappa_{ab}\Lambda_{M,an}\lambda_{(Mi)(nj)(ab)}, \end{aligned}$$

$$\chi^{rrr}_{(mi)(nj)(kl),(ab)} = \tfrac{1}{2}k^2_{ab}\Lambda_{,amnk}\lambda_{(mi)(nj)(kl)(ab)},$$
$$\chi^{ppr}_{(Mi)(Nj),(kl),(ab)} = \tfrac{1}{2}k^2_{ab}\Lambda_{MN,ak}\lambda_{(Mi)(Nj)(kl)(ab)}$$

and within the tensor Λ, whose elements are defined as

$$\Lambda_{M\ldots N,i\ldots j} = \int_{-\pi}^{\pi} \cos(A\theta)\ldots\cos(M\theta)\,\cdot\,\sin(i\theta)\ldots\sin(j\theta)\,d\theta. \tag{4.20}$$

The tensors Λ can be computed using recursive formulas

$$\Lambda_{M,i} = 0,\quad \Lambda_{,ij} = \pi\delta_{ij},\quad \Lambda_{MN,} = \pi\delta_{MN},\ M^2+N^2\neq 0,\ \Lambda_{00,} = 2\pi,$$
$$\Lambda_{M\ldots NK,i\ldots j} = \tfrac{1}{2}(\Lambda_{M\ldots|N-K|,i\ldots j} + \Lambda_{M\ldots|N+K|,i\ldots j}),$$
$$\Lambda_{M\ldots N,i\ldots ljk} = \tfrac{1}{2}(\Lambda_{M\ldots|j-k|,i\ldots l} - \Lambda_{M\ldots|j+k|,i\ldots l}).$$

The tensors λ are defined by the formula

$$\lambda_{(Ab)\ldots(Mn)} = \int_0^1 r\mathcal{R}_{Ab}(r)\ldots\mathcal{R}_{Mn}(r)\,dr. \tag{4.21}$$

Partial derivatives of (4.19) with respect to generalized coordinates are

$$\frac{\partial A^p_{Ab}}{\partial p_{Df}} = \Lambda_{AD,}\delta_{bf} + \sum_{M,i}^{I_\theta,I_r}\chi^{pp}_{(Mi)(Df),(Ab)}p_{Mi} + \sum_{NK,jl}^{I_\theta,I_r}\chi^{ppp}_{(Df)(Nj)(Kl),(Ab)}p_{Nj}p_{Kl} + \sum_{nk,jl}^{I_\theta,I_r}\chi^{prr}_{(Df),(nj)(kl),(Ab)}r_{nj}r_{kl}, \tag{4.22a}$$

$$\frac{\partial A^p_{Ab}}{\partial r_{df}} = \sum_{m,i}^{I_\theta,I_r}\chi^{rr}_{(mi)(df),(Ab)}r_{mi} + 2\sum_{Mn,ij}^{I_\theta,I_r}\chi^{prr}_{(Mi),(nj)(df),(Ab)}p_{Mi}r_{nj}, \tag{4.22b}$$

$$\frac{\partial A^r_{ab}}{\partial p_{Df}} = \sum_{n,j}^{I_\theta,I_r}\chi^{pr}_{(Df),(nj),(ab)}r_{nj} + 2\sum_{Mn,ij}^{I_\theta,I_r}\chi^{ppr}_{(Mi)(Df),(nj),(ab)}p_{Mi}r_{nj}, \tag{4.22c}$$

$$\frac{\partial A^r_{ab}}{\partial r_{df}} = \Lambda_{,ad}\delta_{bf} + \sum_{M,i}^{I_\theta,I_r}\chi^{pr}_{(Mi),(df),(ab)}p_{Mi} + \sum_{mn,ij}^{I_\theta,I_r}\chi^{rrr}_{(mi)(nj)(df),(ab)}r_{mi}r_{nj} + \sum_{MN,ij}^{I_\theta,I_r}\chi^{ppr}_{(Mi)(Nj),(df),(ab)}p_{Mi}p_{Nj},\quad I_\theta, I_r\to\infty. \tag{4.22d}$$

The third derivation stage leads to analytical expressions for $A^{pp}_{(Ab)(Mn)}$, $A^{rr}_{(ab)(mn)}$, and $A^{pr}_{(Ab),(mn)}$, where only second-order terms, $O(\epsilon^{2/3})$,

are preserved. The $O(1)$-order terms can be obtained from linear modal theory. The result is

$$A^{pp}_{(Ab)(Mn)} = \Lambda_{AM,}\delta_{bn}\kappa_{Ab} + \sum_{K,l}^{I_\theta,I_r} \Pi^{p,p}_{(Kl),(Ab)(Mn)} p_{Kl} + \sum_{KC,ld}^{I_\theta,I_r} \Pi^{p,pp}_{(Kl)(Cd),(Ab)(Mn)} p_{Kl}p_{Cd} + \sum_{kc,ld}^{I_\theta,I_r} \Pi^{p,rr}_{(kl)(cd),(Ab)(Mn)} r_{kl}r_{cd}, \quad (4.23a)$$

$$A^{rr}_{(ab)(mn)} = \Lambda_{,am}\delta_{bn}\kappa_{ab} + \sum_{K,l}^{I_\theta,I_r} \Pi^{r,p}_{(Kl),(ab)(mn)} p_{Kl} + \sum_{KC,ld}^{I_\theta,I_r} \Pi^{r,pp}_{(Kl)(Cd),(ab)(mn)} p_{Kl}p_{Cd} + \sum_{kc,ld}^{I_\theta,I_r} \Pi^{r,rr}_{(kl)(cd),(ab)(mn)} r_{kl}r_{cd}, \quad (4.23b)$$

$$A^{pr}_{(Ab),(mn)} = \sum_{k,l}^{I_\theta,I_r} \Pi^{r}_{(kl),(Ab),(mn)} r_{kl} + \sum_{Kc,ld}^{I_\theta,I_r} \Pi^{pr}_{(Kl),(cd),(Ab),(mn)} p_{Kl}r_{cd}, \quad (4.23c)$$

where

$$\Pi^{p,p}_{(Kl),(Ab)(Mn)} = \Lambda_{AMK,}G^{(11)}_{(Ab)(Mn),(Kl)} + \Lambda_{K,AM}G^{(12)}_{(Ab)(Mn),(Kl)},$$
$$\Pi^{r,p}_{(Kl),(ab)(mn)} = \Lambda_{K,am}G^{(11)}_{(ab)(mn),(Kl)} + \Lambda_{amK,}G^{(12)}_{(ab)(mn),(Kl)},$$
$$\Pi^{r}_{(kl),(Ab),(mn)} = \Lambda_{A,mk}G^{(11)}_{(Ab)(mn),(kl)} - \Lambda_{m,Ak}G^{(12)}_{(Ab)(mn),(kl)},$$
$$\Pi^{p,pp}_{(Kl)(Cd),(Ab)(Mn)} = \Lambda_{AMKC,}G^{(21)}_{(Ab)(Mn),(Kl)(Cd)} + \Lambda_{KC,AM}G^{(22)}_{(Ab)(Mn),(Kl)(Cd)},$$
$$\Pi^{p,rr}_{(kl)(cd),(Ab)(Mn)} = \Lambda_{AM,kc}G^{(21)}_{(Ab)(Mn),(kl)(cd)} + \Lambda_{,AMkc}G^{(22)}_{(Ab)(Mn),(kl)(cd)},$$
$$\Pi^{r,pp}_{(Kl)(Cd),(ab)(mn)} = \Lambda_{KC,am}G^{(21)}_{(ab)(mn),(Kl)(Cd)} + \Lambda_{KCam,}G^{(22)}_{(ab)(mn),(Kl)(Cd)},$$
$$\Pi^{r,rr}_{(kl)(cd),(ab)(mn)} = \Lambda_{,amkc}G^{(21)}_{(ab)(mn),(kl)(cd)} + \Lambda_{am,kc}G^{(22)}_{(ab)(mn),(kl)(cd)},$$
$$\Pi^{pr}_{(Kl),(cd),(Ab),(mn)} = 2[\Lambda_{AK,mc}G^{(21)}_{(Ab)(mn),(Kl)(cd)} - \Lambda_{Km,Ac}G^{(22)}_{(Ab)(mn),(Kl)(cd)}];$$
$$G^{(11)}_{(Ab)(Mn),(Kl)} = \lambda'_{(Ab)(Mn),(Kl)} + \kappa_{Ab}\kappa_{Mn}\lambda_{(Ab)(Mn)(Kl)},$$
$$G^{(12)}_{(Ab)(Mn),(Kl)} = AM\bar{\lambda}_{(Ab)(Mn)(Kl)},$$
$$G^{(21)}_{(Ab)(Mn),(Kl)(Cd)} = \tfrac{1}{2}[(\kappa_{Ab}+\kappa_{Mn})\lambda'_{(Ab)(Mn),(Kl)(Cd)} + (k^2_{Ab}\kappa_{Mn} + k^2_{Mn}\kappa_{Ab})\lambda_{(Ab)(Mn)(Kl)(Cd)}],$$
$$G^{(22)}_{(Ab)(Mn),(Kl)(Cd)} = \tfrac{1}{2}AM(\kappa_{Ab}+\kappa_{Mn})\bar{\lambda}_{(Ab)(Mn)(Kl)(Cd)}$$

and

$$\lambda'_{(Ab)(Mn),(Cd)\dots(Ef)} = \int_0^1 r\mathcal{R}'_{Ab}(r)\mathcal{R}'_{Mn}(r)\,\cdot\,\mathcal{R}_{Cd}(r)\dots\mathcal{R}_{Ef}(r)\,dr,$$
$$\bar{\lambda}_{(Ab)\dots(Mn)} = \int_0^1 r^{-1}\,\mathcal{R}_{Ab}(r)\dots\mathcal{R}_{Mn}(r)\,dr. \tag{4.24}$$

The partial derivatives of the expressions in (4.23) with respect to the generalized coordinates are

$$\frac{\partial A^{pp}_{(Ab)(Cd)}}{\partial p_{Ef}} = \Pi^{p,p}_{(Ef),(Ab)(Cd)} + 2\sum_{M,i}^{I_\theta,I_r}\Pi^{p,pp}_{(Mi)(Ef),(Ab)(Cd)}p_{Mi}, \tag{4.25a}$$

$$\frac{\partial A^{pp}_{(Ab)(Cd)}}{\partial r_{ef}} = 2\sum_{m,i}^{I_\theta,I_r}\Pi^{p,rr}_{(mi)(ef),(Ab)(Cd)}r_{mi}, \tag{4.25b}$$

$$\frac{\partial A^{rr}_{(ab)(cd)}}{\partial p_{Ef}} = \Pi^{r,p}_{(Ef),(ab)(cd)} + 2\sum_{M,i}^{I_\theta,I_r}\Pi^{r,pp}_{(Mi)(Ef),(ab)(cd)}p_{Mi}, \tag{4.25c}$$

$$\frac{\partial A^{rr}_{(ab)(cd)}}{\partial r_{ef}} = 2\sum_{m,i}^{I_\theta,I_r}\Pi^{r,rr}_{(mi)(ef),(ab)(cd)}r_{mi}, \tag{4.25d}$$

$$\frac{\partial A^{pr}_{(Ab),(cd)}}{\partial p_{Ef}} = \sum_{n,j}^{I_\theta,I_r}\Pi^{pr}_{(Ef),(nj),(Ab)(cd)}r_{nj}, \tag{4.25e}$$

$$\frac{\partial A^{pr}_{(Ab),(cd)}}{\partial r_{ef}} = \Pi^{r}_{(ef),(Ab),(cd)} + \sum_{M,i}^{I_\theta,I_r}\Pi^{pr}_{(Mi),(ef),(Ab)(cd)}p_{Mi}. \tag{4.25f}$$

At the fourth derivation stage, the kinematic equations (4.10) must be solved with respect to the generalized hydrodynamic velocities P_{Ab} and R_{ab}. Postulating the following

$$P_{Ab} = \frac{1}{\kappa_{Ab}}\dot{p}_{Ab} + \sum_{MN,ij}^{I_\theta,I_r}V^{pp}_{(Mi),(Nj),(Ab)}\dot{p}_{Mi}p_{Nj} + \sum_{mn,ij}^{I_\theta,I_r}V^{rr}_{(mi),(nj),(Ab)}\dot{r}_{mi}r_{nj}$$
$$+ \sum_{Mnk,ijl}^{I_\theta,I_r}V^{prr}_{(Mi),(nj),(kl),(Ab)}\dot{p}_{Mi}r_{nj}r_{kl} + \sum_{MNK,ijl}^{I_\theta,I_r}V^{ppp}_{(Mi),(Nj),(Kl),(Ab)}\dot{p}_{Mi}p_{Nj}p_{Kl}$$

$$+\sum_{Mnk,ijl}^{I_\theta,I_r} V^{rpr}_{(nj),(Mi),(kl),(Ab)}\dot{r}_{nj}p_{Mi}r_{kl}, \quad (4.26a)$$

$$R_{ab} = \frac{1}{\kappa_{ab}}\dot{r}_{ab} + \sum_{Mn,ij}^{I_\theta,I_r} V^{pr}_{(Mi),(nj),(ab)}\dot{p}_{Mi}r_{nj} + \sum_{Mn,ij}^{I_\theta,I_r} V^{rp}_{(nj),(Mi),(ab)}\dot{r}_{nj}p_{Mi}$$
$$+ \sum_{mnk,ijl}^{I_\theta,I_r} V^{rrr}_{(mi),(nj),(kl),(ab)}\dot{r}_{mi}r_{nj}r_{kl} + \sum_{MNk,ijl}^{I_\theta,I_r} V^{rpp}_{(kl),(Mi),(Nj),(ab)}\dot{r}_{kl}p_{Mi}p_{Nj}$$
$$+\sum_{MNk,ijl}^{I_\theta,I_r} V^{ppr}_{(Mi),(Nj),(kl),(ab)}\dot{p}_{Mi}p_{Nj}r_{kl}, \quad (4.26b)$$

Substituting (4.26) into the kinetic subsystem (4.10) and grouping similar terms, we derive the formulas for the coefficients in (4.26)

$$V^{pp}_{(Mi),(Nj),(Ab)} = \frac{1}{\Lambda_{AA}\kappa_{Ab}}\left[\chi^{pp}_{(Nj)(Mi),(Ab)} - \frac{\Pi^{p,p}_{(Nj),(Ab)(Mi)}}{\kappa_{Mi}}\right],$$
$$V^{rr}_{(mi),(nj),(Ab)} = \frac{1}{\Lambda_{AA}\kappa_{Ab}}\left[\chi^{rr}_{(nj)(mi),(Ab)} - \frac{\Pi^{r}_{(nj),(Ab),(mi)}}{\kappa_{mi}}\right],$$
$$V^{rp}_{(nj),(Mi),(ab)} = \frac{1}{\Lambda_{aa}\kappa_{ab}}\left[\chi^{pr}_{(Mi),(nj),(ab)} - \frac{\Pi^{r,p}_{(Mi),(ab)(nj)}}{\kappa_{nj}}\right],$$
$$V^{pr}_{(Mi),(nj),(ab)} = \frac{1}{\Lambda_{aa}\kappa_{ab}}\left[\chi^{pr}_{(Mi),(nj),(ab)} - \frac{\Pi^{r}_{(nj),(Mi),(ab)}}{\kappa_{Mi}}\right],$$

$$V^{ppp}_{(Mi),(Nj),(Kl),(Ab)} = \frac{1}{\Lambda_{AA}\kappa_{Ab}}\left[\chi^{ppp}_{(Mi)(Nj)(Kl),(Ab)} - \frac{\Pi^{p,pp}_{(Nj)(Kl),(Ab)(Mi)}}{\kappa_{Mi}}\right.$$
$$\left. - \sum_{C,d}^{I_\theta,I_r} V^{pp}_{(Mi),(Nj),(Cd)}\Pi^{p,p}_{(Kl),(Ab)(Cd)}\right],$$
$$V^{prr}_{(Mi),(nj),(kl),(Ab)} = \frac{1}{\Lambda_{AA}\kappa_{Ab}}\left[\chi^{prr}_{(Mi),(nj)(kl),(Ab)} - \frac{\Pi^{p,rr}_{(nj)(kl),(Ab)(Mi)}}{\kappa_{Mi}}\right.$$
$$\left. - \sum_{c,d}^{I_\theta,I_r} V^{pr}_{(Mi),(nj),(cd)}\Pi^{r}_{(kl),(Ab),(cd)}\right],$$

$$V^{rrr}_{(mi),(nj),(kl),(ab)} = \frac{1}{\Lambda_{aa}\kappa_{ab}}\left[\chi^{rrr}_{(nj)(kl)(mi),(ab)} - \frac{\Pi^{r,rr}_{(nj)(kl),(ab)(mi)}}{\kappa_{mi}}\right.$$

$$- \sum_{C,d}^{I_\theta,I_r} V^{rr}_{(mi),(nj),(Cd)} \Pi^{r}_{(kl),(Cd),(ab)} \Bigg],$$

$$V^{rpp}_{(kl),(Mi),(Nj),(ab)} = \frac{1}{\Lambda_{aa}\kappa_{ab}} \Bigg[\chi^{ppr}_{(Mi)(Nj),(kl),(ab)} - \frac{\Pi^{r,pp}_{(Mi)(Nj),(ab)(kl)}}{\kappa_{kl}} - \sum_{c,d}^{I_\theta,I_r} V^{rp}_{(kl),(Mi),(cd)} \Pi^{r,p}_{(Nj),(ab),(cd)} \Bigg],$$

$$V^{ppr}_{(Mi),(Nj),(kl),(ab)} = \frac{1}{\Lambda_{aa}\kappa_{ab}} \Bigg[2\chi^{ppr}_{(Mi)(Nj),(kl),(ab)} - \frac{\Pi^{pr}_{(Nj),(kl),(Mi)(ab)}}{\kappa_{Mi}} - \sum_{C,d}^{I_\theta,I_r} V^{pp}_{(Mi),(Nj),(Cd)} \Pi^{r}_{(kl),(Cd),(ab)} - \sum_{c,d}^{I_\theta,I_r} V^{pr}_{(Mi),(kl),(cd)} \Pi^{r,p}_{(Nj),(ab)(cd)} \Bigg],$$

$$V^{rpr}_{(nj),(Mi),(kl),(Ab)} = \frac{1}{\Lambda_{AA}\kappa_{Ab}} \Bigg[2\chi^{prr}_{(Mi),(kl)(nj),(Ab)} - \frac{\Pi^{pr}_{(Mi),(kl),(Ab)(nj)}}{\kappa_{nj}} - \sum_{C,d}^{I_\theta,I_r} V^{rr}_{(nj),(kl),(Cd)} \Pi^{p,p}_{(Mi),(Ab)(Cd)} - \sum_{c,d}^{I_\theta,I_r} V^{rp}_{(nj),(Mi),(cd)} \Pi^{r}_{(kl),(Ab),(cd)} \Bigg].$$

At the fifth derivation stage, the expressions (4.22), (4.25), and (4.26) are substituted into the dynamic modal equations (4.11). Excluding terms of the order $o(\epsilon)$, we obtain the sought-after *adaptive nonlinear modal equations*

$$\sum_{M,i}^{I_\theta,I_r} \ddot{p}_{Mi} \Bigg[\delta_{ME}\delta_{if} + \sum_{N,j}^{I_\theta,I_r} d^{pp,(Ef)}_{(Mi),(Nj)} p_{Nj} + \sum_{NK,jl}^{I_\theta,I_r} d^{ppp,(Ef)}_{(Mi),(Nj),(Kl)} p_{Nj}p_{Kl} + \sum_{nk,jl}^{I_\theta,I_r} d^{prr,(Ef)}_{(Mi),(nj),(kl)} r_{nj}r_{kl} \Bigg] + \sum_{mn,ij}^{I_\theta,I_r} \ddot{r}_{mi}r_{nj} \Bigg[d^{rr,(Ef)}_{(mi),(nj)} + \sum_{K,l}^{I_\theta,I_r} d^{rrp,(Ef)}_{(mi),(nj),(Kl)} p_{Kl} \Bigg]$$
$$+ \sum_{MN,ij}^{I_\theta,I_r} \dot{p}_{Mi}\dot{p}_{Nj} \Bigg[t^{pp,(Ef)}_{(Mi),(Nj)} + \sum_{K,l}^{I_\theta,I_r} t^{ppp,(Ef)}_{(Mi),(Nj),(Kl)} p_{Kl} \Bigg] + \sum_{Mnk,ijl}^{I_\theta,I_r} t^{prr,(Ef)}_{(Mi),(nj),(kl)} \dot{p}_{Mi}\dot{r}_{nj}r_{kl}$$
$$+ \sum_{mn,ij}^{I_\theta,I_r} \dot{r}_{mi}\dot{r}_{nj} \Bigg[t^{rr,(Ef)}_{(mi),(nj)} + \sum_{K,l}^{I_\theta,I_r} t^{rrp,(Ef)}_{(mi),(nj),(Kl)} p_{Kl} \Bigg] + \bar{\sigma}^2_{Ef} p_{Ef}$$
$$= -(\ddot{\eta}_1 - g\eta_5 - S_b\ddot{\eta}_5)\delta_{1E}\kappa_{1f}\, P_f;\; E = 0, \ldots, I_\theta;\; f = 1, \ldots, I_r, \quad (4.27a)$$

$$\sum_{m,i}^{I_\theta,I_r}\ddot{r}_{mi}\left[\delta_{me}\delta_{ij}+\sum_{N,j}^{I_\theta,I_r}d^{rp,(ef)}_{(mi),(Nj)}p_{Nj}+\sum_{NK,jl}^{I_\theta,I_r}d^{rpp,(ef)}_{(mi),(Nj),(Kl)}p_{Nj}p_{Kl}\right.$$
$$\left.+\sum_{nk,jl}^{I_\theta,I_r}d^{rrr,(ef)}_{(mi),(nj),(kl)}r_{nj}r_{kl}\right]+\sum_{Mn,ij}^{I_\theta,I_r}\ddot{p}_{Mi}r_{nj}\left[d^{pr,(ef)}_{(Mi),(nj)}+\sum_{K,l}^{I_\theta,I_r}d^{prp,(ef)}_{(Mi),(nj),(Kl)}p_{Kl}\right]$$
$$+\sum_{Mn,ij}^{I_\theta,I_r}\dot{p}_{Mi}\dot{r}_{nj}\left[t^{pr,(ef)}_{(Mi),(nj)}+\sum_{K,l}^{I_\theta,I_r}t^{prp,(ef)}_{(Mi),(nj),(Kl)}p_{Kl}\right]$$
$$+\sum_{MNk,ijl}^{I_\theta,I_r}t^{ppr,(ef)}_{(Mi),(Nj),(kl)}\dot{p}_{Mi}\dot{p}_{Nj}r_{kl}+\sum_{mnk,ijl}^{I_\theta,I_r}t^{rrr,(ef)}_{(mi),(nj),(kl)}\dot{r}_{mi}\dot{r}_{nj}r_{kl}+\bar{\sigma}^2_{ef}r_{ef}$$
$$=-(\ddot{\eta}_2+g\eta_4+S_b\ddot{\eta}_4)\delta_{1e}\kappa_{1f}P_f;\ e=1,\ldots,I_\theta;\ f=1,\ldots,I_r, \quad (4.27b)$$

where the dimensionless natural frequencies

$$\bar{\sigma}_{Ef}=\frac{\sigma_{Et}}{\sigma} \quad (4.28)$$

are defined in (4.5), P_f and S_b are given in (4.7) and (4.12), respectively, and the hydrodynamic coefficients in nonlinear quantities can be explicitly computed as functions of the dimensionless depth h

$$d^{pp,(Ef)}_{(Mi),(Nj)}=\frac{\kappa_{Ef}}{\Lambda_{EE}}\left[\Lambda_{EE}V^{pp}_{(Mi),(Nj),(Ef)}+\frac{\chi^{pp}_{(Nj)(Ef),(Mi)}}{\kappa_{Mi}}\right],$$

$$d^{ppp,(Ef)}_{(Mi),(Nj),(Kl)}=\frac{\kappa_{Ef}}{\Lambda_{EE}}\left[\Lambda_{EE}V^{ppp}_{(Mi),(Nj),(Kl),(Ef)}+\frac{\chi^{ppp}_{(Ef)(Nj)(Kl),(Mi)}}{\kappa_{Mi}}\right.$$
$$\left.+\sum_{A,b}^{I_\theta,I_r}V^{pp}_{(Mi),(Nj),(Ab)}\chi^{pp}_{(Kl)(Ef),(Ab)}\right],$$

$$d^{prr,(Ef)}_{(Mi),(nj),(kl)}=\frac{\kappa_{Ef}}{\Lambda_{EE}}\left[\Lambda_{EE}V^{prr}_{(Mi),(nj),(kl),(Ef)}+\frac{\chi^{prr}_{(Ef),(nj)(kl),(Mi)}}{\kappa_{Mi}}\right.$$
$$\left.+\sum_{a,b}^{I_\theta,I_r}V^{pr}_{(Mi),(nj),(ab)}\chi^{pr}_{(Ef),(kl),(ab)}\right],$$

$$d^{rr,(Ef)}_{(mi),(nj)}=\frac{\kappa_{Ef}}{\Lambda_{EE}}\left[\Lambda_{EE}V^{rr}_{(mi),(nj),(Ef)}+\frac{\chi^{pr}_{(Ef),(nj),(mi)}}{\kappa_{mi}}\right],$$

$$d^{rrp,(Ef)}_{(mi),(nj),(Kl)} = \frac{\kappa_{Ef}}{\Lambda_{EE}}\left[\Lambda_{EE}V^{rpr}_{(mi),(Kl),(nj),(Ef)} + \frac{2\chi^{ppr}_{(Kl)(Ef),(nj),(mi)}}{\kappa_{mi}} + \sum_{a,b}^{I_\theta,I_r} V^{rp}_{(mi),(Kl),(ab)}\chi^{pr}_{(Ef),(nj),(ab)} + \sum_{A,b}^{I_\theta,I_r} V^{rr}_{(mi),(nj),(Ab)}\chi^{pp}_{(Kl)(Ef),(Ab)}\right],$$

$$t^{pp,(Ef)}_{(Mi),(Nj)} = \frac{\kappa_{Ef}}{\Lambda_{EE}}\left[\Lambda_{EE}V^{pp}_{(Mi),(Nj),(Ef)} + \frac{\Pi^{p,p}_{(Ef),(Mi)(Nj)}}{2\kappa_{Mi}\kappa_{Nj}}\right],$$

$$t^{ppp,(Ef)}_{(Mi),(Nj),(Kl)} = \frac{\kappa_{Ef}}{\Lambda_{EE}}\left[\Lambda_{EE}\bar{V}^{ppp}_{(Mi),(Nj),(Kl),(Ef)} + \frac{\Pi^{p,pp}_{(Kl)(Ef),(Mi)(Nj)}}{\kappa_{Mi}\kappa_{Nj}} + \sum_{A,b}^{I_\theta,I_r} V^{pp}_{(Mi),(Nj),(Ab)}\chi^{pp}_{(Kl)(Ef),(Ab)} + \sum_{A,b}^{I_\theta,I_r}\frac{\Pi^{p,p}_{(Ef),(Mi)(Ab)}}{\kappa_{Mi}}V^{pp}_{(Nj),(Kl),(Ab)}\right],$$

$$t^{rr,(Ef)}_{(mi),(nj)} = \frac{\kappa_{Ef}}{\Lambda_{EE}}\left[\Lambda_{EE}V^{rr}_{(mi),(nj),(Ef)} + \frac{\Pi^{r,p}_{(Ef),(mi)(nj)}}{2\kappa_{mi}\kappa_{nj}}\right],$$

$$t^{rrp,(Ef)}_{(mi),(nj),(Kl)} = \frac{\kappa_{Ef}}{\Lambda_{EE}}\left[\Lambda_{EE}V^{rpr}_{(mi),(Kl),(nj),(Ef)} + \frac{\Pi^{r,pp}_{(Kl)(Ef),(mi)(nj)}}{\kappa_{mi}\kappa_{nj}} + \sum_{A,b}^{I_\theta,I_r} V^{rr}_{(mi),(nj),(Ab)}\chi^{pp}_{(Kl)(Ef),(Ab)} + \sum_{a,b}^{I_\theta,I_r}\frac{\Pi^{r,p}_{(Ef),(mi)(ab)}}{\kappa_{mi}}V^{rp}_{(nj),(Kl),(ab)}\right],$$

$$t^{prr,(Ef)}_{(Mi),(nj),(kl)} = \frac{\kappa_{Ef}}{\Lambda_{EE}}\left[\Lambda_{EE}\bar{V}^{prr}_{(Mi),(nj),(kl),(Ef)} + \frac{\Pi^{pr}_{(Ef),(kl),(Mi)(nj)}}{\kappa_{Mi}\kappa_{nj}} + \sum_{a,b}^{I_\theta,I_r}\left(\bar{V}^{pr}_{(Mi),(nj),(ab)}\chi^{pr}_{(Ef),(kl),(ab)} + \frac{1}{\kappa_{nj}}V^{pr}_{(Mi),(kl),(ab)}\Pi^{r,p}_{(Ef),(ab)(nj)}\right) + \sum_{A,b}^{I_\theta,I_r}\frac{\Pi^{p,p}_{(Ef),(Mi)(Ab)}}{\kappa_{Mi}}V^{rr}_{(nj),(kl),(Ab)}\right],$$

$$d^{pr,(ef)}_{(Mi),(nj)} = \frac{\kappa_{ef}}{\Lambda_{ee}}\left[\Lambda_{ee}V^{pr}_{(Mi),(nj),(ef)} + \frac{\chi^{rr}_{(nj),(ef),(Mi)}}{\kappa_{Mi}}\right],$$

$$d^{prp,(ef)}_{(Mi),(nj),(Kl)} = \frac{\kappa_{ef}}{\Lambda_{ee}}\left[\Lambda_{ee}V^{ppr}_{(Mi),(Kl),(nj),(ef)} + \frac{2\chi^{prr}_{(Kl),(nj)(ef),(Mi)}}{\kappa_{Mi}}\right.$$

$$+\sum_{A,b}^{I_\theta,I_r} V^{pp}_{(Mi),(Kl),(Ab)}\chi^{rr}_{(nj)(ef),(Ab)} + \sum_{a,b}^{I_\theta,I_r} V^{pr}_{(Mi),(nj),(ab)}\chi^{pr}_{(Kl),(ef),(ab)}\Bigg],$$

$$d^{rp,(ef)}_{(mi),(Nj)} = \frac{\kappa_{ef}}{\Lambda_{ee}}\left[\Lambda_{ee}V^{rp}_{(mi),(Nj),(ef)} + \frac{\chi^{pr}_{(Nj),(ef),(mi)}}{\kappa_{mi}}\right],$$

$$d^{rpp,(ef)}_{(mi),(Nj),(Kl)} = \frac{\kappa_{ef}}{\Lambda_{ee}}\Bigg[\Lambda_{ee}V^{rpp}_{(mi),(Nj),(Kl),(ef)} + \frac{\chi^{ppr}_{(Nj)(Kl),(ef),(mi)}}{\kappa_{mi}} + \sum_{a,b}^{I_\theta,I_r} V^{rp}_{(mi),(Nj),(ab)}\chi^{pr}_{(Kl),(ef),(ab)}\Bigg],$$

$$d^{rrr,(ef)}_{(mi),(nj),(kl)} = \frac{\kappa_{ef}}{\Lambda_{ee}}\Bigg[\Lambda_{ee}V^{rrr}_{(mi),(nj),(kl),(ef)} + \frac{\chi^{rrr}_{(nj)(kl)(ef),(mi)}}{\kappa_{mi}} + \sum_{A,b}^{I_\theta,I_r} V^{rr}_{(mi),(nj),(Ab)}\chi^{rr}_{(kl)(ef),(Ab)}\Bigg],$$

$$t^{pr,(ef)}_{(Mi),(nj)} = \frac{\kappa_{ef}}{\Lambda_{ee}}\left[\Lambda_{ee}\bar{V}^{pr}_{(Mi),(nj),(ef)} + \frac{\Pi^{r}_{(ef),(Mi),(nj)}}{\kappa_{Mi}\kappa_{nj}}\right],$$

$$t^{prp,(ef)}_{(Mi),(nj),(Kl)} = \frac{\kappa_{ef}}{\Lambda_{ee}}\Bigg[\Lambda_{ee}\bar{V}^{rpp}_{(nj),(Mi),(Kl),(ef)} + \frac{\Pi^{pr}_{(Kl),(ef),(Mi)(nj)}}{\kappa_{Mi}\kappa_{nj}} + \sum_{a,b}^{I_\theta,I_r} \bar{V}^{pr}_{(Mi),(nj),(ab)}\chi^{pr}_{(Kl),(ef),(ab)} + \sum_{a,b}^{I_\theta,I_r} \frac{V^{rp}_{(nj),(Kl),(ab)}}{\kappa_{Mi}}\Pi^{r}_{(ef),(Mi),(ab)} + \sum_{A,b}^{I_\theta,I_r} \frac{V^{pp}_{(Mi),(Kl),(Ab)}}{\kappa_{nj}}\Pi^{r}_{(ef),(Ab),(nj)}\Bigg],$$

$$t^{ppr,(ef)}_{(Mi),(Nj),(kl)} = \frac{\kappa_{ef}}{\Lambda_{ee}}\Bigg[\Lambda_{ee}V^{ppr}_{(Mi),(Nj),(kl),(ef)} + \frac{\Pi^{p,rr}_{(kl)(ef),(Mi)(Nj)}}{\kappa_{Mi}\kappa_{Nj}} + \sum_{A,b}^{I_\theta,I_r} V^{pp}_{(Mi),(Nj),(Ab)}\chi^{rr}_{(kl)(ef),(Ab)} + \sum_{a,b}^{I_\theta,I_r} \frac{V^{pr}_{(Nj),(kl),(ab)}}{\kappa_{Mi}}\Pi^{r}_{(ef),(Mi),(ab)}\Bigg],$$

$$t^{rrr,(ef)}_{(mi),(nj),(kl)} = \frac{\kappa_{ef}}{\Lambda_{ee}}\Bigg[\Lambda_{ee}\bar{V}^{rrr}_{(mi),(nj),(kl),(ef)} + \frac{\Pi^{r,rr}_{(kl)(ef),(mi)(nj)}}{\kappa_{mi}\kappa_{nj}}$$

$$+\sum_{A,b}^{I_\theta,I_r} V^{rr}_{(mi),(nj),(Ab)}\chi^{rr}_{(kl)(ef),(Ab)} + \sum_{A,b}^{I_\theta,I_r} \frac{V^{rr}_{(mi),(kl),(Ab)}}{\kappa_{nj}}\Pi^{r}_{(ef),(Ab),(nj)}\Bigg];$$

$$\bar{V}^{ppp}_{(Mi),(Nj),(Kl),(Ab)} = V^{ppp}_{(Mi),(Nj),(Kl),(Ab)} + V^{ppp}_{(Mi),(Kl),(Nj),(Ab)},$$
$$\bar{V}^{prr}_{(Mi),(nj),(kl),(Ab)} = V^{prr}_{(Mi),(nj),(kl),(Ab)} + V^{prr}_{(Mi),(kl),(nj),(Ab)} + V^{rpr}_{(nj),(Mi),(kl),(Ab)},$$
$$\bar{V}^{pr}_{(Mi),(nj),(ab)} = V^{pr}_{(Mi),(nj),(ab)} + V^{rp}_{(nj),(Mi),(ab)},$$
$$\bar{V}^{rrr}_{(mi),(nj),(kl),(ab)} = V^{rrr}_{(mi),(nj),(kl),(ab)} + V^{rrr}_{(mi),(kl),(nj),(ab)},$$
$$\bar{V}^{rpp}_{(kl),(Mi),(Nj),(ab)} = V^{rpp}_{(kl),(Mi),(Nj),(ab)} + V^{rpp}_{(kl),(Nj),(Mi),(ab)} + V^{ppr}_{(Mi),(Nj),(kl),(ab)}.$$

The system of ordinary differential equations (4.27) can be interpreted as a mechanical system composed with an infinite number of degrees of freedom without damping. If we neglect the nonlinear terms by p_{Mi} and r_{mi}, the system splits into an infinite set of linear oscillators. Hence, these uncoupled oscillators (in our case, related to p_{Mi} and r_{mi}) interact exclusively in a linear manner. The nonlinearity ensures an energy transfer between degrees of freedom of the hydrodynamic system, here, the generalized coordinates of p_{Mi} and r_{mi}.

4.4. On damping in the linear modal theory

Consider the damped linear standing waves in an upright cylindrical container. These decaying standing waves are associated with natural sloshing modes (4.2) and can be modeled using the linear approximation of the modal system (4.27) by incorporating linear damping coefficients into the linearized system (4.27). The resulting linear equations (system (4.27)) then resemble a system of independent linear oscillators without a right-hand (forcing) terms, i.e.,

$$\ddot{p}_{Mi} + \boxed{2\xi_{Mi}\bar{\sigma}_{Mi}\dot{p}_{Mi}} + \bar{\sigma}^2_{Mi}p_{Mi} = 0; \quad \ddot{r}_{mi} + \boxed{2\xi_{mi}\bar{\sigma}_{mi}\dot{r}_{mi}} + \bar{\sigma}^2_{mi}r_{mi} = 0, \quad (4.29)$$

where the framed terms represent the viscous damping.

Normally, the damping rates ξ_{Mi} are associated with logarithmic decrement of the natural sloshing modes. The rates are supposed to be small

dimensionless parameters and account for the cumulative effect of various dissipative phenomena, including the viscous laminar boundary layer on the wetted tank surface [160]. Additional factors include viscous affects at the liquid–tank–gas contact line [158], free-surface contamination [94], and, for sufficiently strong wave perturbations, the wave breakings [10]. When ξ_{Mi} are relatively small, these can be assumed that the frequencies of standing waves remain approximately equal to those given by the ideal liquid surface theory (4.5).

According to Henderson and Miles [160] who investigated both experimental and theoretical values of ξ_{Mi}, the damping rates ξ_{Mi} in (4.29) are mainly contributed by the viscous boundary layer on the wetted tank surface and by viscous bulk friction. Theoretical values of ξ_{Mi} can be asymptotically derived via the *Galilei number* [230], $Ga \gg 1$ (which implies the ratio between gravity and viscosity), or, more precisely, in terms of the small parameter

$$\delta = \mathrm{Ga}^{-1/4} = \sqrt{\nu/(g^{1/2}R_0^{3/2})} \ll 1, \tag{4.30}$$

where ν is the kinematic viscosity, which provides an asymptotic estimate of the viscous layer thickness along the wetted tank surface.

The leading-order asymptotic contribution, $\xi_{Mi}^{surf} = O(\delta)$, is associated with the laminar viscous boundary layer on the wetted tank walls. The value of ξ_{Mi}^{surf} can be estimated using the Keulegan method [158]. The second-order asymptotic contribution, $\xi_{Mi}^{bulk} = O(\delta^2)$, is related to the bulk viscosity (internal friction). According to [159] and [160], the sum

$$\xi_{Mi} = \xi_{Mi}^{surf} + \xi_{Mi}^{bulk} \tag{4.31}$$

provides good agreement with experimental results regarding the damping decrements of standing linear waves.

To estimate the damping coefficients ξ_{Mi} in formula (4.31), one can study [4] the energy loss of the standing wave over the natural sloshing period. The derivation procedure for (4.31) is described in detail in the book [4]. The result is

$$\xi_{Mi}^{surf} = \delta\, \frac{\mu_{Mi}^{(1)} + \frac{1}{2}J_{Mi}^2(k_{Mi})(\mu_{Mi}^{(2)} + \mu_{Mi}^{(3)})}{2\sqrt{2}\,\kappa_{Mi}^{5/4}\,\mu_{Mi}^{(0)}}, \tag{4.32}$$

where

$$\mu_{Mi}^{(0)} = \int_0^1 r J_{Mi}^2(k_{Mi}r)dr,$$
$$\mu_{Mi}^{(1)} = \int_0^1 r k_{Mi}^2 J_{Mi}^{'2}(k_{Mi}r)dr + M^2 \int_0^1 \frac{J_{Mi}^2(k_{Mi}r)}{r}dr, \tag{4.33}$$
$$\mu_{Mi}^{(2)} = M^2 \left(\frac{\tanh(k_{Mi}h)}{k_{Mi}} + \frac{h}{\cosh^2(k_{Mi}h)} \right),$$
$$\mu_{Mi}^{(3)} = k_{Mi}^2 \left(\frac{\tanh(k_{Mi}h)}{k_{Mi}} - \frac{h}{\cosh^2(k_{Mi}h)} \right)$$

and

$$\xi_{Mi}^{bulk} = \delta^2 \left[\frac{2k_{Mi}^2}{\kappa_{Mi}^{1/2}} - \frac{J_{Mi}^2(k_{Mi})\,\mu_{Mi}^{(2)}}{2\kappa_{Mi}^{3/2}\,\mu_{Mi}^{(0)}} \right]. \tag{4.34}$$

4.5. The damped Narimanov-Moiseev–type modal equations

We consider an upright circular base rigid tank of the radius R_0 performing small-amplitude (relative to the radius) oscillatory periodic translatory motions in the horizontal plane that are governed by the generalized time-periodic coordinate $\eta_1(t)$. The excitation period is close to the higher natural sloshing period so that the contained liquid is in resonance, that is, in particular, that the surface-wave magnitude is much larger that the excitation amplitude.

Combining the Miles-Lukovsky variational and Narimanov-Moiseev asymptotic approaches, a rather compact weakly nonlinear system of ordinary differential equations was derived in [4, 7]. This Narimanov-Moiseev–type modal system is applicable when the excitation frequency σ is close to the lowest natural sloshing frequency σ_{11}, i.e., $\bar{\sigma}_{11} \to 1$, the non-dimensional liquid depth $1.02 \lesssim h$ (this provides no secondary resonances [1, 7, 74] in the hydrodynamic system) and the nondimensional (R_0-scaled) excitation amplitude is small

$$\eta_1 = O(\epsilon) \ll 1. \tag{4.35}$$

Within the framework of the Narimanov-Moiseev–type multimodal modelling, the nondimensional generalised hydrodynamic coordinates satisfy the asymptotic relations

$$p_{11} \sim r_{11} = O(\epsilon^{1/3}),\ p_{0i} \sim p_{2i} \sim r_{2i} = O(\epsilon^{2/3}),$$
$$p_{3i} \sim r_{3i} \sim p_{1\,i+1} \sim r_{1\,i+1} = O(\epsilon),\ i \geq 1, \quad (4.36)$$

but the modal system neglects the $o(\epsilon)$ terms and takes the form [4, 7]

$$\ddot{p}_{11} + \boxed{2\xi_{11}\bar{\sigma}_{11}\dot{p}_{11} + \mathcal{Q}_{11}(\dot{p}_{11})} + \bar{\sigma}_{11}^2 p_{11} + d_1 p_{11}\left(\ddot{p}_{11}p_{11} + \ddot{r}_{11}r_{11} + \dot{p}_{11}^2 + \dot{r}_{11}^2\right)$$
$$+ d_2[r_{11}(\ddot{p}_{11}r_{11} - \ddot{r}_{11}p_{11}) + 2\dot{r}_{11}(\dot{p}_{11}r_{11} - \dot{r}_{11}p_{11})$$
$$+ \sum_{j=1}^{I_r}\Big[d_3^{(j)}(\ddot{p}_{11}p_{2j} + \ddot{r}_{11}r_{2j} + \dot{p}_{11}\dot{p}_{2j} + \dot{r}_{11}\dot{r}_{2j}) + d_4^{(j)}(\ddot{p}_{2j}p_{11} + \ddot{r}_{2j}r_{11})$$
$$+ d_5^{(j)}\left(\ddot{p}_{11}p_{0j} + \dot{p}_{11}\dot{p}_{0j}\right) + d_6^{(j)}\ddot{p}_{0j}p_{11}\Big] = -\ddot{\eta}_1\kappa_{11}P_1, \quad (4.37a)$$

$$\ddot{r}_{11} + \boxed{2\xi_{11}\bar{\sigma}_{11}\dot{r}_{11} + \mathcal{Q}_{11}(\dot{r}_{11})} + \bar{\sigma}_{11}^2 r_{11} + d_1 r_{11}\left(\ddot{p}_{11}p_{11} + \ddot{r}_{11}r_{11} + \dot{p}_{11}^2 + \dot{r}_{11}^2\right)$$
$$+ d_2[p_{11}(\ddot{r}_{11}p_{11} - \ddot{p}_{11}r_{11}) + 2\dot{p}_{11}(\dot{r}_{11}p_{11} - \dot{p}_{11}r_{11})$$
$$\sum_{j=1}^{I_r}\Big[d_3^{(j)}\left(\ddot{p}_{11}r_{2j} - \ddot{r}_{11}p_{2j} + \dot{p}_{11}\dot{r}_{2j} - \dot{p}_{2j}\dot{r}_{11}\right)$$
$$+ d_4^{(j)}(\ddot{r}_{2j}p_{11} - \ddot{p}_{2j}r_{11}) + d_5^{(j)}(\ddot{r}_{11}p_{0j} + \dot{r}_{11}\dot{p}_{0j}) + d_6^{(j)}\ddot{p}_{0j}r_{11}\Big] = 0; \quad (4.37b)$$

$$\ddot{p}_{2k} + \boxed{2\xi_{2k}\bar{\sigma}_{2k}\dot{p}_{2k}} + \bar{\sigma}_{2k}^2 p_{2k} + d_{7,k}(\dot{p}_{11}^2 - \dot{r}_{11}^2) + d_{9,k}(\ddot{p}_{11}p_{11} - \ddot{r}_{11}r_{11}) = 0, \quad (4.38a)$$

$$\ddot{r}_{2k} + \boxed{2\xi_{2k}\bar{\sigma}_{2k}\dot{r}_{2k}} + \bar{\sigma}_{2k}^2 r_{2k} + 2d_{7,k}\dot{p}_{11}\dot{r}_{11} + d_{9,k}(\ddot{p}_{11}r_{11} + \ddot{r}_{11}p_{11}) = 0, \quad (4.38b)$$

$$\ddot{p}_{0k} + \boxed{2\xi_{0k}\bar{\sigma}_{0k}\dot{p}_{0k}} + \bar{\sigma}_{0k}^2 p_{0k} + d_{8,k}(\dot{p}_{11}^2 + \dot{r}_{11}^2) + d_{10,k}(\ddot{p}_{11}p_{11} + \ddot{r}_{11}r_{11}) = 0; \quad (4.38c)$$

$$\ddot{p}_{3k} + \boxed{2\xi_{3k}\bar{\sigma}_{3k}\dot{p}_{3k}} + \bar{\sigma}_{3k}^2 p_{3k} + d_{11,k}[\ddot{p}_{11}(p_{11}^2 - r_{11}^2) - 2p_{11}r_{11}\ddot{r}_{11}]$$
$$+ d_{12,k}[p_{11}(\dot{p}_{11}^2 - \dot{r}_{11}^2) - 2r_{11}\dot{p}_{11}\dot{r}_{11}] + \sum_{j=1}^{I_r}\Big[d_{13,k}^{(j)}(\ddot{p}_{11}p_{2j} - \ddot{r}_{11}r_{2j})$$
$$+ d_{14,k}^{(j)}(\ddot{p}_{2j}p_{11} - \ddot{r}_{2j}r_{11}) + d_{15,k}^{(j)}(\dot{p}_{2j}\dot{p}_{11} - \dot{r}_{2j}\dot{r}_{11})\Big] = 0, \quad (4.39a)$$

$$\ddot{r}_{3k}+\boxed{2\xi_{3k}\bar{\sigma}_{3k}\dot{r}_{3k}}+\bar{\sigma}_{3k}^2 r_{3k}+d_{11,k}\left[\ddot{r}_{11}(p_{11}^2-r_{11}^2)+2p_{11}r_{11}\ddot{p}_{11}\right]$$
$$+d_{12,k}\left[r_{11}(\dot{p}_{11}^2-\dot{r}_{11}^2)+2p_{11}\dot{p}_{11}\dot{r}_{11}\right]+\sum_{j=1}^{I_r}\Big[d_{13,k}^{(j)}(\ddot{p}_{11}r_{2j}+\ddot{r}_{11}p_{2j})$$
$$+d_{14,k}^{(j)}(\ddot{p}_{2j}r_{11}+\ddot{r}_{2j}p_{11})+d_{15,k}^{(j)}(\dot{p}_{2j}\dot{r}_{11}+\dot{r}_{2j}\dot{p}_{11})\Big]=0,\ k=1,...,I_r;\quad (4.39b)$$

$$\ddot{p}_{1n}+\boxed{2\xi_{1n}\bar{\sigma}_{1n}\dot{p}_{1n}}+\bar{\sigma}_{1n}^2 p_{1n}+d_{16,n}(\ddot{p}_{11}p_{11}^2+r_{11}p_{11}\ddot{r}_{11})+d_{17,n}(\ddot{p}_{11}r_{11}^2-r_{11}p_{11}\ddot{r}_{11})$$
$$+d_{18,n}p_{11}(\dot{p}_{11}^2+\dot{r}_{11}^2)+d_{19,n}(r_{11}\dot{p}_{11}\dot{r}_{11}-p_{11}\dot{r}_{11}^2)$$
$$+\sum_{j=1}^{I_r}\Big[d_{20,n}^{(j)}(\ddot{p}_{11}p_{2j}+\ddot{r}_{11}r_{2j})+d_{21,n}^{(j)}(p_{11}\ddot{p}_{2j}+r_{11}\ddot{r}_{2j})+d_{22,n}^{(j)}(\dot{p}_{11}\dot{p}_{2j}+\dot{r}_{11}\dot{r}_{2j})$$
$$+d_{23,n}^{(j)}\ddot{p}_{11}p_{0j}+d_{24,n}^{(j)}p_{11}\ddot{p}_{0j}+d_{25,n}^{(j)}\dot{p}_{11}\dot{p}_{0j}\Big]=-\ddot{\eta}_1\kappa_{1n}P_n,\quad (4.40a)$$

$$\ddot{r}_{1n}+\boxed{2\xi_{1n}\bar{\sigma}_{1n}\dot{r}_{1n}}+\bar{\sigma}_{1n}^2 r_{1n}+d_{16,n}(\ddot{r}_{11}r_{11}^2+r_{11}p_{11}\ddot{p}_{11})+d_{17,n}(\ddot{r}_{11}p_{11}^2-r_{11}p_{11}\ddot{p}_{11})$$
$$+d_{18,n}r_{11}(\dot{p}_{11}^2+\dot{r}_{11}^2)+d_{19,n}(p_{11}\dot{p}_{11}\dot{r}_{11}-r_{11}\dot{p}_{11}^2)$$
$$+\sum_{j=1}^{I_r}\Big[d_{20,n}^{(j)}(\ddot{p}_{11}r_{2j}-\ddot{r}_{11}p_{2j})+d_{21,n}^{(j)}(p_{11}\ddot{r}_{2j}-r_{11}\ddot{p}_{2j})+d_{22,n}^{(j)}(\dot{p}_{11}\dot{r}_{2j}-\dot{r}_{11}\dot{p}_{2j})$$
$$+d_{23,n}^{(j)}\ddot{r}_{11}p_{0j}+d_{24,n}^{(j)}r_{11}\ddot{p}_{0j}+d_{25,n}^{(j)}\dot{r}_{11}\dot{p}_{0j}\Big]=0,\ n=2,...,I_r,\quad (4.40b)$$

where

$$P_j=\frac{1}{k_{1j}}\sqrt{\frac{2}{k_{1j}^2-1}}\qquad (4.41)$$

and the non-dimensional hydrodynamic coefficients at the nonlinear quantities are the given functions of the non-dimensional liquid depth h which are tabled in [4].

Following [4], the nonlinear Narimanov-Moiseev–type equations (4.37)–(4.40) are equipped with extra framed terms which are not derivable from the original mathematical statement but are needed to account for the viscous damping. The terms include linear components with the damping coefficients $2\xi_{Mi}\bar{\sigma}_{Mi}$ ($0<\xi_{Mi}\ll 1$ are the viscous damping rates) which can physically be related to logarithmic decrements of the natural sloshing modes when the free-surface nonlinearity does not matter. In addition, the nonlinear damping

quantity $\mathcal{Q}_{11}$ is introduced in (4.37) governing the lowest-order (dominant) generalised hydrodynamic coordinates $p_{11}(t)$ and $r_{11}(t)$.

Experimental estimates of the damping rates ξ_{Mi} might be done by measuring the logarithmic decrements [1, 160, 219] of the corresponding natural sloshing modes (standing waves). The procedure of restoring ξ_{Mi} from these measurements could mathematically be interpreted as a [machine] learning of the linearised modal equations (4.37)–(4.40). Theoretical predictions of ξ_{Mi} are derivable by solving a spectral boundary value problem on linear sloshing of viscous liquid [48, 230]. Alternatively, the theoretical damping rates ξ_{Mi} can be estimated by employing asymptotic formulas by Keulegan [4, 158, 160, 219] that assumes laminar viscous flow near the wetted tank surface.

Specifically, all the aforementioned approaches to estimating the damping rates ξ_{Mi} are invalid for nonlinear resonant sloshing when total energy loss is seriously affected by energy flow from lower to higher natural sloshing modes [220]. This means that ξ_{Mi} in (4.37)–(4.40) are poorly predicted by existing theories [4, 48, 158, 160, 219]. The latter is also true for experiments when the free-surface nonlinearity is not negligible.

The nonlinear Narimanov-Moiseev–type modal system (4.38)–(4.40) is of asymptotic nature. It neglects the $o(\epsilon)$-order quantities including whose associated with viscous damping. Furthermore, one should recall that the damping rates ξ_{Mi} should be small. It is because they should be proportional to the viscous boundary layer thickness at the liquid boundary but the thickness must be small if an inviscid-liquid hydrodynamic model is adopted.

In [4], the damping rates ξ_{Mi} are assumed being of the $O(\epsilon^{2/3})$-order that made it possible to completely neglect viscous damping in (4.38)–(4.40) and require $\mathcal{Q}_{11} \equiv 0$. Under this asymptotic assumption, the Narimanov-Moiseev–type modal theory completely fails to fit the measured data in [10] on the phase lag for the steady-state swirling wave mode. On the other hand, the authors [215] showed that assuming the $O(\epsilon^{1/3})$-order damping rates in the Narimanov-Moiseev–type modal equations for sloshing in a rectangular tank makes it possible to fit analogous measurements in [11]. Let us further

follow [215] and, therefore, postulate $\xi_{Mi} = O(\epsilon^{1/3})$ and

$$\mathcal{Q}_{11}(f) = \xi_1 \frac{3\pi}{4} f\,|f| + o(f^2), \quad \xi_1 = O(\epsilon^{1/3}). \tag{4.42}$$

4.6. Steady-state resonant sloshing

The nonlinear modal equations (4.37)–(4.40) were derived assuming resonant excitation of the lowest natural sloshing mode. Consider the harmonic resonant longitudinal forcing of a small amplitude, i.e.,

$$\eta_1(t) = \eta_{1a} \cos t, \quad \eta_{1a} = O(\epsilon) \ll 1, \tag{4.43}$$

when the excitation (equal to the characteristic) frequency σ is close to the first natural sloshing frequency σ_{11} as well as the Moiseev asymptotic detuning is satisfied,

$$\Lambda = \bar{\sigma}_{11}^2 - 1 = \frac{\sigma_{11}^2}{\sigma^2} - 1 = O(\epsilon^{2/3}). \tag{4.44}$$

Even though the Narimanov-Moiseev–type equations (4.37)–(4.40) are equipped with extra damping terms, its asymptotic periodic solution can be constructed by combining asymptotic and Fourier harmonic analysis from [4, 7]. The starting point consists of considering the first (lowest) order asymptotic approximation which is associated with amplitudes at the lowest Fourier harmonics in the dominant generalised hydrodynamic coordinates

$$p_{11}(t) = a \cos t + \bar{a} \sin t + O(\epsilon); \quad r_{11}(t) = \bar{b} \cos t + b \sin t + O(\epsilon), \tag{4.45}$$

where the non-dimensional amplitude parameters $a, \bar{a}, \bar{b}$, and $b = O(\epsilon^{1/3})$. Why these four lowest order amplitudes are of the lowest asymptotic order $O(\epsilon^{1/3})$ in the Narimanov-Moiseev–type approximation.

Substitution of (4.45) into (4.38) derives

$$\begin{aligned} p_{0k}(t) = {} & s_{0k}(a^2 + \bar{a}^2 + b^2 + \bar{b}^2) \\ & + s_{1k}\left[(a^2 - \bar{a}^2 - b^2 + \bar{b}^2)\cos 2t + 2(a\bar{a} + b\bar{b})\sin 2t\right] \\ & + s_{2k}\left[-2(a\bar{a} + b\bar{b})\cos 2t + (a^2 - \bar{a}^2 - b^2 + \bar{b}^2)\sin 2t\right] + o(\epsilon), \end{aligned} \tag{4.46a}$$

$$p_{2k}(t) = c_{0k}(a^2 + \bar{a}^2 - b^2 - \bar{b}^2)$$

$$+ c_{1k}\left[(a^2-\bar{a}^2+b^2-\bar{b}^2)\cos 2t + 2(a\bar{a}-b\bar{b})\sin 2t\right]$$
$$+ c_{2k}\left[-2(a\bar{a}-b\bar{b})\cos 2t + (a^2-\bar{a}^2+b^2-\bar{b}^2)\sin 2t\right] + o(\epsilon), \quad (4.46b)$$

$$r_{2k}(t) = 2c_{0k}(a\bar{b}+b\bar{a}) + 2c_{1k}\left[(a\bar{b}-b\bar{a})\cos 2t + (ab+\bar{a}\bar{b})\sin 2t\right]$$
$$+ 2c_{2k}\left[-(ab+\bar{a}\bar{b})\cos 2t + (a\bar{b}-b\bar{a})\sin 2t\right] + o(\epsilon), \quad (4.46c)$$

where

$$\begin{aligned} s_{0k} &= \frac{d_{10,k}-d_{8,k}}{2\bar{\sigma}_{0k}^2};\ s_{1k} = \frac{d_{10,k}+d_{8,k}}{2\Delta_{0k}}(\bar{\sigma}_{0k}^2-4), \\ s_{2k} &= 2\frac{d_{10,k}+d_{8,k}}{\Delta_{0k}}\xi_{0,k}\bar{\sigma}_{0k};\ c_{0k} = \frac{d_{9,k}-d_{7,k}}{2\bar{\sigma}_{2k}^2}, \\ c_{1k} &= \frac{d_{9,k}+d_{7,k}}{2\Delta_{2k}}(\bar{\sigma}_{2k}^2-4);\ c_{2k} = 2\frac{d_{9,k}+d_{7,k}}{\Delta_{2k}}\xi_{2,k}\bar{\sigma}_{2k} \end{aligned} \quad (4.47)$$

and

$$\Delta_{0k} = (\bar{\sigma}_{0k}^2-4)^2 + 16\xi_{0k}^2\bar{\sigma}_{0k}^2; \quad \Delta_{2k} = (\bar{\sigma}_{2k}^2-4)^2 + 16\xi_{2k}^2\bar{\sigma}_{2k}^2. \quad (4.48)$$

Inserting (4.45) and (4.46) into (4.37) and collecting the terms in front of the first Fourier harmonics, $\cos t$ and $\sin t$, deduce the necessary solvability (secular) conditions

$$a\left[\Lambda + m_1(a^2+\bar{a}^2+\bar{b}^2) + m_3b^2 - 2(m_7-m_6)b\bar{b}\right]$$
$$+ \bar{a}\left[(m_1-m_3)\bar{b}b + (\xi_0+\xi_1A) - (m_6+m_7)(a^2+\bar{a}^2+b^2)\right.$$
$$\left.-(3m_6-m_7)\bar{b}^2\right] = \epsilon_x = \kappa_{11}P_1\eta_{1a}, \quad (4.49a)$$

$$\bar{a}\left[\Lambda + m_1(a^2+\bar{a}^2+b^2) + m_3\bar{b}^2 + 2(m_7-m_6)b\bar{b}\right] + a\left[(m_1-m_3)\bar{b}b\right.$$
$$\left.-(\xi_0+\xi_1A) + (m_6+m_7)(a^2+\bar{a}^2+\bar{b}^2) + (3m_6-m_7)b^2\right] = 0, \quad (4.49b)$$

$$b\left[\Lambda + m_1(b^2+\bar{b}^2+\bar{a}^2) + m_3a^2 + 2(m_7-m_6)a\bar{a}\right] + \bar{b}\left[(m_1-m_3)\bar{a}a\right.$$
$$\left.-(\xi_0+\xi_1B) + (m_6+m_7)(b^2+\bar{b}^2+a^2) + (3m_6-m_7)\bar{a}^2\right] = 0, \quad (4.49c)$$

$$\bar{b}\left[\Lambda + m_1(b^2+\bar{b}^2+a^2) + m_3\bar{a}^2 - 2(m_7-m_6)a\bar{a}\right] + b\left[(m_1-m_3)\bar{a}a\right.$$
$$\left.+(\xi_0+\xi_1B) - (m_6+m_7)(b^2+\bar{b}^2+\bar{a}^2) - (3m_6-m_7)a^2\right] = 0 \quad (4.49d)$$

with respect to $a, \bar{a}, \bar{b}$ and b, $\xi_0 = 2\xi_{11}$, so that the system (4.49) defines the amplitude parameters as functions the frequency parameter Λ by (4.44). The coefficients m_i are calculated by the formulas

$$m_1 = -\tfrac{1}{2}d_1 + \sum_{j=1}^{I_r}\Big[c_{1j}\left(\tfrac{1}{2}d_3^{(j)} - 2d_4^{(j)}\right) + s_{1j}\left(\tfrac{1}{2}d_5^{(j)} - 2d_6^{(j)}\right) - s_{0j}d_5^{(j)} - c_{0j}d_3^{(j)}\Big], \quad (4.50a)$$

$$m_3 = \tfrac{1}{2}d_1 - 2d_2 + \sum_{j=1}^{I_r}\Big[c_{1j}\left(\tfrac{3}{2}d_3^{(j)} - 6d_4^{(j)}\right) + s_{1j}\left(-\tfrac{1}{2}d_5^{(j)} + 2d_6^{(j)}\right) - s_{0j}d_5^{(j)} + c_{0j}d_3^{(j)}\Big], \quad (4.50b)$$

$$m_6 = \sum_{j=1}^{I_r} c_{2j}\left(\tfrac{1}{2}d_3^{(j)} - 2d_4^{(j)}\right); \quad m_7 = \sum_{j=1}^{I_r} s_{2j}\left(\tfrac{1}{2}d_5^{(j)} - 2d_6^{(j)}\right), \quad (4.50c)$$

which are formally functions of h and $\bar{\sigma}_{11} = 1 + O(\epsilon^{2/3})$ so that excluding the higher-order terms in m_k implies considering $\bar{\sigma}_{0k}^2$ and $\bar{\sigma}_{2k}^2$ in expressions (4.47) and (4.48) independent of σ^2 and equal to $\sigma_{0k}^2/\sigma_{11}^2$ and $\sigma_{2k}^2/\sigma_{11}^2$, respectively.

Following [8], we introduce the integral amplitudes

$$A = \sqrt{a^2 + \bar{a}^2} \quad \text{and} \quad B = \sqrt{\bar{b}^2 + b^2} > 0, \quad (4.51)$$

which link the original amplitude parameters as follows

$$a = A\cos\psi, \quad \bar{a} = A\sin\psi, \quad \bar{b} = B\cos\varphi, \quad b = B\sin\varphi, \quad (4.52)$$

where ψ and φ are the phase lags.

By substituting (4.52) into expressions $[\bar{a}\,(4.49a) - a\,(4.49b)]$, $[\bar{b}\,(4.49c) - b\,(4.49d)]$, $[a\,(4.49a) + \bar{a}\,(4.49b)]$ and $[b\,(4.49c) + \bar{b}\,(4.49d)]$, we arrive at the following alternative secular equations

$$\begin{cases} \boxed{1}: A[\Lambda + m_1A^2 + (\mathcal{F} + \mathcal{H})B^2] = \epsilon_x\cos\psi, \\ \boxed{2}: B[\Lambda + m_1B^2 + (\mathcal{F} - \mathcal{H})A^2] = 0, \\ \boxed{3}: A[(\mathcal{D} + \mathcal{G})B^2 + (\xi_0 + \xi_1A) - (m_6 + m_7)A^2] = \epsilon_x\sin\psi, \\ \boxed{4}: B[(\mathcal{D} - \mathcal{G})A^2 - (\xi_0 + \xi_1B) + (m_6 + m_7)B^2] = 0, \end{cases} \quad (4.53)$$

where

$$\begin{aligned}
\mathcal{F} &= \mathcal{F}_\alpha = m_1\cos^2\alpha + m_3\sin^2\alpha,\\
\mathcal{D} &= \mathcal{D}_\alpha = (m_3 - m_1)\sin\alpha\cos\alpha,\\
\mathcal{G} &= \mathcal{G}_\alpha = m_7 - 3m_6 + 2(m_6 - m_7)\cos^2\alpha,\\
\mathcal{H} &= \mathcal{H}_\alpha = 2(m_6 - m_7)\sin\alpha\cos\alpha,
\end{aligned} \tag{4.54}$$

and $\alpha = \varphi - \psi$. The secular systems (4.49) and (4.53) are mathematically equivalent. Having known $A, B,\ \psi, \varphi$ from (4.53), we can define $a, \bar{a}, b, \bar{b}$ and *vice versa*. There are two physically different solutions which determine planar and swirling steady-state waves.

The *planar* steady-state waves correspond to $B = 0$ and $A > 0$ (phase lag φ is not defined), where A and ψ are analytically represented by

$$\begin{aligned}
&A^2\left[(\Lambda + m_1A^2)^2 + (\xi_0 + \xi_1A - (m_6 + m_7)A^2)^2\right] = \epsilon_x^2\\
&\qquad\qquad\Updownarrow\\
&-1 < \Lambda_{[A]} = \pm\sqrt{\frac{\epsilon_x^2}{A^2} - (\xi_0 + \xi_1A - (m_6 + m_7)A^2)^2} - m_1A^2,\\
&\psi_{[A]} = \operatorname{atan2}\left(\frac{A(\xi_0 + \xi_1A - (m_6 + m_7)A^2)}{\epsilon_x}, \frac{A(\Lambda_{[A]} + m_1A^2)}{\epsilon_x}\right),
\end{aligned} \tag{4.55}$$

which parametrically determine the wave amplitude ($\sigma/\sigma_1 = (\Lambda_{[A]} + 1)^{-1/2}, A, 0$) and phase lag ($\sigma/\sigma_1 = (\Lambda_{[A]} + 1)^{-1/2}, \psi_{[A]}, 0$) response curves as functions of $A_{min} < A < A_{max}$, where A_{max} comes from the positiveness of expression under the square root and A_{min} is associated with the equality $-1 < \Lambda_{[A]}$.

The *swirling* steady-state wave regime is associated with solution of (4.53) when $B > 0$. To get this solution, the secular system should be rewritten in the form

$$\boxed{4}:\ A^2_{[B,\alpha]} = \frac{\xi_0 + \xi_1B - (m_6 + m_7)B^2}{\mathcal{D}_\alpha - \mathcal{G}_\alpha} > 0, \tag{4.56a}$$

$$\boxed{2}:\ \Lambda_{[B,\alpha]} = -m_1B^2 - (\mathcal{F}_\alpha - \mathcal{H}_\alpha)A^2_{[B,\alpha]} > -1, \tag{4.56b}$$

$$\begin{aligned}
\boxed{1}^2 + \boxed{4}^2:\ \epsilon_x^2 = A^2_{[B,\alpha]}\Bigg(&\left[\Lambda_{[B,\alpha]} + m_1A^2_{[B,\alpha]} + (\mathcal{F}_\alpha + \mathcal{H}_\alpha)B^2\right]^2\\
&+ \left[(\xi_0 + \xi_1A_{[B,\alpha]}) - (m_6 + m_7)A^2_{[B,\alpha]} + (\mathcal{D}_\alpha + \mathcal{G}_\alpha)B^2\right]^2\Bigg),
\end{aligned} \tag{4.56c}$$

$$\boxed{1},\ \boxed{4}: \qquad \psi_{[B,\alpha]} = \operatorname{atan2}\left(\frac{A_{[B,\alpha]}\left(\xi_0+\xi_1 A_{[B,\alpha]}-(m_6+m_7)A^2_{[B,\alpha]}\right)}{\epsilon_x},\right.$$
$$\left.\frac{A_{[B,\alpha]}\left(\Lambda_{[B,\alpha]}+m_1 A^2_{[B,\alpha]}\right)}{\epsilon_x}\right), \quad (4.56d)$$

$$\varphi_{[B,\alpha]} = \alpha + \psi_{[B,\alpha]} \quad (4.56e)$$

whose consequently usage makes it possible to draw the amplitude/phase-lag response branchings, parametrically, as functions of B.

Summarizing the above derivations implies that we proved the following theorem.

Theorem 4.1. *Getting the branches for the swirling wave mode implies following the computational procedure:*

1^0. *Consider a trial fixed value* $B > 0$.

2^0. *Because* $\mathcal{D}_\alpha, \mathcal{G}_\alpha, \mathcal{F}_\alpha$, *and* $\mathcal{H}_\alpha$ *are the* π*–periodic functions of* α, *one can find intervals* (α_i, α_{i+1}), $0 \le \alpha_i < \pi$, *where inequality (4.56a) is satisfied for the chosen* B *and, therefore, the real* $A > 0$ *exists.*

3^0. *Substitute (4.56a) and (4.56b) into (4.56c) to get (for the chosen fixed* B*) an equation with respect to* α *defined on the above computed intervals* (α_i, α_{i+1}), $0 \le \alpha_i < \pi$. *Denote these roots as* $\alpha^{[k]}_{[B]}$, $k = 1, ..., N_B$.

4^0. *Consequently inserting* B *and* $\alpha = \alpha^{[k]}_{[B]}$, $k = 1, ..., N_B$ *into (4.56a), (4.56b) and (4.56e) determines* N_B *points on the amplitude*

$$\left(\sigma/\sigma_1 = (\Lambda_{\left[B,\alpha^{[k]}_{[B]}\right]}+1)^{-1/2}, A_{\left[B,\alpha^{[k]}_{[B]}\right]}, B\right), \ k = 1, ..., N_B \quad (4.57)$$

and phase-lag

$$\left(\sigma/\sigma_1 = (\Lambda_{\left[B,\alpha^{[k]}_{[B]}\right]}+1)^{-1/2}, \psi_{\left[B,\alpha^{[k]}_{[B]}\right]}, \varphi_{\left[B,\alpha^{[k]}_{[B]}\right]}\right), \ k = 1, ..., N_B \quad (4.58)$$

response curves.

5^0. *Varying* B *between* 0 *and* B_{max} *which obviously exists since the right-hand side of (4.56c) increases with increasing* B *draws the response curves by (4.57) and (4.58).*

4.7. Learning the damping coefficients ξ_{0i}, ξ_{2i}, ξ_0 and ξ_1

Based on analytical solutions (4.55) and (4.56) and experimental data on the phase lag, one can, following [215], construct a learning procedure to compute the positive damping rates ξ_{0i}, ξ_{2i} as well as ξ_0 and ξ_1 (denote all of them as the vector $\boldsymbol{\xi} \geq 0$).

Appropriate measurements of the phase lag ψ for stable swirling were done in [10]. These measurements were employed in [4] to show that assuming the damping rates (= viscous boundary layer thickness) of the order $O(\epsilon^{2/3})$ (which means $\xi_{0i} = \xi_{2i} = 0$ and $\xi_1 = 0$ when neglecting the $o(\epsilon)$-order terms in the modal system) makes it impossible to fit, even qualitatively, the measured phase-lag data within the framework of the Narimanov-Moiseev–type modal theory.

Assume the given experimental measurements of the phase lag with the same liquid depth but, possibly, different forcing amplitudes, ϵ_x, are presented by the pairs

$$(\sigma/\sigma_{11} = s_j(\epsilon_x), \psi = p_j(\epsilon_x)),\ j = 1, ..., N \tag{4.59}$$

and consider the theoretical phase-lag branch

$$\left([\sigma/\sigma_{11}]_{\left[B,\alpha^{[*]}_{[B]}\right]}(\epsilon_x, \boldsymbol{\xi}) = \left(\Lambda_{\left[B,\alpha^{[*]}_{[B]}\right]}(\epsilon_x, \boldsymbol{\xi}) + 1\right)^{-1/2}, \psi_{\left[B,\alpha^{[*]}_{[B]}\right]}(\epsilon_x, \boldsymbol{\xi})\right) \tag{4.60}$$

as a function of $0 < B \leq B_{max}$.

Similar to [215], we also introduce the distance function between the measured (4.59) and theoretical (4.60) phase-lag branches as follows

$$D(\epsilon_x, \boldsymbol{\xi}, j) = \left(\min_{0 \leq B \leq B_{max}} \left(s_j(\epsilon_x) - [\sigma/\sigma_{11}]_{\left[B,\alpha^{[*]}_{[B]}\right]}(\epsilon_x, \boldsymbol{\xi})\right)^2 + \left(p_j(\epsilon_x) - \psi_{\left[B,\alpha^{[*]}_{[B]}\right]}(\epsilon_x, \boldsymbol{\xi})\right)^2\right)^{1/2}, \tag{4.61}$$

which is determined for each fixed experimental point j with the excitation amplitude ϵ_x and the trial vector $\boldsymbol{\xi} \geq 0$ of the damping rates. The integral (summarised) distance reads as

$$C(\boldsymbol{\xi}) = \sum_{j=1}^{N} \sum_{\epsilon_x} D(\epsilon_x, \boldsymbol{\xi}, j). \tag{4.62}$$

It appears as the cost function in the learning procedure. Minimisation of the cost function (4.62) can be done by the gradient descent method.

To the authors best knowledge, the research paper [10] is a unique case when its authors measured the phase lag for steady-state resonant sloshing in an upright circular base tank exposed to a horizontal harmonic excitation. The measurements were done for the swirling-wave regime when the nondimensional mean liquid depth $h = 1.5$ and the excitation amplitude $\eta_{2a} = 0.045$. These were already employed in [4, 9] to investigate applicability of the Narimanov-Moiseev–type theory with $\xi_{11} \neq 0$ but $\xi_1 = \xi_{0k} = \eta_{2k} = 0, k = 1, ..., N_r$, which corresponds to the $O(\epsilon^{2/3})$-order viscous boundary layer thickness. Similar failure was reported in [11] which used analogous assumptions to the Narimanov-Moiseev–type modal system [3] on sloshing in a two=dimensional rectangular tank. The present authors [215] showed that the latter modal system effectively fits the experimental data from [11] with viscous damping terms associated with the $O(\epsilon^{1/3})$-asymptotics for the viscous boundary layer.

Fig. 4.2 demonstrates results of the developed (machine) learning procedure resulted from feature data on the phase lag in [10]. The left panel is drown when the learning procedure adopts the whole set of measurements including those where experimental observations discovered severe wave breakings with the free-surface fragmentation. The computed damping coefficients are $\xi_0 = 1.019368961 \cdot 10^{-4}, \xi_1 = 2.259451 \cdot 10^{-2}$, $\xi_{01} = 2.6424261 \cdot 10^{-2}, \xi_{02} = 6.4908885462 \cdot 10^{-3}, \xi_{03} = 0.21416321$, and $\xi_{21} = 0.150823783, \xi_{22} = 7.008502736 \cdot 10^{-3}, \xi_{23} = 7.00062716 \cdot 10^{-3}$. The right panel in Fig. 4.2 compares theory and experiments when feature data corresponding to severe breaking waves in [10] are excluded. The computed damping coefficients are $\xi_0 = 0.0, \xi_1 = 8.393626 \cdot 10^{-3}$, $\xi_{01} = 2.74034543 \cdot 10^{-2}, \xi_{02} = 8.7304159 \cdot 10^{-3}, \xi_{03} = 0.2148668$, and $\xi_{21} = 0.15094845, \xi_{22} = 7.138907 \cdot 10^{-3}, \xi_{23} = 7.31498666 \cdot 10^{-3}$.

The computed damping coefficients show that damping of higher natural sloshing modes plays the primary role to fit experimental feature data. The damping rates ξ_{0i} and ξ_{2i} weakly change with the choice of the full or

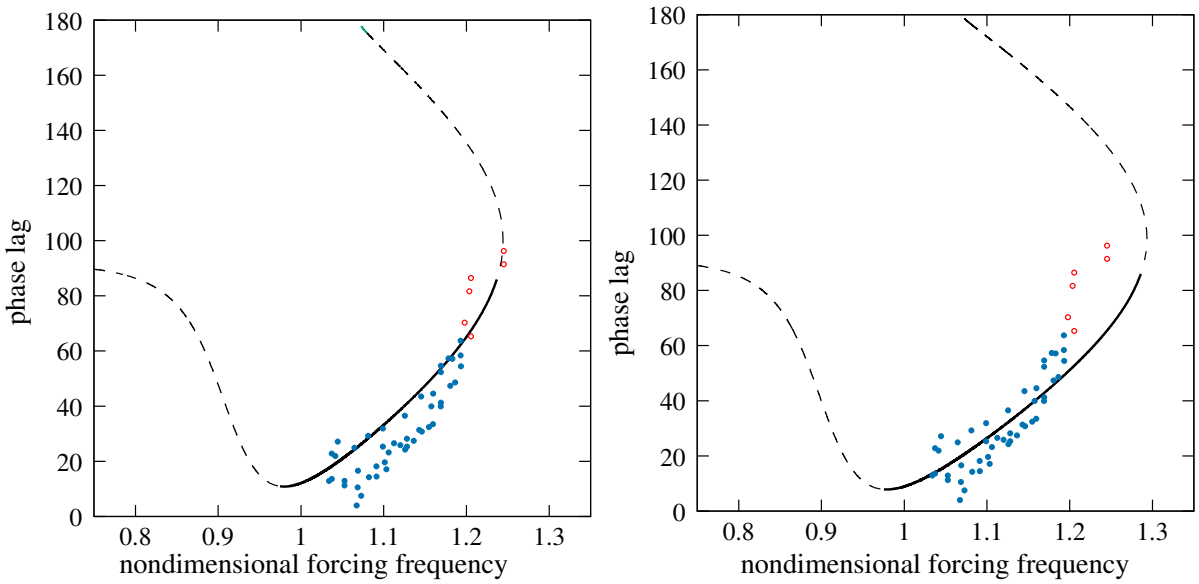

Figure 4.2. Theoretical and experimental phase lag ψ (vertical axis, grad) versus the nondimensional forcing frequency σ/σ_{11} (horizontal axis) for longitudinal tank excitations with the nondimensional forcing amplitude $\eta_{2a} = 0.045$ and $h = 1.5$. Steady-state swirling waves. The measured values (circles) are taken from [10]. The theoretical response curves are marked by lines: the solid lines correspond to stable steady-state swirling (according to [4]) and the dashed lines imply instable waves. The empty (red) circles are experimental data for which [10] reports severe wave breaking with fragmentation of the free surface that can significantly affect, as discussed in [215], the measured data. The solid (deep blue) circles mark measurements done with stable swirling wave which is also accompanied by the breaking wave phenomenon but not much severe. The left panel demonstrates the results when all the measurement from [10] are adopted as feature data but the right panel was drown based on feature data which are marked by the solid circles.

limited (trusted) feature data set. Linear damping of the lowest natural sloshing modes (generalized coordinates $p_{11}(t)$ and $r_{11}(t)$) can be practically neglected. However, the coefficient in the non-linear damping term, ξ_1, is not zero and determines the theoretical branching behavior versus the reliable (feature) experimental data.

4.8. Conclusions to the chapter

The chapter shows how to get nonlinear modal equations of a special form, (4.10), (4.11), which describe sloshing under small-amplitude resonant excitations of an upright circular base tank with four degrees of freedom $\eta_i(t)$, $i = 1, 2, 4, 5$ as illustrated in Fig. 4.1. The non-dimensional rigid-body degrees of freedom $\eta_i(t)$ satisfy the condition (4.1). The characteristic size is equal to the radius R_0 and the characteristic time $1/\sigma$, where σ is the forcing

frequency. The generalized hydrodynamic coordinates and velocities in the derived modal equations satisfy (4.9) and the asymptotic terms of order $o(\epsilon)$ are neglected.

The system of ordinary differential equations (4.10), (4.11) assume that the $o(\eta_i)$-order quantities can be neglected. At the same time, the asymptotic condition (4.9) expresses the resonant nature of liquid sloshing, that is, the resonance response amplitude in (4.10), (4.11) should be of a lower asymptotic order than the forcing amplitude. That is why, the generalized hydrodynamic coordinates and velocities are included into modal equations 'as is'.

In [4, 9], the Narimanov-Moiseev–type modal theory was applied to derive the steady-state periodic solution and compare the theoretical results on the phase lags with experimental data on the phase lag measured for the resonant steady-state swirling wave in [10]. These studies followed a rather typical assumption that viscous damping in the hydrodynamic system is mainly associated with energy dissipation of the dominant (lowest-order) generalized hydrodynamic coordinate. This is the same as in [11] but for resonant sloshing in a rectangular tank. However, following this assumption failed to fit experimental data: for rectangular tank in [11] but for vertical circular tank – [10].

The solution on how to get agreement with experiments for rectangular tank was proposed in [215] where the present authors assumed that viscous damping is of strongly nonlinear character. These results are reported in the previous chapter. The present results [231] demonstrate that this idea (approach) can be expanded to the case in [10]. The focus has been on steady-state swirling wave regime.

Physically, this success of the machine learning methods to teach the model system accounting for the viscous damping can be interpreted as that viscous damping terms and, therefore, boundary layer thickness become in the nonlinear resonant case of the lowest asymptotic order.

Chapter 5

Conclusions

Based on the hidden physics concept, the present PhD thesis (dissertation) conducts an analytical study of (simplified) reduced order models on resonant liquid sloshing in rigid containers exposed to longitudinal harmonic excitation of the lowest natural sloshing frequency. The focus has been on upright tanks of rectangular (two-dimensional flows) and circular base (three-dimensional waves). The simplified (reduced order) hydrodynamic models are a product of combined usage of both variational and asymptotic methods applied to the original free-surface boundary value problem on the liquid sloshing dynamics. As it is usually accepted in the analytical sloshing theories, the original hydrodynamic model suggests a perfect incompressible liquid with irrotational flows. Applying the reduced order modeling leads to the Narimanov-Moiseev–type multi-modal equations with respect to the generalized hydrodynamic coordinates which describe perturbations of the natural sloshing modes. Because viscosity is not accounted for in the original hydrodynamic model, the approximate reduced order models are not able to describe physical phenomena for which viscous damping matters. A machine learning technique makes it possible to remove these failures by 'learning' special kind damping terms with *apriori* unknown coefficients and, thereby, correctly account for viscous damping phenomena by asymptotic multi-modal equations of the Narimanov-Moiseev–type. These phenomena were considered by the authors of [4,11] who also attempted speculatively describe them by incorporating linear damping terms in similar reduced order modal equations but without success.

When conducting the present dedicated applied matthematical studies, the following results were obtained:

- Derivations of multi-modal equations of both Miles-Lukovsky' and Narimanov-Moiseev' types are revisited for upright rectangular and circular base containers. The derivations are treated as a first step of the Reduced Order Modeling in sloshing problems. The derived nonlinear ordinary differential (modal) equations of the Miles-Lukovsky-type couple the generalized hydrodynamic coordinates and velocities. They imply discrete infinite dimensional mathematical models/conservative mechanical systems which are fully equivalent to the original free-surface boundary value problem. Employing, in addition, the Narimanov-Moiseev asymptotics significantly simplifies analytical structure of these discrete mathematical models so that they may admit dedicated analytical studies and, as the study shows, construct analytical periodic solutions which are associated with steady-state resonant waves.

- The Reduced Order Modeling suggests both derivation of discrete mathematical models by using a Galerkin–type projective and asymptotic methods (that has been done in the dissertation for two tank shapes) and development of Machine Learning algorithm to discover or infer the underlying governing differential equations and system parameters from limited and/or noisy observational data. Effectively, these mathematical models leverage Machine Learning to make the implicit or "hidden" physical laws. The Narimanov-Moiseev–types asymptotic modal equations for sloshing in upright rectangular and circular base tanks are, therefore modified with extra terms responsible for viscous damping in the hydrodynamic system. In the linear (non-resonant) case, this damping-equipped discrete modal formulation appears as an infinite set of uncoupled damped linear oscillators where each degree of freedom corresponds to perturbations of natural sloshing mode. The damping rates can then be interpreted as those coming from measuring logarithmic decrement of the natural sloshing modes. For resonant sloshing, the resulting damping becomes strongly nonlinear, affected by numerous dissipative physical factors (in addition to the boundary layer effect on the mean wetted tank surface) and also imply an energy transfer

from primary-excited to other (higher) natural sloshing modes.

- The single-dominant modal equations from [3] are re-derived and equipped with *apriori* unknown nonlinear damping terms. Theorem 3.1 establishes analytical structure of these terms to fit the Narimanov-Moiseev–type asymptotics. Theorem 3.2 deduces the asymptotic steady-state wave (periodic) solution of the damped modal equations. The solution is analytically derived by using the Moiseev's asymptotic scheme. It becomes a function of three unknown parameters, ξ_1, ξ_2 and ξ which are responsible for damping in the hydrodynamic system.

- Having known experimental measurements of the phase lags makes it possible to effectively compute the aforementioned three *apriori* unknown damping-related parameters. Measurements by [11] are employed by the author to demonstrate abilities of the proposed machine learning procedure. The results were published in [215]. In contrast to numerical speculations with damping coefficients in [11], an excellent agreement is demonstrated except when, according to visual observations in [11], the single-dominant modal system is not applicable. Conclusions from these numerical results are:

  – confirmation that damping effect of higher natural sloshing modes cannot be neglected (reason is nonlinear energy transfer from the primary-excited to higher modes with forthcoming viscous damping of these modes);

  – viscous damping of the primary-excited (first) natural sloshing mode should, generally speaking, be a function of the resonant wave amplitude and, moreover, for the considered case, this function is just the linear regression;

  – proposed learning technique can be an efficient tool for estimating the viscous damping (logarithmic decrements) of the lowest (dominant) natural sloshing mode, but it fails for higher (order) natural sloshing modes.

- In [4, 9], the Narimanov-Moiseev–type nonlinear modal theory was applied to derive the steady-state periodic solution and compare theoretical results on the phase lags with experimental data on the phase lag measured for the resonant steady-state swirling wave in [10]. These studies followed a rather typical assumption that viscous damping in the hydrodynamic system is mainly associated with energy dissipation of the dominant (lowest-order) generalized hydrodynamic coordinates. However, following this assumption failed to fit experimental data in [10]. The obtained results (see, also, [231]) on Machine Learning of the Narimanov-Moiseev–type modal equations to account for damping of the steady-state swirling wave regime in a circular base tank (based on experiments in [10]) showed that, similar to the case of rectangular tank,
  - viscous damping of higher natural sloshing modes cannot be neglected;
  - viscous damping of the primary-excited (first) natural sloshing modes is strongly nonlinear and, therefore, is a function of the resonant wave amplitude;
- The success of learning hydrodynamic systems on sloshing to account for viscous damping can be explained by the fact that boundary layer thickness become in the nonlinear resonant case larger of the lowest asymptotic order in the Narimanov-Moiseev–type asymptotics. The results can be improved by using adaptive multi-modal system from [75]. Such adaptive modal system is also required for better prediction of the resonance steady-state wave-amplitude response curves.

Bibliography

1. Faltinsen OM, Timokha AN. Sloshing. Cambridge: Cambridge University Press; 2009.

2. Lukovsky I, Timokha A. Multimodal method in sloshing. Journal of Mathematical Sciences. 2017;220(3):239-53.

3. Faltinsen OM, Rognebakke OF, Lukovsky IA, Timokha AN. Multidimensional modal analysis of nonlinear sloshing in a rectangular tank with finite water depth. Journal of Fluid Mechanics. 2000;407:201-34.

4. Raynovskyy I, Timokha A. Sloshing in upright circular containers: Theory, analytical solutions, and applications. CRC Press/Taylor & Fransis group; 2021.

5. Rebouillat S, Liksonov D. Fluid-structure interaction in partially filled liquid containers: A comparative review of numerical approaches. Computers & Fluids. 2010;39:739-46.

6. Ikeda T, Ibrahim RA, Harata Y, Kuriyama T. Nonlinear liquid sloshing in a square tank subjected to obliquely horizontal excitation. Journal of Fluid Mechanics. 2012;700:304-28.

7. Faltinsen OM, Lukovsky IA, Timokha AN. Resonant sloshing in an upright annular tank. Journal of Fluid Mechanics. 2016;804:608-45.

8. Faltinsen OM, Timokha AN. Resonant three-dimensional nonlinear sloshing in a square-base basin. Part 4. Oblique forcing and linear viscous damping. Journal of Fluid Mechanics. 2017;822:139-69.

9. Raynovskyy I, Timokha A. Damped steady-state resonant sloshing in a circular base container. Fluid Dynamics Research. 2018;50:Article ID 045502.

10. Royon-Lebeaud A, Hopfinger EJ, Cartellier A. Liquid sloshing and wave breaking in circular and square-base cylindrical containers. Journal of Fluid Mechanics. 2007;577:467-94.

11. Bäuerlein B, Avila K. Phase lag predicts nonlinear response maxima in liquid-sloshing experiments. Journal of Fluid Mechanics. 2021;925(A22):1-29.

12. Ostrogradsky MA. Mémoire sur la propagation des ondes dans un bassin cylindrique. Mémoires a l'Academie Royale des Sciences, De l'Institut de France. 1832;III:23-44.

13. Feschenko SF, Lukovsky IA, Rabinovich BI, Dokuchaev LV. Methods of determining the added liquid mass in mobile cavities. Kiev: Naukova Dumka (in Russian); 1969.

14. Hutton RE. An investigation of nonlinear, nonplanar oscillations of fluid in cylindrical container. NASA; D-1870: NASA; 1963.

15. Lukovsky IA. Nonlinear Dynamics: Mathematical Models for Rigid Bodies with a Liquid. De Gruyter; 2015.

16. Abramson HN. The dynamic behavior of liquids in moving containers with applications to space vehicle technology. Washington: NASA; 1966. NASA, SP-106.

17. Cooper RM. Dynamic of liquid in moving containers. ARS Journal. 1960;30(8):725-9.

18. Fontenot LL. Dynamic stability of space vehicles. Vol. 7. The dynamics of liquid in fixed and moving containers. Washington: NASA; 1968. NASA, CR-941.

19. Stofan AJ, Armsted AL. Analytical and experimental investigation of forces and frequencies resulting from liquid sloshing in a spherical tank. NASA, Lewis Research Center, Clevelend, Ohio; 1962. D–1281.

20. Sumner IE. Experimental investigations of stability boundaries for planar and nonplanar sloshing in spherical tanks. NASA, TN D-3210; 1966.

21. Sumner IE, Stofan AJ. An experimental investigation of the viscous damping of liquid sloshing in spherical tanks. NASA Technical Note, TN D-1991; 1963.

22. Abgaryan KA, Rapoport IM. Rockets dynamics. Moscow: Mashinostroenie; 1969. In Russian.

23. Kolesnikov KS. Propellant rocket as a control object. Moscow: Mashinostroenie; 1969. In Russian.

24. Kubenko VD, Koval'chuk PS. Nonlinear problems of the dynamics of elastic shells partialiy filled with a liquid. International Applied Mechanics. 2000;36(4):421-48.

25. Mikishev GN, Rabinovich BI. Dynamics of a Solid Body with Cavities Partially Filled with Liquid. Mashinostroenie; 1968. In Russian.

26. Mikishev GN, Rabinovich BI. Dynamics of Thin-Walled Structures with Compartments Containing a Liquid. Mashinostroenie; 1971. In Russian.

27. Moiseev NN. Variational problems in the theory of oscillations of a liquid and a body with a liquid. In: Variational methods in the problems of oscillations of a liquid and a body with a liquid. Moscow; 1962. p. 9-118. In Russian.

28. Moiseev NN, Petrov AA. Numerical methods for computing the eigenoscillations of a limited liquid volume. Computer Center of Academy of Sciences of USSR; 1966. In Russian.

29. Moiseyev NN, Rumyantsev VV. Dynamic Stability of Bodies Containing Fluid. Vol. 6. Applied Physics and Engineering. Berlin, Heidelberg: Springer; 1968.

30. Rabinovich BI. Introduction to dynamics of spacecraft. Moscow: Mashinostroenie; 1975. In Russian.

31. Bogomaz GI, Sirota SA. Oscillations of a liquid in containers: methods and results of experimental studies. Dnepropetrovsk: National Space Agency of Ukraine; 2002. In Russian.

32. Bogoryad IB. Oscillations of a viscous liquid in a cavity of a rigid body. Tomsk: Tomsk University; 1999. In Russian.

33. Bogoryad IB, Druzhinin IA, Druzhinina GZ, Libin EE. Introduction to the dynamics of vessels with a liquid. Tomsk: Tomsk University; 1977. In Russian.

34. Narimanov GS. Motions of a solid body whose cavity is partly filled by a liqud. Applied Mathematics and Mechanics (PMM). 1956;20(1):21-38.

35. Okhotsimskii DE. On the theory of a body motions when there is a cavity partly filled by a liquid. Applied Mathematics and Mechanics (PMM). 1956;20(1):3-20.

36. Rabinovich BI. Equations of perturbed motions of a solid body with a cylindrical cavity partly filled by a liquid. Applied Mathematics and Mechanics (PMM). 1956;20(1):39-49.

37. Lukovsky IA, Barnyak MY, Komarenko AN. Approximate Methods of Solving the Problems of the Dynamics of a Limited Liquid Volume. Kiev: Naukova Dumka; 1984. In Russian.

38. Trotsenko YV. Frequencies and modes of vibration of a cylindrical shell with attached rigid body. Journal of Sound and Vibration. 2006;292:535-51.

39. Morand J, Ohayon R. Fluid structure interaction. Applied numerical methods. Chichester-New York-Brisbane-Toronto-Singapore: John Wiley & Sons; 1995.

40. Faltinsen OM, Timokha AN. A multimodal method for liquid sloshing in a two-dimensional circular tank. Journal of Fluid Mechanics. 2010;665:457-79.

41. Kolaei A, Rakheja S, Richard MJ. Effects of tank cross-section on dynamic fluid slosh loads and roll stability of a partly–filled tank truck. European Journal of Mechanics B/Fluids. 2014;46:46-58.

42. Kolaei A, Rakheja S, Richard MJ. A coupled multimodal and boundary-element method for analysis of anti-slosh effectiveness of partial baffles in a partly-filled container. Computers & Fluids. 2015;107:43-58.

43. Yan-Sheng Y, Xing-Rui M, Ben-Li W. Multidimensional modal analysis of liquid nonlinear sloshing in right circular cylindrical tank. Applied Mathematics and Mechanics – English Edition. 2007;28(8):1997-018.

44. Joukowski N. On motions of a rigid body with cavity filled by homogeneous liquid. Journal of Russian Physical-Mathematical Society. 1885;XVI:30-85. In Russian.

45. Craik ADD. The origin of water wave theory. Annual Review of Fluid Mechanics. 2004;36:1-28.

46. Eastham M. An eigenvalue problem with parameter in the boundary condition. Quarterly Journal of Mathematics. 1962;13:304-20.

47. Kopachevsky ND, Krein SG. Operator approach to linear problems of hydrodynamics. Volume 2: Nonself-adjoint problems for viscous fluid. Basel – Boston – Berlin: Birkhauser Verlag; 2003.

48. Krein SG. Oscillations of a viscous fluid in a container. Doklady Akademii Nauk SSSR. 1964;159:262-5. In Russian.

49. Chernous'ko F. Motion of a rigid body with cavities containing viscous liquid. Nauka; 1968.

50. Chernous'ko FL. On free oscillations of a viscous fluid in a vessel. Journal of Applied Mathematics and Mechanics. 1966;30(5):990-1003.

51. Myshkis AD, Babskii VG, Kopachavskii AD, Slobozhanin LA, Tiuptsov AD. Low-gravity fluid mechanics: Mathematical theory of capillary phenomena. Berlin and New York: Springer-Verlag; 1987.

52. Kopachevsky ND, Krein SG. Operator approach to linear problems of hydrodynamics. Volume 1: Self-adjoint problems for an ideal fluid. Basel – Boston – Berlin: Birkhauser Verlag; 2003.

53. N KY. On the Oscillation of a Physical Pendulum Containing a Two-Layer Liquid Separated by an Elastic Membrane // Solid Body Mechanics. Interdepartmental Collection of Scientific Works — 2001. — Issue 31. — pp. 105–110; 2001. In Russian.

54. Kononov Yu N RVF, A DY. Axisymmetric Vibrations of Elastic Foundations and an Ideal Liquid in a Rigid Cylindrical Tank. Bulletin of Zaporizhzhia National University Physical and Mathematical Sciences. 2015;(2):106-15.

55. Budiansky B. Sloshing of liquid in circular canals and spherical tanks. Journal of Aerospace Sciences. 1960;27(3):161-72.

56. Vekua IN. On completeness of a system of harmonic polynomials in space. Doklady Akademii Nauk SSSR. 1953;90:495-8.

57. Vekua IN. New methods for solving elliptic equations. New York: Interscience Publishers John Wiley & Sons, Inc.; 1967.

58. Komarenko A. Asymptotic expansion of eigenfunctions of a problem with a parameter in the boundary conditions in a neighborhood of angular boundary points. Ukrainian Mathematical Journal. 1980;32(5):433-7.

59. Komarenko A. Asymptotics of solutions of spectral problems of hydrodynamics in the neighborhood of angular points. Ukrainian Mathematical Journal. 1998;50(6):912-21.

60. Wigley NM. Asymptotic expansions at a corner of solutions of mixed boundary value problems (Asymptotic expansions at corner of solutions of elliptic second order partial differential equations in two variables). Journal of Mathematics and Mechanics. 1964;13:549-76.

61. Wigley NM. Mixed boundary value problems in plane domains with corners. Mathematische Zeitschrift. 1970;115:33-52.

62. Faltinsen OM, Timokha AN. Analytically approximate natural sloshing modes and frequencies in two-dimensional tanks. European Journal of Mechanics B/Fluids. 2014;47:176-87.

63. Shao YL, Faltinsen OM. Fully-Nonlinear Wave-Current-Body Interaction Analysis by a Harmonic Polynomial Cell (HPC) Method. In: 32nd International Conference on Ocean, Offshore and Arctic Engineering, Nantes, France, June 9-14, 2013; 2013. Paper ID: OMAE2013-10185.

64. Shao YL, Faltinsen OM. A harmonic polynomial cell (HPC) method for 3D Laplace equation with application in marine hydromechanics. Journal of Computational Physics. 2014;274:312-32.

65. Faltinsen OM, Timokha AN. Natural sloshing frequencies and modes in a rectangular tank with a slat-type screen. Journal of Sound and Vibration. 2011;330:1490-503.

66. Faltinsen OM, Timokha AN. Analytically approximate natural sloshing modes for a spherical tank shape. Journal of Fluid Mechanics. 2012;703:391-401.

67. Faltinsen OM, Timokha AN. On sloshing modes in a circular tank. Journal of Fluid Mechanics. 2012;695:467-77.

68. Gavrilyuk I, Lukovsky I, Trotsenko Y, Timokha A. Sloshing in a vertical circular cylindrical tank with an annular baffle. Part 1. Linear fundamental solutions. Journal of Engineering Mathematics. 2006;54:71-88.

69. Penny WG, Price AT. Finite periodic stationary waves in a perfect liquid. Philosophical Transactions of the Royal Society, A. 1952;244:254-84.

70. Moiseev NN. On the theory of nonlinear vibrations of a liquid of finite volume. Journal of Applied Mathematics and Mechanics. 1958;22(5):860-72.

71. Narimanov GS. Movement of a tank partly filled by a fluid: the taking into account of non-smallness of amplitude. Prikl Math Mech. 1957;21:513-24.

72. Moore RE, Perko LM. Inviscid fluid flow in an accelerating cylindrical container. Journal of Fluid Mechanics. 1964;22:305-20.

73. Perko LM. Large-amplitude motions of liquid-vapour interface in an accelerating container. Journal of Fluid Mechanics. 1969;35:77-96.

74. Bryant PJ. Nonlinear progressive waves in a circular basin. Journal of Fluid Mechanics. 1989;205:453-67.

75. Faltinsen OM, Timokha AN. Adaptive multimodal approach to nonlinear sloshing in a rectangular tank. Journal of Fluid Mechanics. 2001;432:167-200.

76. Faltinsen OM, Timokha AN. Asymptotic modal approximation of nonlinear resonant sloshing in a rectangular tank with small fluid depth. Journal of Fluid Mechanics. 2002;470:319-57.

77. Wu GX. Second-order resonance of sloshing in a tank. Ocean Engineering. 2007;34:2345-9.

78. Faltinsen OM. A nonlinear theory of sloshing in rectangular tanks. Journal of Ship Research. 1974;18:224-41.

79. Ockendon JR, Ockendon H. Resonant surface waves. Journal of Fluid Mechanics. 1973;59:397-413.

80. Bauer HF, Eidel W. Non-linear liquid motion in conical container. Acta Mechanica. 1988;73(1-4):11-31.

81. Maggio ODD, Rehm AS. Nonlinear free oscillations of a perfect fluid in a cylindical container. AIAA Symposium on Structural Dynamics and Aeroelasticity. 1965;30:156-61.

82. Solaas F, Faltinsen OM. Combined numerical and analytical solution for sloshing in two-dimensional tanks of general shape. Journal of Ship Research. 1997;41(2):118-29.

83. Miles JW. Internally resonant surface waves in circular cylinder. Journal of Fluid Mechanics. 1984;149:1-14.

84. Miles JW. Resonantly forces surface waves in circular cylinder. Journal of Fluid Mechanics. 1984;149:15-31.

85. Bateman H. Partial differential equations of mathematical physics. Cambridge University Press; 1932.

86. Hargneaves R. A pressure-integral as kinetic potential. Philosophical Magazine. 1908;16:436-44.

87. Luke JG. A variational principle for a fluid with a free surface. Journal of Fluid Mechanics. 1967;27:395-7.

88. Holmes P. Chaotic motions in a weakly nonlinear model for surface waves. Journal of Fluid Mechanics. 1986;162:365-88.

89. Funakoshi M, Inoue S. Surface waves due to resonant oscillation. Journal of Fluid Mechanics. 1988;192:219-47.

90. Funakoshi M, Inoue S. Bifurcations in resonantly forced water waves. European Journal of Mechanics B/Fluids. 1991;10:31-6.

91. Henderson DM, Miles JW. Faraday waves in 2:1 resonance. Journal of Fluid Mechanics. 1991;222:449-70.

92. Miles JW. Parametrically excited, progressive cross-waves. Journal of Fluid Mechanics. 1988;186:129-46.

93. Miles JW. Parametrically excited, standing cross-waves. Journal of Fluid Mechanics. 1988;186:119-27.

94. Miles JW. Faraday waves: rolls versus squares. Journal of Fluid Mechanics. 1994;269:353-71.

95. Krasnopolskaya TS, Shvets AY. Dynamical chaos for a limited power supply for fluid oscillations in cylindrical tanks. Journal of Sound and Vibration. 2009;322:532-53.

96. Shvets AY, Sirenko VA. Peculiarities of transition to chaos in nonideal hydrodynamics systems. Chaotic Modeling and Simulation. 2012;2:303-10.

97. Stolbetsov VI. Nonsmall liquid oscillations in a right circular cylinder. Fluid Dynamics. 1967;2(2):41-5.

98. Stolbetsov VI. Oscillations of liquid in a vessel in the form of a rectangular parallelepiped. Fluid Dynamics. 1967;2(1):44-9.

99. Stolbetsov VI. Equations of nonlinear oscillations of a container partially filled with a liquid. Fluid Dynamics. 1969;4(2):95-9.

100. Stolbetsov VI, Fishkis VM. A mechanical model of a liquid performing small oscillations in a spherical cavity. Fluid Dynamics. 1968;3(5):79-81.

101. Lukovsky IA. Nonlinear sloshing in tanks of complex geometrical shape. Kiev: Naukova Dumka; 1975. In Russian.

102. Lukovsky IA. Introduction to nonlinear dynamics of rigid bodies with the cavities partially filled by a fluid. Kiev: Naukova Dumka; 1990. In Russian.

103. Narimanov GS, Dokuchaev LV, Lukovsky IA. Nonlinear dynamics of flying apparatus with liquid. Moscow: Mashinostroenie; 1977. In Russian.

104. Gavrilyuk I, Lukovsky I, Trotsenko Y, Timokha A. Sloshing in a vertical circular cylindrical tank with an annular baffle. Part 2. Nonlinear resonant waves. Journal of Engineering Mathematics. 2007;57:57-78.

105. Lukovskii IA. Variational formulation of nonlinear dynamic boundary problems of a finite liquid volume performing specified spatial motion. Soviet Applied Mechanics. 1980;16(2):164-9.

106. Lukovskii IA. Approximate method of solution of nonlinear problems in the dynamics of a liquid in a vessel executing a prescribed motion. Soviet Applied Mechanics. 1981;17(2):172-8.

107. Lukovskii IA. Variational methods of solving dynamic problems for fluid-containing bodies. International Applied Mechanics. 2004;40(10):1092-128.

108. Seliger E, Whitham GB. Variational principles in continuum mechanics. Proceedings of the Royal Society A. 1968;305:1-25.

109. Whitham GB. Non-linear dispersion of water waves. Journal of Fluid Meachanics. 1967;27:399-412.

110. Whitham GB. Linear and nonlinear waves. New York: Interscience; 1974.

111. Miles JW. Nonlinear surface waves in closed basins. Journal of Fluid Mechanics. 1976;75(3):419-48.

112. Lukovsky IA. Variational method in the nonlinear problems of the dynamics of a limited liquid volume with free surface. In: Oscillations of elastic constructions with liquid. Moscow: Volna; 1976. p. 260-4. In Russian.

113. Faltinsen OM, Timokha AN. Multimodal analysis of weakly nonlinear sloshing in a spherical tank. Journal of Fluid Mechanics. 2013;719:129-64.

114. Gavrilyuk I, Hermann M, Lukovsky I, Solodun O, Timokha A. Weakly-nonlinear sloshing in a truncated circular conical tank. Fluid Dynamics Research. 2013;45(ID 055512):1-30.

115. Lukovsky IA, Timokha AN. Modal modeling of nonlinear sloshing in tanks with non-vertical walls. Non-conformal mapping technique. International Journal of Fluid Mechanics Research. 2002;29(2):216-42.

116. Lukovsky IA. A mathematical problem of wave liquid motions in reseivor with inclined walls. Transactions of Institute of mathematics of NASU. 2005;2(1):227-53.

117. Lukovsky IA. Usage of variational principle to derivations of equations of the body-liquid dynamics. In: Dynamics of spacecraft apparatus and study of the space. Moscow; 1986. p. 182-94. In Russian.

118. Hermann M, Timokha A. Modal modelling of the nonlinear resonant sloshing in a rectangular tank I: A single-dominant model. Mathematical Models and Methods in Applied Sciences. 2005;15(9):1431-58.

119. Lukovsky IA, Ovchynnykov DV, Timokha AN. Asymptotic nonlinear multimodal method for liquid sloshing in an upright circular cylindrical tank. Part 1: Modal equations. Nonlinear Oscillations. 2012;14(4):512-25.

120. Lukovsky IA, Timokha AN. Combining Narimanov–Moiseev' and Lukovsky–Miles' schemes for nonlinear liquid sloshing. Journal of Numerical and Applied Mathematics. 2011;105(2):69-82.

121. Bogoryad IB, Druzhinin IA, Chakhlov SV. Study of transient processes with large disturbances of the free surface of a liquid in a closed compartment. In: Dynamics of spacecraft apparatus and investigation of the space. Moscow: Mashinostroenie; 1986. p. 194-203. In Russian.

122. Druzhinin IA, Chakhlov SV. Computation of nonlinear oscillations of liquid in a vessel (the Cauchy problem). In: Dynamics of Elastic and Rigid Vodies interacting with a Liquid. Tomsk: Tomsk University; 1981. .

123. Limarchenko OS. Direct method for solution of nonlinear dynamic problem on the motion of a tank with fluid. Dopovidi Akademii Nauk Ukrains'koi RSR, Series A. 1978;11(11):99-1002. In Ukrainian.

124. Limarchenko OS. Variational-method investigation of problems of nonlinear dynamics of a reservoir with a liquid. Soviet Applied Mechanics. 1980;16(1):74-9.

125. Limarchenko OS. Direct method of solving problems on the combined spatial motions of a body-fluid system. Soviet Applied Mechanics. 1983;19(8):715-21.

126. Limarchenko OS. Specific features of application of perturbation techniques in problems of nonlinear oscillations of a liquid with free surface in cavities of noncylindrical shape. Ukrainian Mathematical Journal. 2007;59:45-69.

127. Limarchenko OS, Yasinskii VV. Nonlinear dynamics of constructions with a fluid. Kiev: Kiev Polytechnical University; 1996. In Russian.

128. Buldakov E. Lagrangian modelling of fluid sloshing in moving tanks. Journal of Fluids and Structures. 2014;45:1-14.

129. Elahi R, Passandideh-Fard M, Javanshir A. Simulation of liquid sloshing in 2D containers using the volume of fluid method. Ocean Enginering. 2015;96:226-44.

130. Guo L, Morita K. Numerical simulation of 3D sloshing in a liquid-solid mixture using particle methods. International Journal for Numerical Methods in Engineering. 2013;95(9):771-90.

131. Sun P, Ming F, Zhang A. Numerical simulation of interactions between free surface and rigid body using a robust SPH method. Ocean Engineering. 2015;98:32-49.

132. Wang L, Wang Z, Li Y. A SPH simulation on large-amplitude sloshing for fluids in a two-dimensional tank. Earthquake Engineering and Engineering Vibration. 2013;12(1):135-42.

133. Zhang C. Application of an improved semi-Lagrangian procedure to fully-nonlinear simulation of sloshing in non-wallsided tanks. Applied Ocean Research. 2015;51:74-92.

134. Zhang C, Li Y, Meng Q. Fully nonlinear analysis of second-order sloshing resonance in a three-dimensional tank. Computes & Fluids. 2015;116:88-104.

135. Ovsyannikov LV, Makarenko NI, Nalimov VI, Lyapidevski VY, Plotnikov PI, Sturova IV, et al. Nonlinear problems of the theory of surface and internal waves. Novosibirsk: Nauka; 1985.

136. La Rocca M, Scortino M, Boniforti MA. A fully nonlinear model for sloshing in a rotating container. Fluid Dynamics Research. 2000;27:225-9.

137. Shankar PN, Kidambi R. A modal method for finite amplitude, nonlinear sloshing. Pramana. 2002;59(4):631-51.

138. Faltinsen OM, Firoozkoohi R, Timokha AN. Effect of central slotted screen with a high solidity ratio on the secondary resonance phenomenon for liquid sloshing in a rectangular tank. Physics of Fluids. 2011;23:Art. No. 062106.

139. Faltinsen OM, Rognebakke OF, Timokha AN. Transient and steady-state amplitudes of resonant three-dimensional sloshing in a square base tank with a finite fluid depth. Physics of Fluids. 2006;18:Article ID 012103.

140. Limarchenko OS. Nonlinear properties for dynamic behavior of liquid with a free surface in a rigid moving tank. International Journal of Nonlinear Sciences and Numerical Simulation. 2000;1(2):105-18.

141. Limarchenko OS, Semenova IY. Nonlinear wave generation on a fluid in a moving parabolic tank. International Applied mechanics. 2011;46(8):864-8.

142. Love JS, Tait MJ. Nonlinear simulation of a tuned liquid damper with damping screens using a modal expansion technique. Journal of Fluids and Structures. 2010;26(7-8):1058-77.

143. Love JS, Tait MJ. Non-linear multimodal model for tuned liquid dampers of arbitrary tank geometry. International Journal of Non-Linear Mechanics. 2011;46(8):1065-75.

144. Love JS, Tait MJ. Nonlinear multimodal model for TLD of irregular tank geometry and small fluid depth. Journal of Fluids and Structures. 2013;43:83-44.

145. Forbes LK. Sloshing of an ideal fluid in a horizontally forced rectangular tank. Journal of Engineering Mathematics. 2010;66(4):395-412.

146. Hermann M, Timokha A. Modal modelling of the nonlinear resonant fluid sloshing in a rectangular tank II: Secondary resonance. Mathematical Models and Methods in Applied Sciences. 2008;18(11):1845-67.

147. Ikeda T. Nonlinear parametric vibrations of an elastic structure with a rectangular liquid tank. Nonlinear Dynamics. 2003;33(1):43-70.

148. Ikeda T. Autoparametric resonances in elastic structures carrying two rectangular tanks partially filled with liquid. Journal of Sound and Vibration. 2007;302(4-5):657-82.

149. Ikeda T, Nakagawa N. Nonlinear vibrations of a structure caused by water sloshing in a rectangular tank. Journal of Sound and Vibration. 1997;201(1):23-41.

150. Lee DY, Choi HS, Faltinsen OM. A study on the sloshing effect on the motion of 2d boxes in regular waves. Journal of Hydrodynamics. 2010;22(5):429-33.

151. Lee DY, Jo GN, Kim YH, Choi HS, Faltinsen OM. The effect of sloshing on the sway motions of 2D rectangular cylinders in regular waves. Journal of Marine Science and Technology. 2011;16(3):323-30.

152. Rognebakke OF, Faltinsen OM. Coupling of sloshing and ship motions. Journal of Ship Research. 2003;47(3):208-21.

153. Waterhouse DD. Resonant sloshing near a critical depth. Journal of Fluid Mechanics. 1994;281:313-8.

154. Fultz D. An experimental note on finite-amplitude standing gravity waves. Journal of Fluid Mechanics. 1962;13(2):192-212.

155. Ockendon H, Ockendon JH, Johnson AD. Resonant sloshing in shallow water. Journal of Fluid Mechanics. 1986;167:465-79.

156. Ockendon JR, Ockendon H, Waterhouse DD. Multi-mode resonance in fluids. Journal of Fluid Mechanics. 1996;315:317-44.

157. Case KM, Parkinson WC. Damping of surface waves in an incompressible liquid. Journal of Fluid Mechanics. 1957;2:172-84.

158. Keulegan G. Energy dissipation in standing waves in rectangular basins. Journal of Fluid Mechanics. 1959;6(1):33-50.

159. Martel A, Nicolás JA, Vega JM. Surface-wave damping in a brimful circular cylinder. Journal of Fluid Mechanics. 1998;360:213-28.

160. Miles JW, Henderson DM. A note on interior vs. boundary-layer damping of surface waves in a cicular cylinder. Journal of Fluid Mechanics. 1998;364:319-23.

161. Utsumi M. Theoretical determination of modal damping ratio of sloshing using a variational method. Journal of Pressure Vessel Technology. 2011;133(Art. No. 011301-1):1-10.

162. Chester W. Resonant oscillation of water waves. I. Theory. Proceedings of Royal Society, London. 1968;308:5-22.

163. Chester W, Bones JA. Resonant oscillation of water waves. II. Experiment. Proceedings of Royal Society, London. 1968;306:23-30.

164. Antuono M, Bouscasse B, Colagrossi A, Lugni C. Two-dimensional modal method for shallow-water sloshing in rectangular basins. Journal of Fluid Mechanics. 2012;700:419-40.

165. Faltinsen OM, Rognebakke OF. Sloshing. In: NAV 2000: International Conference on Ship and Shipping Research : 13th Congress, 19-22 September 2000, Venice (Italy) : Proceedings, 2000; 2000. .

166. Faltinsen OM, Firoozkoohi R, Timokha AN. Analytical modeling of liquid sloshing in a two-dimensional rectangular tank with a slat screen. Journal of Engineering Mathematics. 2011;70(1-2):93-109.

167. Faltinsen OM, Firoozkoohi R, Timokha AN. Steady-state liquid sloshing in a rectangular tank with a slat-type screen in the middle: quasi-linear modal analysis and experiments. Physics of Fluids. 2011;23:Art. No 042101.

168. Blevins RD. Applied Fluid Dynamics. Krieger Publishing Company, Malabar, FL; 1992.

169. Hamelin JA, Love JS, Tait MJ, Wilson JC. Tuned liquid dampers with a Keulegan-Carpenter number-dependent screen drag coefficient. Journal of Fluids and Structures. 2013;43:271-86.

170. Love JS, Tait MJ. Parametric depth ratio study on tuned liquid dampers: Fluid modelling and experimental work. Computers & Fluids. 2013;79:13-26.

171. Faltinsen OM, Rognebakke OF, Timokha AN. Resonant three-dimensional nonlinear sloshing in a square base basin. Journal of Fluid Mechanics. 2003;487:1-42.

172. Faltinsen OM, Rognebakke OF, Timokha AN. Resonant three-dimensional nonlinear sloshing in a square base basin. Part 3. Base ratio perturbation. Journal of Fluid Mechanics. 2006;551:93-116.

173. Faltinsen OM, Rognebakke OF, Timokha AN. Classification of three-dimensional nonlinear sloshing in a square-base tank with finite depth. Journal of Fluids and Structures. 2005;20(1):81-103.

174. Faltinsen OM, Lagodzinskyi O, Timokha AN. Resonant three-dimensional nonlinear sloshing in a square base basin. Part 5. Three-dimensional non-parametric tank forcing. Journal of Fluid Mechanics. 2020;894(A10):1-42.

175. Bridges TJ. On secondary bifurcation of three-dimensional standing waves. SIAM Journal of Appied Mathematics. 1986;47:40-59.

176. Bridges TJ. Secondary bifurcation and change of type for three dimensional standing waves in finite depth. Journal of Fluid Mechanics. 1987;179:137-53.

177. Faltinsen OM, Rognebakke OF, Timokha AN. Resonant three-dimensional nonlinear sloshing in a square base basin. Part 2. Effect of higher modes. Journal of Fluid Mechanics. 2005;523:199-218.

178. Lukovsky IA, Pilkevich AM. On liquid motions in an upright oscillating circular tank. In: Numerical-analytical studies of the dynamics and stability of multidimensional systems. Kiev: Institute of Mathematics; 1985. p. 3-11. In Russian.

179. Abramson HN, Chu WH, Kana DD. Some studies of nonlinear lateral sloshing in rigid containers. Journal of Applied Mechanics. 1966;33(4):66-74.

180. Ikeda T, Ibrahim RA. Nonlinear random responses of a structure parametrically coupled with liquid sloshing in a cylindrical tank. Journal of Sound and Vibration. 2005;284:75-102.

181. Gavrilyuk I, Lukovsky I, Timokha AN. A multimodal approach to nonlinear sloshing in a circular cylindrical tank. Hybrid Methods in Engineering. 2000;2(4):463-83.

182. Pilkevich AM. Analysis of forced liquid sloshing in co-axial cylindical reseivors. In: Applied methods of studying the physical-mechanical processes. Kiev: Institute of Mathematics; 1979. p. 49-63. In Russian.

183. Pilkevich AM. Constructing the approximate solutions of nonlinear equations on wave motions of a liquid in a container. In: Dynamics and stability of mechanical systems. Kiev: Institute of Mathematics; 1980. p. 16-21. In Russian.

184. Takahara H, Kimura K. Frequency response of sloshing in an annular cylindrical tank subjected to pitching excitation. Journal of Sound and Vibration. 2012;331(13):3199-212.

185. Takahara H, Hara K, Ishida T. Nonlinear liquid oscillation in a cylindrical tank with an eccentric core barrel. Journal of Fluids and Structures. 2012;35:120-32.

186. Lukovsky IO, Solodun OV. A nonlinear model of liquid motions in cylindrical compartment tanks. Dopovidi NANU. 2001;(5):51-5. In Ukrainian.

187. Lukovsky IO, Solodun OV. Study of the forced liquid sloshing in circular tanks by using a seven-mode model of the third order. In: Problems of the dynamics and stability of multidimensional systems. Transactions of Institute of Mathematics of NASU. vol. 47. Kiev: Institite of Mathematics; 2003. p. 161-79. In Ukrainian.

188. Lukovsky IA. On constructing a solution of a nonlinear problem on free oscillations of a liquid in basins of arbitray shape. Dopovidi AN UkrSSR, Ser A. 1969;(3):207-10. In Ukrainian.

189. Lukovsky IA. Variational method for solving the nonlinear problem on liquid sloshing in tanks of complicated shape. In: Dynamics and stability of managed systems. Kiev: Institute of Mathematics; 1977. p. 45-61. In Russian.

190. Bauer HF. Flüssigkeitsschwingungen in Kegelbehälterformen. Acta Mechanica. 1982;43:185-200.

191. Dokuchaev LV. On the solution of a boundary value problem on the sloshing of a liquid in conical cavities. Applied Mathematics and Mechanics (PMM). 1964;28(1):601-2.

192. Lukovsky IA, Bilyk AN. Forced sloshing in movable axisymmetic conical tanks. In: Numerical-analytical studies of the dynamics and stability

of multidimensional systems. Kiev: Institute of Mathematics; 1985. p. 12-26. In Russian.

193. Lukovsky IA, Bilyk AN. Study of forcced nonlinear sloshing in conical tanks with a small apex angle. In: Applied problems in the dynamics and stability of mechanical systems. Kiev: Institute of Mathematics; 1987. p. 5-14. In Russian.

194. Gavrilyuk I, Hermann M, Lukovsky I, Solodun O, Timokha A. Natural sloshing frequencies in rigid truncated conical tanks. Engineering Computations. 2008;25(6):518-40.

195. Gavrilyuk I, Hermann M, Lukovsky I, Solodun O, Timokha A. Multimodal method for linear liquid sloshing in a rigid tapered conical tank. Engineering Computations. 2012;29(2):198-220.

196. Gavrilyuk IP, Lukovsky IA, Timokha AN. Linear and nonlinear sloshing in a circular conical tank. Fluid Dynamics Research. 2005;37:399-429.

197. Lukovsky IA, Solodun OV, Timokha AN. Eigen oscillations of a liquid sloshing in truncated conical tanks. Acoustic Bulletin. 2006;9:42-61. In Russian.

198. Lukovsky IA. On solving spectral problems on linear sloshing in conical tanks. Dopovidi NANU. 2002;(5):53-8. In Ukrainian.

199. Gavrilyuk I, Lukovsky I, Timokha AN. Sloshing in circular conical tank. Hybrid Methods in Engineering. 2001;3(4):322-78.

200. Casciati F, Stefano AD, Matta E. Simulating a conical tuned liquid damper. Simulation Modelling Practice and Theory. 2003;11:353-70.

201. Barkowiak K, Gampert B, Siekmann J. On liquid motion in a circular cylinder with horizontal axis. Acta Mechanica. 1985;54:207-20.

202. Barnyak M, Gavrilyuk I, Hermann M, Timokha A. Analytical velocity potentials in cells with a rigid spherical wall. ZAMM. 2011;91(1):38-45.

203. Faltinsen OM, Timokha AN. Nonlinear sloshing in a spherical tank. In: OMAE 2013. Proceedings of the ASME 32nd International Conference on Ocean, Offshore and Arctic Engineering. June 9-14, Nantes, France; 2013. .

204. Chernova MA, Timokha AN. Sloshing in a two-dimensional circular tank. Weakly-nonlinear modal equations. Transactions of Institute of Mathematics of NAS of Ukraine. 2013;10(3):262-83.

205. Chernova MO, Lukovsky IA, Timokha AN. Generalizing the multimodal method for the levitating drop dynamics. ISRN Mathematical Physics. 2012;Article ID 869070:1-19.

206. Gavrilyuk I, Hermann M, Lukovsky I, Ovchynnykov D, Timokha A. Computer-based multimodal modeling of liquid sloshing in a circular cylindrical tank. Reports on Numerical Mathematics, FSU Jena. 2010;(10-03):1-14.

207. Reclari M. Hydrodynamics of orbital shaken bioreactors [Thesis No 5759 (2013)]. Ècole Polytechnique Federale de Lausanne; 2013.

208. Bouvard J, Herreman W, Moisy F. Mean mass transport in an orbitally shaken cylindrical container. Physical Review Fluids. 2017;2:Paper No 084801.

209. Ducci A, Weheliye WH. Orbitally Shaken Bioreactors-Viscosity Effects on Flow Characteristics. AIChE Journal. 2014;60(11):3951-68.

210. Weheliye W, Yianneskis M, Ducci A. On the fluid dynamics of shaken bioreactors – flow characterization and transition. AIChE. 2013;59(1):334-44.

211. Reclari M, Dreyer M, Tissot S, Obreschkow D, Wurm FM, Farhat M. Surface wave dynamics in orbital shaken cylindrical containers. Physics of Fluids. 2014;26:Paper ID 052104.

212. Raynovskyy I, Timokha A. Steady-state resonant sloshing in an upright cylindrical container performing a circular orbital motion. Mathematical Problems in Engineering. 2018;2018(Article ID 5487178):1-11.

213. Billingham J. Nonlinear sloshing in zero gravity. Journal of Fluid Mechanics. 2002;464:365-91.

214. Billingham J. On a model for the motion of a contact line on a smooth solid surface. European Journal of Applied Mathematics. 2006;17:347-82.

215. Miliaev A, Timokha A. Viscous damping of steady-state resonant sloshing in a clean rectangular tank. Journal of Fluid Mechanics. 2023;965(R1):1-11.

216. Milyaev AO, Timokha AN. Learning the single-dominant model system on resonant sloshing in a rectangular tank. Dopov Nac Akad Nauk Ukraine. 2022;(3):17-22.

217. Lukovsky IA, Timokha AN. Variational methods in nonlinear problems of the dynamics of a limited liquid volume. Institute of Mathematics of NASU; 1995. In Russian.

218. Barnyak MY, Barnyak OM. Normal oscillations of viscous liquid in a horizontal channel. International Applied Mechanics. 1996;32(7):56-566.

219. Miles JW. Surface-wave damping in closed basins. Proceedings of Royal Society London. 1967;A297:459-75.

220. Pilipchuk VN. Nonlinear interactions and energy exchange between liquid sloshing modes. Physica D. 2013;263:21-40.

221. Raissi M, Karniadakis GE. Hidden physics models: Machine learning of nonlinear partial differential equations. Journal of Computational Physics. 2018;357:125-41.

222. Raissi M, Perdikaris P, Karniadakis GE. Physics-informed neural networks: A deep learning framework for solving forward and inverse prob-

lems involving nonlinear partial differential equations. Journal of Computational Physics. 2019;378:686-707.

223. Ahmed SE, Pawar S, San O, Rasheed A, Iliescu T, Noack D. On closures for reduced order models – A spectrum of first-principle to machine-learned avenues. Physics of Fluids. 2021.

224. Saltari F, Pizzoli M, Coppotelli G, Gambioli F, Cooper JF, Mastroddi F. Experimental characterisation of sloshing tank dissipative behaviour in vertical harmonic excitation. Journal of Fluids and Structures. 2022;109(Paper ID 103474).

225. NASA S. Propellant slosh loads. NASA Space Vehicle Design Criteria (Structures), NASA SP-8009; 1968.

226. Miles JW. Stability of forced oscillations of a spherical pendulum. Quarterly of Applied Mathematics. 1962;20(1):21-32.

227. Aliabadi S, Johnson A, Abedi J. Comparison of finite element and pendulum models for simulating of sloshing. Computers and Fluids. 2003;32:535-45.

228. Godderidge B, Turnock SR, Tan M. A rapid method for the simulation of sloshing using a mathematical model based on the pendulum equation. Computers & Fluids. 2012;57:163-71.

229. Raynovskyy I, Timokha A. Resonant liquid sloshing in an upright circular tank performing a periodic motion. Journal of Numerical and Applied Mathematics. 2016;122:71-82.

230. Barnyak MY, Leschuk OP. Construction of solutions of the problem of free oscillations of viscous fluid in a half-filled spherical tank. Nonlinear Oscillations. 2008;11(4):461-83.

231. Miliaev AO, Timokha AN. Damping of the swirling wave mode. Nelinijyni Kolyvannya. 2024;27(4):517-28.

Appendix A

List of publications and approbation of results

This appendix contains the list of publications of the PhD candidate on the thesis' topic as well as information about the approbation of the thesis' results.

Scientific works in which the scientific results of the thesis were published:

1. Milyaev A.O., Timokha A.N., Learning the single-dominant model system on resonant sloshing in a rectangular tank, *Доповіді Національної Академії Наук України*, № 6 (2022), 46-53, 10.15407/dopovidi2022.06.046. (Фаховий журнал категорії Б).

2. Miliaiev A.O., Timokha A.N., Viscous damping of steady-state resonant sloshing in a clean rectangular tank, *Journal of Fluid Mechanics* **965**, R1 (2023), 11 pp., 10.1017/jfm.2023.372. (Scopus – Q1, WoS – Q1, SJR – Q1).

3. Miliaiev A.O., Timokha A.N., Damping of the swirling wave mode, *Нелінійні коливання* **27**, № 4 (2024), 517-528, 10.3842/nosc.v27i4.1494. (Фаховий журнал категорії А).
   Перевидано за кордоном:
   Miliaiev A.O., Timokha A.N., Damping of the swirling wave mode, *Journal of Mathematical Sciences (USA)* **295**, № 6 (2025), 726-738, 10.1007/s10958-026-08219-3. (Scopus – Q3, SJR – Q3).

Certifying the approbation of the thesis' materials:

1. Timokha A., Miliaiev A. Hidden physics models in sloshing: machine learning of multimodal equations. Bogolyubov Kyiv Conference "Problems of Theoreticall and Mathematical Physics" dedicated to the 115th anniversary of MM Bogiolyubov (1909-1992), September 24-26, 2024, Kyiv, Ukraine, Program, Section 5 Mathematics, Wednesday, September 25, 10:00. https://imath.kiev.ua/∼institute/BKC2024/Program%20Sec5%20Bogolubov%202024.pdf.

2. Miliaiev A., Timokha A. Machine learning approach for studying damped resonant sloshing. VIII міжнародна наукова конференція СУЧАСНІ ПРОБЛЕМИ МЕХАНІКИ. Kyiv, 28-29 серпня 2025 року, Abstracts, http://tamd.univ.kiev.ua/wp-content/uploads/2025/08/ABSTRACTS_MPM_2025.pdf.

3. Miliaiev A.O., Timokha A.N. Differential equations of damped resonant sloshing. XX Міжнародна наукова конференція імені академіка Михайла Кравчука. 17–20 листопада 2025 р., Тези доповідей, сторінка 83, https://matan.kpi.ua/media/2025/kravchuk-conf-2025/kravchuk-conf-2025-abstracts.pdf.

Information on the approbation of the thesis' results. The main results of the thesis were reported and discussed at:

- Seminar of Department of Mathematical Problems of Mechanics and Control Theory (Kyiv, 2020–2026);
- Bogolyubov Kyiv Conference "Problems of Theoreticall and Mathematical Physics" dedicated to the 115th anniversary of MM Bogiolyubov (1909-1992), September 24-26, 2024, Kyiv, Ukraine;
- VIII міжнародна наукова конференція СУЧАСНІ ПРОБЛЕМИ МЕХАНІКИ. Київ, 28-29 серпня 2025 року;
- XX Міжнародна наукова конференція імені академіка Михайла Кравчука. 17–20 листопада 2025 р.